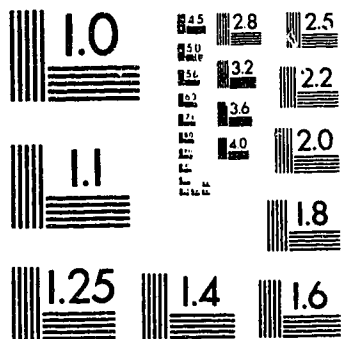


2

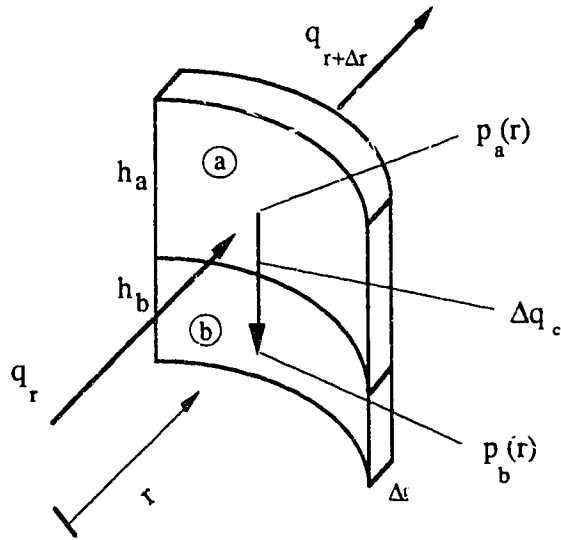
of/de

2

PM-1 3½"x4" PHOTOGRAPHIC MICROCOPY TARGET
NBS 1010a ANSI/ISO #2 EQUIVALENT



Consider a thin ring behind the flood front as follows (only a section of the ring is drawn):



A mass balance for Section a above gives:

$$q_r - (q_{r+\Delta r} + \Delta q_c) = 0 \quad \dots\dots\dots(8.2)$$

Now, using Darcy's equation and rearranging we obtain

$$\frac{2\pi r h_a k_a}{\mu_a} \frac{\partial p_a}{\partial r} \Big|_{r+\Delta r} - \frac{2\pi r h_a k_a}{\mu_a} \frac{\partial p_a}{\partial r} \Big|_r = \frac{4\pi r \Delta r}{\frac{\mu_a h_a}{k_a} + \frac{\mu_b h_b}{k_b}} \cdot (p_a - p_b), \quad \dots\dots\dots(8.3)$$

where p_a and p_b are the average pressures of the corresponding sections taken from each section center. Taking the limit as Δr approaches zero, the following differential form of Eq. (8.3) results.

$$\frac{\partial^2 p_a}{\partial r^2} = \alpha_1 (p_a - p_b) \quad \dots\dots\dots(8.4)$$

where $\alpha_1 = \frac{2}{h_a^2 (1 + M_{ab} \frac{h_b}{h_a})}$ and $M_{ab} = \frac{k_a/\mu_a}{k_b/\mu_b}$ is the mobility ratio of the fluid in Section a

to that in Section b. If a similar procedure is carried out for Sections b and a, c and d, and d and c, the following equations can be derived:

$$\frac{\partial^2 p_b}{\partial r^2} = \alpha_2 (p_b - p_a), \quad \dots\dots\dots(8.5)$$

$$\frac{\partial^2 p_c}{\partial r^2} = \alpha_3 (p_c - p_d), \quad \dots\dots\dots(8.6)$$

and $\frac{\partial^2 p_d}{\partial r^2} = \alpha_4 (p_d - p_c), \quad \dots\dots\dots(8.7)$

where $\alpha_2 = \frac{2}{h_b^2 (1 + M_{ba} \frac{h_a}{h_b})}$, $\alpha_3 = \frac{2}{h_c^2 (1 + M_{cd} \frac{h_d}{h_c})}$, $\alpha_4 = \frac{2}{h_d^2 (1 + M_{dc} \frac{h_c}{h_d})}$ and where the

M's are the mobility ratios for the corresponding sections. It can be seen that the only difference between the linear flow case and the radial flow case is the independent displacement direction variable: x and r for the linear and radial cases, respectively. Solving Eqs. (8.4) and (8.5) simultaneously, and Eqs. (8.6) and (8.7) simultaneously, the following solutions result

$$p_a(r) = c_1 + c_2 r + c_3 \left(\frac{\alpha_1}{m}\right) \cdot \sinh(r\sqrt{m} + c_4), \quad \dots\dots\dots(8.8)$$

$$p_b(r) = c_1 + c_2 r + c_3 \left(\frac{\alpha_1}{m} - 1\right) \cdot \sinh(r\sqrt{m} + c_4), \quad \dots\dots\dots(8.9)$$

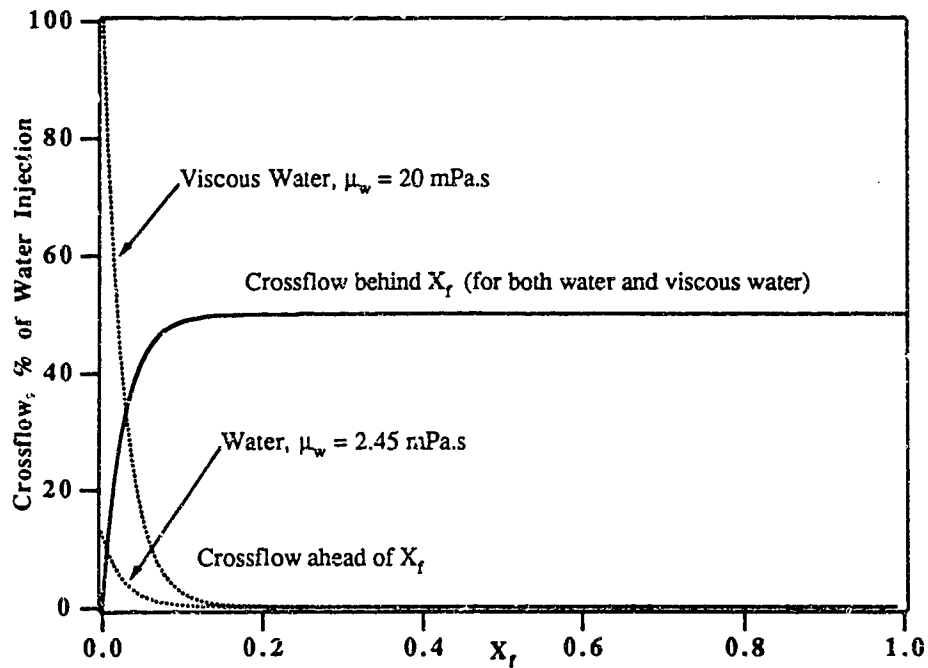
$$p_c(r) = c'_1 + c'_2 r + c'_3 \left(\frac{\alpha_3}{n}\right) \cdot \sinh(r\sqrt{n} + c'_4), \quad \dots\dots\dots(8.10)$$

and $p_d(r) = c'_1 + c'_2 r + c'_3 \left(\frac{\alpha_3}{n} - 1\right) \cdot \sinh(r\sqrt{n} + c'_4); \quad \dots\dots\dots(8.11)$

where $m = \alpha_1 + \alpha_2$ and $n = \alpha_3 + \alpha_4$.

Thus, it can be seen that when crossflow exists in a two-layer system, the pressure distribution is similar for both linear and radial systems, depending on the boundary conditions.

The unconsolidated sand model used in Barnes' study³ was one-eighth of a five-spot well pattern under bottom-water conditions. His visual model experiments showed that when the viscosity of the injected water was increased, crossflow ahead of the flood front increased. The crossflow equations can be used to study this phenomenon mathematically. Because the radial flow boundary conditions for a five-spot well pattern are not clearly defined, an approximation suggested by Rapoport and Leas⁴⁰ was used to study the crossflow effect. By replacing the actual quadrant by a linear section of equivalent area, the crossflows behind and ahead of the flood front were plotted for both water and viscous water injection in Fig. 8.4. For a waterflood using a low viscosity viscous water ($\mu_w = 2.45 \text{ mPa}\cdot\text{s}$), oil crossflow into the bottom-water zone ahead of the flood front is 13% of the injected water at $X_f = 0$, whereas a value of 100% is obtained when viscous water ($\mu_w = 20 \text{ mPa}\cdot\text{s}$) was used. Both of these values were calculated using Eq. (4.13) at $X_f = 0$, using Barnes' experimental data (Fig. 8.4). When viscous water was used in Barnes' study, a much larger amount of crossflow was observed. Notice that while crossflow ahead of the flood front increased substantially when viscous water was used, crossflow behind the flood front remained unchanged (Fig. 8.4). This is true only if the same water viscosity was used for both the oil and water zones behind the flood front. However, in a real situation, the large oil bank formed by the injection of viscous water reduces the mobility of water in the bottom-water zone, which improves water displacement in the oil zone. Thus, a higher oil rate was observed in Barnes' experiments when using a viscous water for flood.



A linear section of equivalent area of a five-spot model

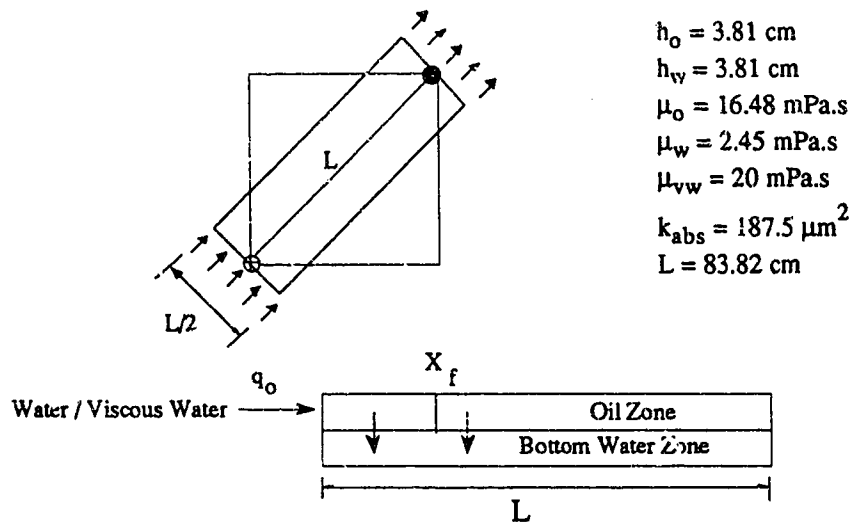


Fig. 8.4: Crossflow as a Function of the Flood Front Position when Waterflooding the Oil Zone in a Linear Equivalent Five-spot Model Used by Barnes³.

8.1.3 The Region of Crossflow

As mentioned in the previous section, crossflow takes place mostly around the injection well; in this section, a mathematical view of the crossflow region is presented.

As can be seen from the previous crossflow figures, crossflow ahead of the flood front starts at a finite value and reaches a minimum at $X_f = 1$, while crossflow behind the flood front starts at zero and reaches a maximum at $X_f = 1$. Notice that both crossflows ahead of and behind the flood front are almost invariant after the flood front reaches approximately 0.1 of the model length (Figs. 8.2a, 8.2b, and 8.2c). In other words, crossflow takes place only near the injection well. Now, to examine how far away from the injection point the crossflow achieves 90% of its minimum or maximum value, solve for x from the crossflow Eqs. (4.12) and (4.13):

$$0.1 = \frac{q_c|_{X_f=x}}{q_c|_{X_f=0}} = \frac{1 - \cosh(x\sqrt{n} - \sqrt{n})}{1 - \cosh(\sqrt{n})} \quad \dots\dots\dots(8.12)$$

for crossflow ahead of the flood front, and

$$0.9 = \frac{q_c|_{X_f=x}}{q_c|_{X_f=1}} = \frac{\cosh(x\sqrt{m} - \sqrt{m}) - \cosh(\sqrt{m})}{1 - \cosh(\sqrt{m})} \quad \dots\dots\dots(8.13)$$

for crossflow behind the flood front.

Solving Eqs. (8.12) and (8.13) for x ,

$$x|_{\text{ahead}} = \frac{\sqrt{n} - \cosh^{-1}(0.9 + 0.1 \cdot \cosh(\sqrt{n}))}{\sqrt{n}} \quad \dots\dots\dots(8.14)$$

for crossflow ahead of the flood front, and

$$x|_{\text{behind}} = \frac{\sqrt{m} - \cosh^{-1}(0.9 + 0.1 \cdot \cosh(\sqrt{m}))}{\sqrt{m}} \quad \dots\dots\dots(8.15)$$

for crossflow behind the flood front.

Recall that $m = \alpha_1 + \alpha_2$ and $n = \alpha_3 + \alpha_4$, where $\alpha_1 = \frac{2}{h_a^2 (1 + M_{ab} \frac{h_b}{h_a})}$, $\alpha_2 = \frac{2}{h_b^2 (1 + M_{ba} \frac{h_a}{h_b})}$,

$\alpha_3 = \frac{2}{h_c^2 (1 + M_{cd} \frac{h_d}{h_c})}$, $\alpha_4 = \frac{2}{h_d^2 (1 + M_{dc} \frac{h_c}{h_d})}$. As an illustration, the data from Run 7 is

used: $h_o = 5.715$ cm, $h_w = 1.905$ cm, $\mu_o = 63$ mPa.s, $\mu_w = 1$ mPa.s, $k_{owr} = 13.4$ μm^2 , $k_w = 18.0$ and $k_{wor} = 3.5$ μm^2 , which give $n = 631.567$ and $m = 910.533$. Substituting n and m into Eqs. (8.14) and (8.15) respectively, regions of crossflow ahead of and behind the flood front are determined. For crossflow ahead of the flood front, 90% of the initial crossflow was dissipated when flood front reached 9.2% of the model length. For crossflow behind the flood front, 90% of the maximum crossflow was attained when the flood front reached 7.6% of the model length. Thus, from an engineering viewpoint, under the bottom-water conditions studied, crossflow is no longer a function of the flood front position once it is beyond 10% of the model length.

It should be noted that the regions of crossflow obtained from Eqs. (8.14) and (8.15) are independent of flow rate. Thus, increasing the injection rate does not affect the crossflow regions. In other words, crossflow is not a function of injection rate as was concluded by Lambeth and Dawe³³ experimentally (i.e., the ratio of q_c to q_{inj} is not a function of the q_{inj}). Furthermore, Eqs. (8.14) and (8.15) are also independent of the injection interval, as confirmed by Runs 7, 12 and 20. In short, it can be concluded that crossflow under bottom-water conditions takes place near the injection end; when the water front passes beyond the regions calculated by Eqs. (8.14) and (8.15), a linear flow regime can be assumed approximately in the individual layers.

8.2 Emulsion Flooding Under Bottom-Water Conditions

8.2.1 Effect of Slug Size on Oil Recovery in the Emulsion-Slug Process

The effect of the emulsion slug size on the Emulsion-Slug Process was examined in Runs 3 to 6 for an emulsion with 0.4% surfactant concentration; the emulsion slug size in these runs was varied from $0.5 PV_{bw}$ to $2 PV_{bw}$. The remaining emulsion slug runs utilized a constant slug size of $1.0 PV_{bw}$.

The results of Runs 3 to 6 show that for the particular surfactant concentration used, i.e. 0.4%, emulsion has an adverse effect on recovery even for a homogeneous porous medium. Figure 8.5 compares cumulative oil recovery from a homogeneous pack for emulsions of different surfactant concentrations as displacing fluids. It can be seen that the emulsion with 0.4% surfactant concentration had the lowest volumetric sweep efficiency: an ultimate oil recovery of 43.4% IOIP as compared to 59.5% IOIP for the waterflood run. On the other hand, from the bottom-water runs, it appears that an emulsion slug first invades the oil zone. If the slug is small, it just blocks the oil zone. Water injected after the emulsion slug thus channels even more readily into the bottom-water than in the absence of the emulsion slug. This is evident when the results of Runs 3 and 7 are compared. In Run 3, a small emulsion slug of $0.5 PV_{bw}$ was injected at the beginning of the run. Because of this small slug size, only 20% IOIP of oil was recovered. On the other hand, in Run 7, waterflood alone gave an ultimate oil recovery of 50.1% IOIP.

If the emulsion slug size is increased, part of the slug starts to block the bottom-water zone, so that some of the water injected is subsequently forced to flow in the oil zone. Thus, as the emulsion slug size increases, recovery increases also. Based on the experiments conducted, an emulsion slug size of $0.5 PV_{bw}$ in Run 3 gave an ultimate oil recovery of 20% IOIP; as the slug size was increased to $0.75 PV_{bw}$ in Run 6, and $1.0 PV_{bw}$ in Run 4, the ultimate oil recovery increased to 25.1% and 23.3% IOIP, respectively.

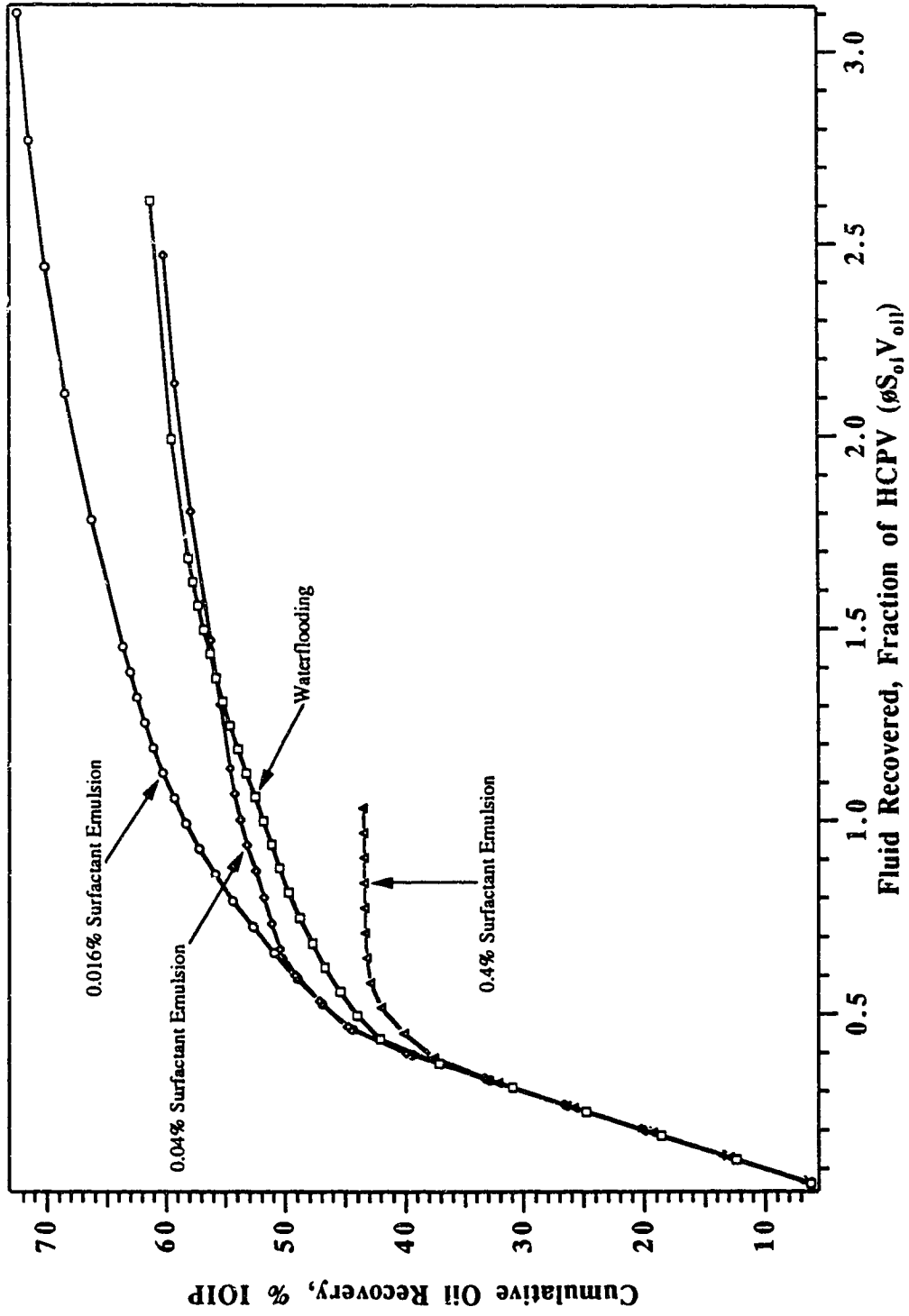


Fig. 8.5: The Effect of Displacing Fluid on Oil Recovery (Base Runs with Homogeneous Pack).

Though recovery increases as the emulsion slug size increases, it appears that once the slug size reached $1.0 PV_{bw}$, further injection of emulsion or water would lead to flow through the bottom-water zone only. Thus, recovery remains unchanged regardless of the emulsion slug size thereafter. The emulsion slug size in Runs 4 and 5 was 1 and $2 PV_{bw}$ respectively, but the recovery for the two differed by less than 1% IOIP.

Thus, based on the results of these experiments, it can be said that when an emulsion has an adverse effect on oil recovery in a homogeneous pack (reservoir), the effect becomes more pronounced under bottom-water conditions.

8.2.2 Effect of Surfactant Concentration of the Emulsion Slug on Oil Recovery

In this study, three different surfactant concentrations were used to prepare stable emulsions as mobility control or blocking agents. It was found that the surfactant concentration of the emulsion plays an important role in oil recovery. It appears that when emulsion is injected into a homogeneous pack, the lower the surfactant concentration in the emulsion, the higher the oil recovery. Of course, it is understood that the surfactant concentration is high enough to ensure emulsion stability. This can be seen readily from Fig. 8.5 for emulsions with different surfactant concentrations injected into a homogeneous pack in Runs 21, 22 and 23. Run 7, the base waterflood, is also plotted in Fig. 8.5 for comparison. From this figure, it can be seen that the emulsion with 0.4% surfactant concentration gave the lowest oil recovery of 43.4% IOIP, compared to the waterflood recovery of 59.5% IOIP in Run 7. When the surfactant concentration was lowered by a factor of 10, to 0.04%, the oil rate after breakthrough was higher than that for the waterflood in Run 7; however, a similar ultimate oil recovery of 59.2% IOIP was obtained. When the surfactant concentration of the injected emulsion was lowered to 0.016%, a significant improvement over the waterflood was observed in both the oil production rate and the ultimate oil recovery: an ultimate oil recovery of 71.5% IOIP was obtained.

The effect of surfactant concentration of the emulsion slug on recovery is more apparent for all methods used under bottom-water conditions. Figures 8.6 to 8.8 show the effect of surfactant concentration on cumulative recovery, under bottom-water conditions, for ESP, AWE process, and DBP. From the figures, except for the initial production of the ESP, all three methods showed an increase in the oil rate and the ultimate oil recovery with a decrease in surfactant concentration.

8.2.3 Effect of Injection Strategies on Recovery Under Bottom-Water Conditions

8.2.3.1 Differences Between the Dynamic-Blocking Procedure (DBP) and Conventional Waterflooding

To elaborate on the differences between a conventional waterflood (with or without the help of a blocking agent) and the DBP injection strategies, the term "single-fluid" and "simultaneous fluids" injection are used for conventional waterflooding and the DBP strategies, respectively. The following sections describe the two strategies individually.

8.2.3.1.1 Conventional Waterflooding

This section covers the single-fluid blocking strategy. Basically, the single-fluid blocking process consists of two distinct modes: blocking and displacing. At any given stage of the process, only one fluid is injected into the model. In an ideal situation, it is desired for the blocking mode to take place in the bottom-water zone, and the displacing mode to take place in the oil zone. Because only one fluid is injected at a time, the two modes operate over different time intervals. Thus, when the displacing mode is active, the blocking action inside the model is not controllable from outside the model. In the ESP and the AWE process, the single fluid blocking method was used, which relies on a blocking agent to modify the flow path. That is, there is only one main flow path from the injection well to the production well. Initially, the main flow path is through the bottom-water zone. Thus, by injecting a blocking agent into the bottom-water zone, the main flow path switches to the oil zone. To illustrate this concept of single fluid blocking, consider the following diagram:

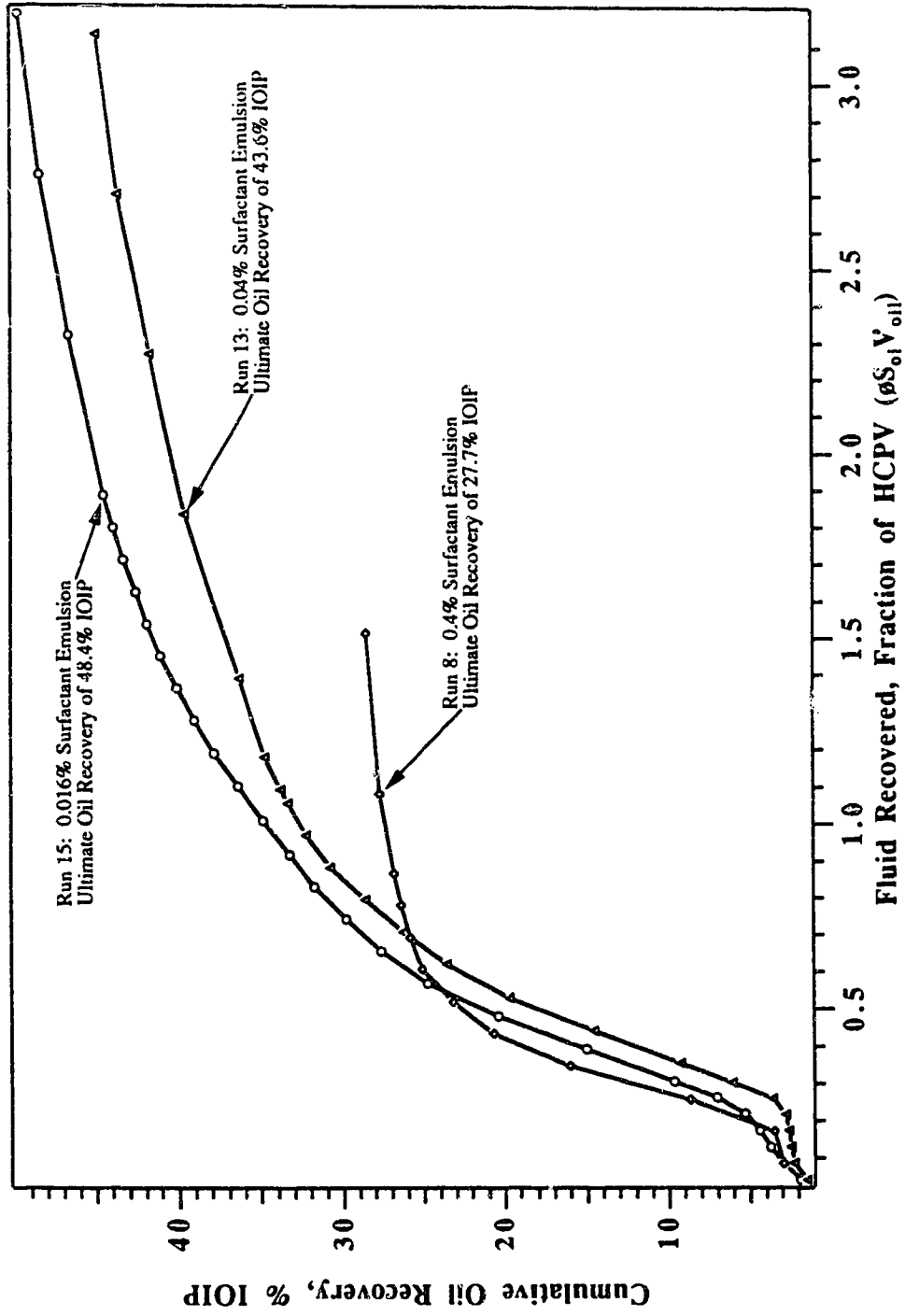


Fig. 8.6: The Effect of Surfactant Concentration on the ESP.

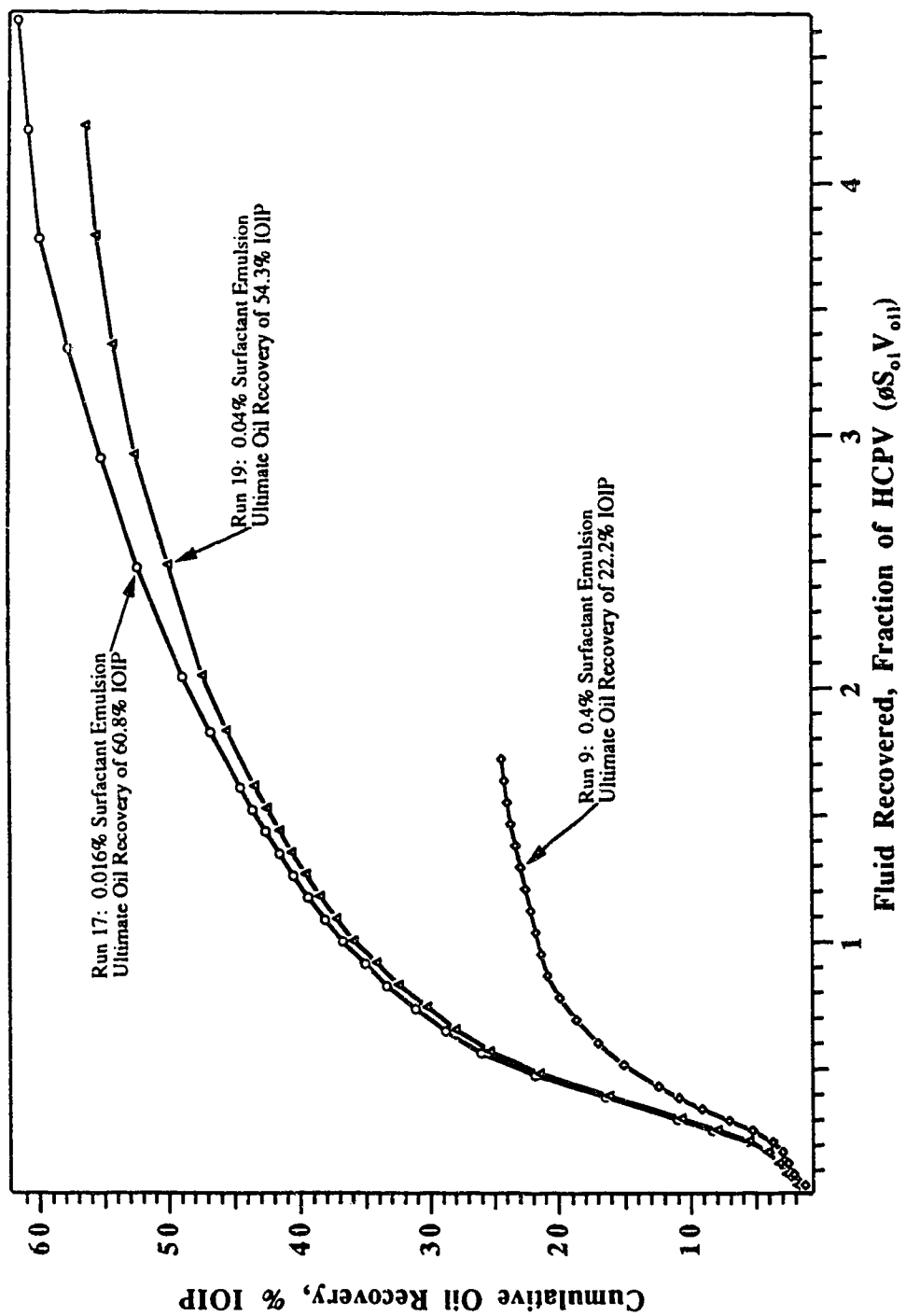


Fig. 8.7: The Effect of Surfactant Concentration on the AWE Process.

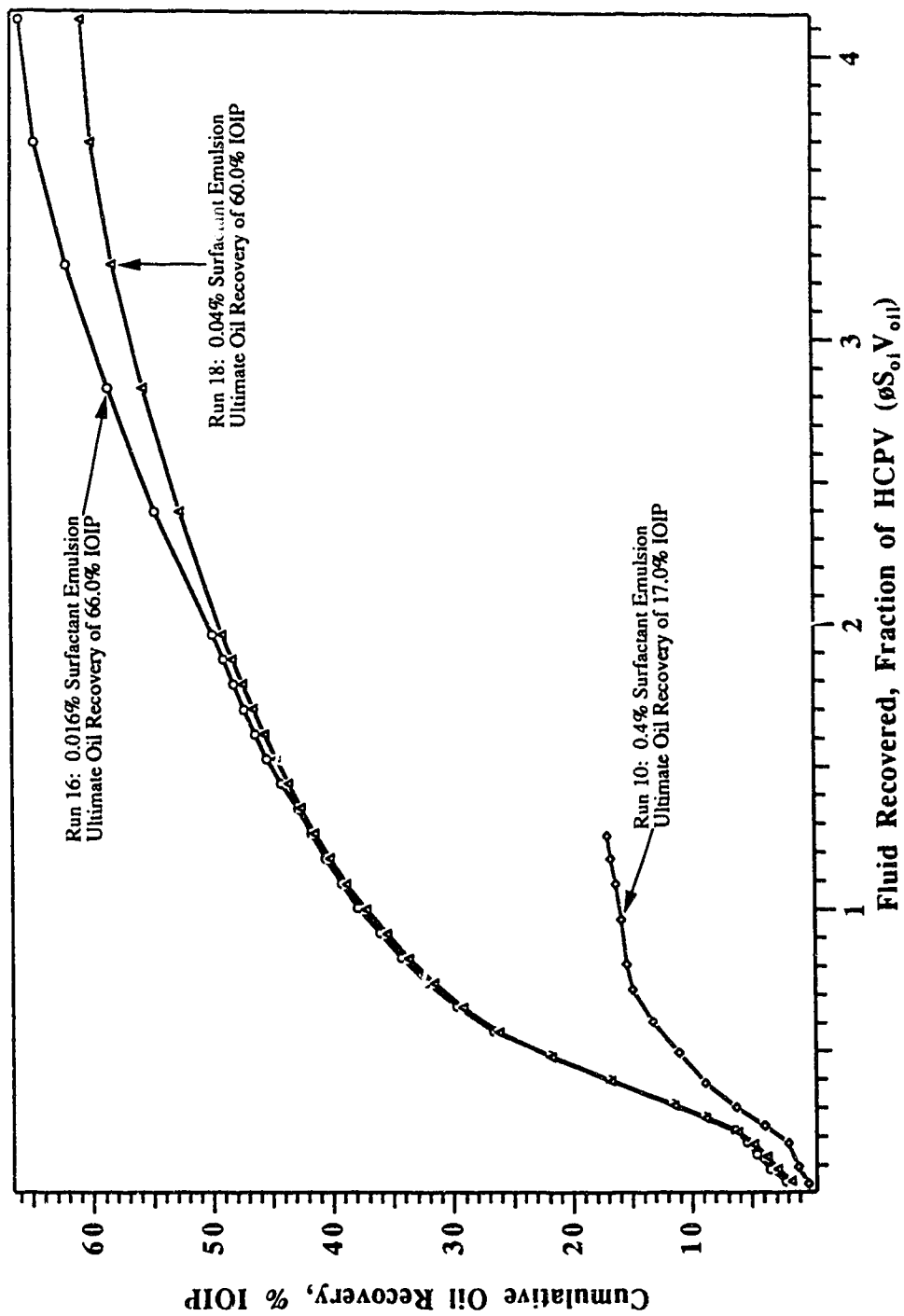
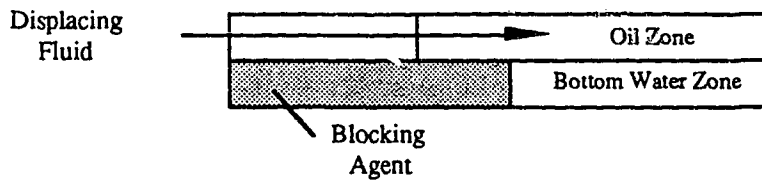
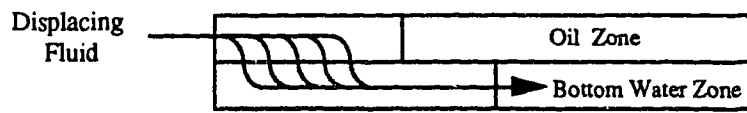


Fig. 8.8: The Effect of Surfactant Concentration on the DBP.



The shaded area represents the blocking agent. From this diagram, it is clear that the blocking process depends very much on the properties of the blocking agent; that is, if the permeability reduction due to the blocking agent is large, a high pressure gradient would be needed for any flow, and most of the injected fluid would then travel along the path shown above. However, if the blocking agent is unable to reduce the permeability of the bottom-water zone such that the main flow path is in the oil zone, it would deteriorate by dilution due to the injected fluid and the main flow path would be as shown below:



Several points should be noted when using the single-fluid blocking method where a single fluid is injected at a time: 1) The changeover of path from the so-called 'undesirable' to the 'desirable' path is not well-defined. Usually the change from one path to another is gradual. Thus, it is difficult to decide when to inject the blocking agent and when to inject the displacing fluid, water or mobility control agent. (Notice that the terms mobility control agent and blocking agent are somewhat different. Though, they can be the same chemical, mobility control is used to displace the oil in such a way that the mobility ratio is favourable. A blocking agent is used to lower the permeability of a layer in such a way that the main flow is redirected). 2) It is obvious that the greater the permeability reduction in the bottom-water zone, the more efficient the displacement process will be in the oil zone. However, if the permeability reduction due to the blocking agent is too large, it will be difficult to inject the blocking agent at the desired location, since the injection of a blocking

agent would divert the flow path as injection continues. On the other hand, if the permeability reduction is small, the blocking process may not be effective. 3) The blocking process is passive in that the permeability reduction depends solely on the properties of the blocking agent. Thus, if the injected fluid generates a large enough pressure gradient such that it can penetrate through (or displace) the blocking agent, then the blocking agent would no longer be effective.

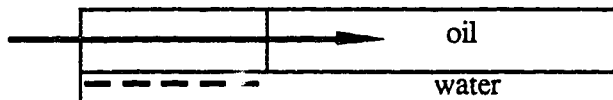
In the last diagram, additional blocking agent is required to replace the previously injected blocking agent so that the unswept oil may be recovered. To do this, the injected blocking agent must travel from the injection well to the shaded area above. From item (2) above, it can be seen that it is physically impossible to block off the desired location without blocking the other region, the oil zone in this case.

8.2.3.1.2 Dynamic-Blocking Procedure

In the following, the Dynamic-Blocking Procedure (DBP) is described. The term simultaneous injection is also used to refer to this process.

In the single-fluid blocking method, the blocking of flow in the bottom-water layer requires a stable material that inhibits flow into this layer. In the DBP method, however, 'blocking' requires the generation of a pressure in the bottom-water layer such that there is no vertical pressure gradient between the oil and the water layers. Under such conditions, no blocking is necessary, since the fluid injected into the oil layer will not migrate into the bottom-water zone. This is accomplished by injecting displacing and blocking fluids into the corresponding layers simultaneously. The Dynamic-Blocking Procedure consists of two modes: displacing and blocking. The main difference from the previous process is that the two modes are operating simultaneously, and because of this, a better control of the displacement process is obtained. That is, during the displacement in the oil zone, the

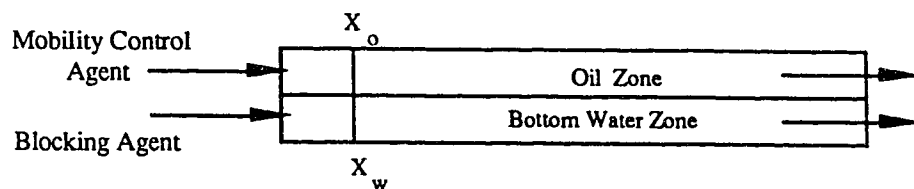
blocking process is externally controllable. In other words, the blocking process is active while displacing the oil. Consider the following situation,



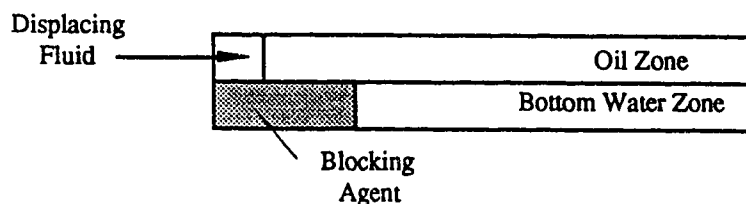
where the broken line represents the generation of a pressure distribution identical to that in the path above. When this happens, all of the fluid displacing the oil would be confined to the oil zone. Because this "blocking" pressure distribution can be monitored during the displacement, this blocking method is said to be dynamic.

Although use of the simultaneous injection method in the field would require a dual injection system, this method is preferred to the single-fluid injection for two reasons. First, the permeability reduction can be monitored as required. This aspect is rather important because the permeability reduction requirement is usually not invariant during oil displacement: a greater permeability reduction is required initially for a faster oil rate response. This is important because the oil rate is extremely low initially in waterflooding reservoirs with contiguous bottom-water zones. Also, the amount of permeability reduction needed is not constant along the oil-displacement path: the crossflow along the porous medium is not constant (i.e., it is a function of the horizontal position). In the single-fluid blocking method, permeability reduction is basically constant within the region occupied by the blocking agent, and if a certain reduction near the injection well is achieved, the region far away would have the same reduction, which may or may not be adequate. Therefore, in using the single-fluid blocking method, permeability reduction away from the injection well should be adequate to insure a high displacement efficiency, which is not practical in most instances³². On the other hand, in the dynamic-blocking method, permeability reduction is variable along the displacement path, as needed, to minimize crossflow.

Another advantage of the dynamic blocking method is that it is a more cost-effective way of flooding than the single fluid blocking method. With both displacing fluid and blocking agent acting at the same time, it is possible to improve (i.e. lower) the mobility ratio in the oil zone. Thus, this process is much more effective than water displacing oil in the single fluid blocking method.



In contrast, in the conventional method, the use of a mobility agent together with a blocking agent is quite difficult. This is due to the passive nature of the method. Consider the following:



If a mobility control agent is used instead of water as the displacing fluid, it would generate a higher pressure gradient than in the case of water. This implies that the blocking agent would have to reduce the permeability more than in the case of water to compensate for this higher pressure gradient need; otherwise, the mobility control agent would go to the bottom-water instead, which defeats its purpose.

8.2.3.2 Experimental Results for the Injection Strategies

In this study, emulsions were used as blocking agents to lower the water mobility in the bottom-water zone. Thus, given the same volume of the emulsion slug, the more emulsion injected into the bottom-water zone, the greater the blocking effect. Three injection methods were used to inject the emulsions into the bottom-water zone: these were ESP, the AWE process and DBP. The operating procedures for these processes were described in the previous sections.

Figures 8.9 to 8.11 show the effect of injection strategies on cumulative oil recovery for three different emulsions used. For the lower surfactant concentration (0.016% and 0.04%) emulsions, cumulative oil recovery shows that the DBP injection method followed by the AWE process resulted in higher recovery than the Emulsion-Slug Process. However, the opposite trend was obtained for the higher surfactant concentration, 0.4%, emulsion; i.e., the ESP showed the highest recovery and the DBP showed the lowest recovery among the injection methods. Recall that the 0.4% surfactant concentration emulsion adversely affected the recovery whereas the lower surfactant concentration emulsions improved recovery in a homogeneous model (see Fig. 8.5). From the bottom-water experiments, it appears that under bottom-water conditions, the DBP and AWE processes yield higher recovery compared to ESP for 0.04% and 0.016% surfactant concentration emulsions, while for the 0.4% surfactant concentration emulsion, the performance of DBP and AWE processes is inferior to that of ESP.

The improved recovery for the AWE process and DBP can be interpreted as a more effective blocking process in the bottom-water zone because more emulsion is injected into the zone. However, the same reasoning apparently did not apply to the higher surfactant concentration, 0.4%, emulsion. One possible explanation is as follows. Consider the case of the DBP injection method. Note that the effect of the AWE process lies between ESP and DBP, because if the slug size in the AWE process increases, the limit would be a single

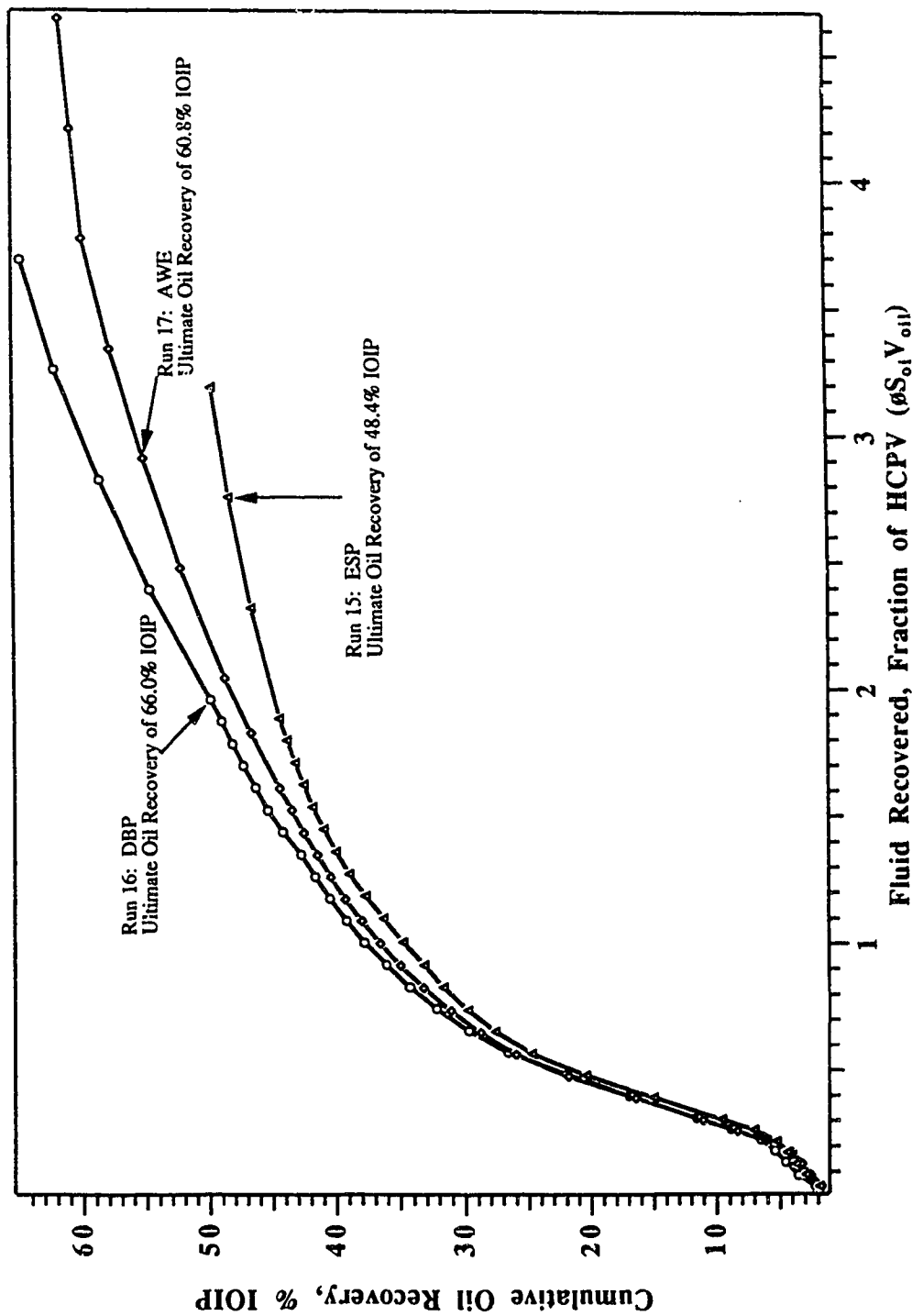


Fig. 8.9: The Effect of the Injection Strategy on Oil Recovery Under Bottom Water Conditions (0.016 % Surfactant Emulsion).

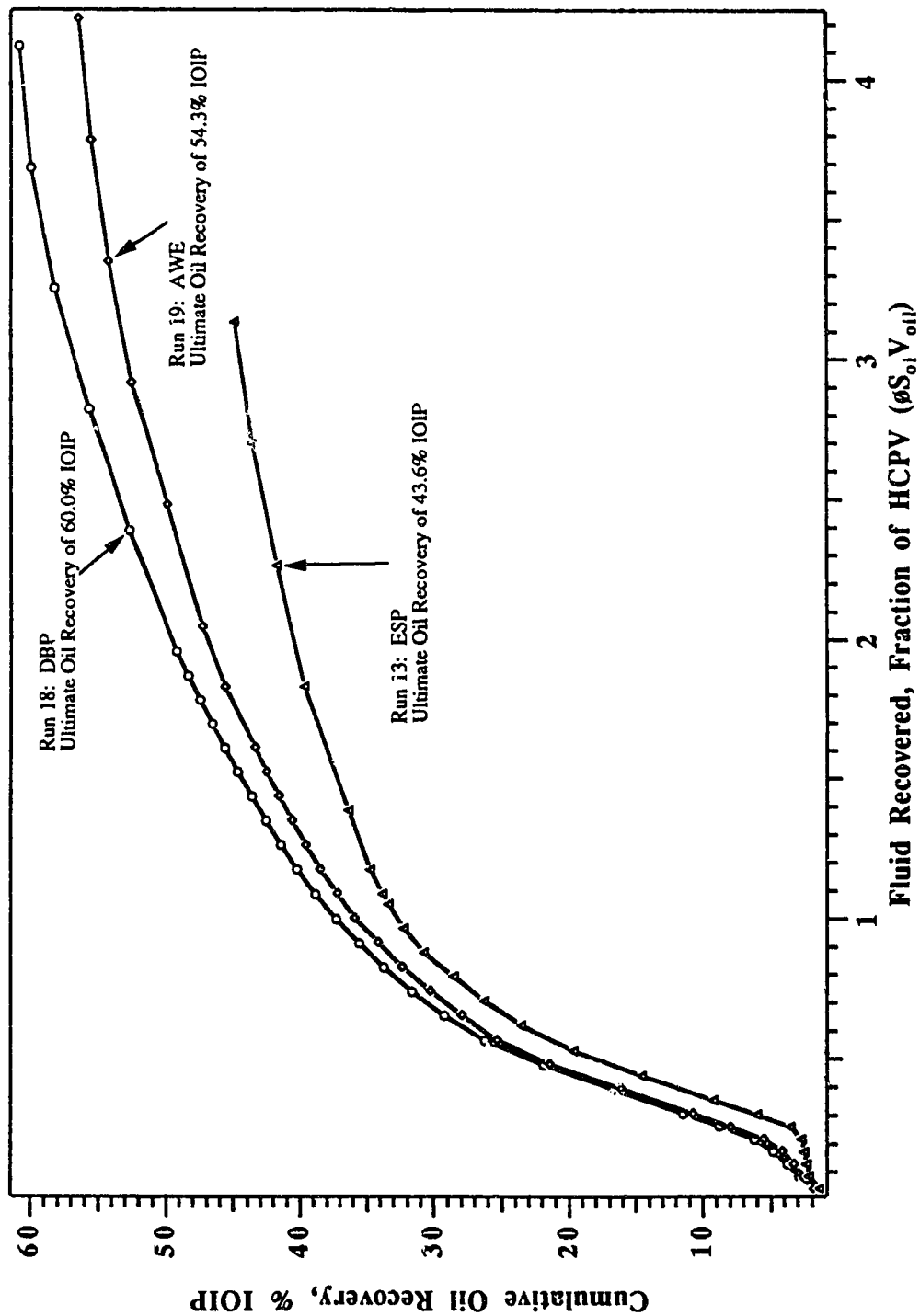


Fig. 8.10: The Effect of the Injection Strategy on Oil Recovery Under Bottom Water Conditions (0.04 % Surfactant Emulsion).

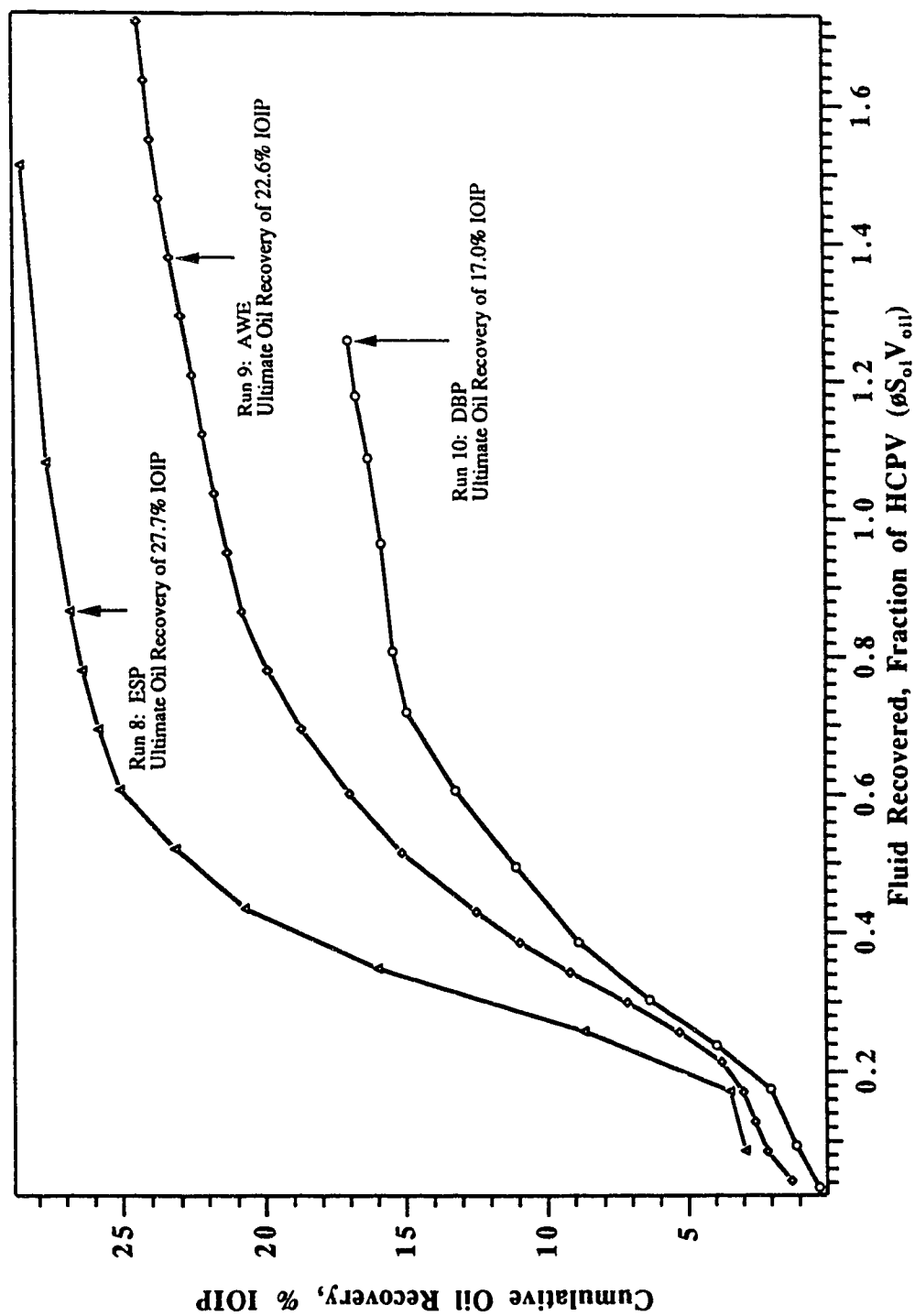
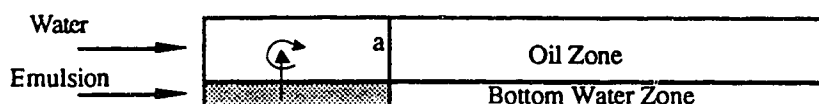


Fig. 8.11: The Effect of the Injection Strategy on Oil Recovery Under Bottom Water Conditions (0.4 % Surfactant Emulsion).

slug injection, i.e. the ESP. On the other hand, if the slug size in the AWE process decreases to be infinitesimally small, in the limit it will be equivalent to injecting two fluids simultaneously, i.e., DBP.



When the injected emulsion crossflow is upwards from the bottom-water zone to the oil zone, the waterflood in the oil zone, Zone a, is disrupted. Since the flow of emulsion into Zone a is vertical and the flow of water in Zone a is horizontal, the result is nonlinear flow as shown. Thus, with the crossflow effect, which leads to nonlinear flow in the oil zone, it is believed that oil recovery by the DBP and AWE processes was less than that by ESP. Of course, the above effect applies to the lower surfactant concentration emulsions also; however, only this high surfactant concentration, 0.4%, emulsion showed an adverse effect on oil recovery from a homogeneous reservoir (Fig. 8.5). The mechanism is complex, and involves mobility ratio and interphase and intraphase transfer of the surfactant.

9. CONCLUSIONS

The present research examined waterflooding when a communicating water zone is present below the oil zone. A simple mathematical model was developed to estimate crossflow of fluids under such conditions. In this study, the effect of different injection strategies for an emulsion slug was examined. Based on the mathematical model and the results of experiments in a physical model, the following conclusions are reached:

- 1) Under bottom-water conditions, the amount of water channelling into the bottom-water zone can be estimated from Eqs. (4.12) and (4.13).
- 2) In a two-layer reservoir, crossflow takes place near the injection end. The regions of crossflow can be estimated from Eqs. (8.14) and (8.15).
- 3) Under bottom-water conditions, waterflood volumetric sweep efficiency is independent of the point of injection.
- 4) The amount of crossflow ahead of the flood front increases as the viscosity of the injected fluid increases in a two-layer reservoir.
- 5) For 10% quality oil-in-water stable emulsion slug injection, the lower the surfactant concentration, the higher the recovery for both homogeneous and bottom-water conditions cases.
- 6) Under bottom-water conditions, the DBP and AWE processes yield higher recovery compared to ESP for 0.04% and 0.016% surfactant concentration emulsions, while for the 0.4% surfactant concentration emulsion, the performance of DBP and AWE processes is inferior to that of ESP.
- 7) The predictions based upon the crossflow equations derived in this work were in good agreement with the experimental results obtained in this work, as well as in previous studies.

10. REFERENCES

1. Pye, D.J., "Improved Secondary Recovery by Control of Water Mobility," J. Pet. Tech. (Aug. 1964) 911-916.
2. Robertson, J.O., Jr., and Oefelein, F.H., "Plugging Thief Zones in Water Injection Wells," J. Pet. Tech. (Aug. 1967) 999-1004.
3. Barnes, A. L., "The Use of a Viscous Slug to Improve Waterflood Efficiency in a Reservoir Partially Invaded by Bottom Water," J. Pet. Tech. (Oct. 1962) 1147-1153.
4. Zaidel, Ya. M., "Polymer Flooding of Oil Formations With Bottom Water," Izv. Akad. Nauk SSSR, Mekh. Zhidk. Gaza, No. 3 (May-June 1986) 84-90.
5. Islam, M.R., Mobility Control in Reservoirs With Bottom Water, Ph.D. Thesis, University of Alberta (1987)
6. Farouq Ali S.M., Islam, M.R., Kaleli, M.K., Yeung K. and Thomas, S., Mobility Control, AOSTRA Contract 438C, Final Report (1988)
7. Islam, M.R., and Farouq Ali, S.M., "Mobility Control in Waterflooding Oil Reservoirs With a Bottom-Water Zone," J. Can. Pet. Tech. (Nov-Dec. 1987) 40-53.
8. Islam, M.R., and Farouq Ali, S.M., "Waterflooding Oil Reservoirs With Bottom Water," Paper CIM 87-38-26, presented at the 38th Annual Technical Meeting of the CIM, Calgary (1987)
9. Islam, M.R., and Farouq Ali, S.M., "An Experimental and Numerical Study of Blocking of a Mobile Water Zone by an Emulsion," Paper 133 presented at the Fourth UNITAR/UNDP Conference on Heavy Crude and Tar Sands (1987)
10. Islam, M.R., and Farouq Ali, S.M., "The Use of Oil/Water Emulsion as a Blocking and Diverting Agent," Paper 5 Session 1, presented at the Advances in Petroleum Recovery and Upgrading Technology Conference (1987)
11. Bansbach, P.L., "The How and Why of Emulsions," Oil and Gas J. (Sept. 1970) 87-93.
12. Uzoigwe, A.C., and Marsden, S.S., "Emulsion Rheology and Flow Through Unconsolidated Synthetic Porous Media," Paper presented at the 45th Annual Fall Meeting of the Society of AIME, Houston, Texas (Oct. 4-7, 1970)
13. McAuliffe, C.D., "Oil-in-water Emulsions and their Flow Properties in Porous Media," J. Pet. Tech. (June 1973) 727-732.
14. McAuliffe, C.D., "Crude Oil-in-Water Emulsions to Improve Fluid Flow in an Oil Reservoir," J. Pet. Tech. (June 1973) 721-726.
15. Johnson, Jr., "Status of Caustic and Emulsion Methods," Soc. Pet. Eng. J. (Jan. 1976) 85-92.

16. Soo, H. and Radke, C.J., "The Flow Mechanism of Dilute, Stable Emulsions in Porous Media," Ind. Eng. Chem. Fund. (1984) 342-347.
17. Schmidt, D.P., Soo, H., and Radke, C.J., "Linear Oil Displacement by the Emulsion Entrapment Process," Soc. Pet. Eng. J. (June 1984) 351-360.
18. French, T.R., Broz, J.S., Lorenz, P.B., and Bertus, K.M., "Use of Emulsions for Mobility Control During Steamflooding," Paper presented at the 56th California Regional Meeting of the SPE, Oakland, CA (April 2-4 1986)
19. Farouq Ali S.M., Thomas, S., Khambharatana, F., Flow of Emulsions in Porous Media, AOSTRA Contract 493, Final Report (1988)
20. Alvarado, K.A., and Marsden Jr., S.S., "Flow of Oil-in-Water Emulsions Through Tubes and Porous Media," Soc. Pet. Eng. J. (Dec. 1979) 369-377.
21. Devereux, O.F., "Emulsion Flow in Porous Solids - I. A Flow Model," Chem. Eng. J. (1974) 121-128.
22. Soo, H., and Radke, C.J., "A Filtration Model for the Flow of Dilute, Stable Emulsions in Porous Media - I. Theory," Chem. Eng. Sci. (1986) 263-272.
23. Soo, H., Williams, M.C., and Radke, C.J., "A Filtration Model for the Flow of Dilute, Stable Emulsions in Porous Media - II. Parameter Evaluation and Estimation," Chem. Eng. Sci. (1986) 273-281.
24. Farouq Ali, S.M. and Abou-Kassem, "Modeling of Emulsion Flow in Porous Media," Paper presented at the International Technical Meeting of CIM/SPE, Calgary, (June 10-13 1990)
25. Abou-Kassem, J.H., and Farouq Ali, S.M., "Evaluation of Emulsion Flow in Porous Media," Submitted for publication to Soc. Pet. Eng. J. (1986)
26. Abou-Kassem, J.H., and Farouq Ali, S.M., "Mathematical Representation of Single-Phase Emulsion Flow in Porous Media," Submitted for publication to Soc. Pet. Eng. J. (1990)
27. Soo, H., Flow of Dilute, Stable Emulsions in Porous Media, Ph.D. Thesis, University of California, Berkely (1983)
28. Soo, H., and Radke, C.J., "Velocity Effects in Emulsion Flow Through Porous Media," J. Coll. Int. Sci. (1984) 462-476.
29. Warren, J.E. and Cosgrove, J.J., "Prediction of Waterflood Behavior in a Stratified System," Soc. Pet. Eng. J. (June 1964) 149-157, Trans., AIME, 149.
30. Root, P.J. and Skiba, F.F., "Crossflow Effects During an Idealized Displacement Process in a Stratified Reservoir," Soc. Pet. Eng. J. (Sept. 1965) Trans., AIME, 234.
31. Goddin, C.S. Jr., Craig, F.F. Jr., Wilkes J.O., Tek M.R., "A Numerical Study of Waterflood Performance In a Stratified System With Crossflow," J. Pet. Tech. (June 1966) 765-771, Trans., AIME, 237.

32. Silva, Luis, and Farouq Ali, S.M., "Waterflood Performance in the Presence of Communicating Strata and Formation Plugging," The Libyan Journal of Science, Vol. 3 (1973) 41-63.
33. Lambeth, N. and Dawe, R.A., "Viscous Effects for Miscible Displacements in Regular Heterogeneous Porous Media," Chem. Eng. Res. Des. (Jan. 1987) 52-62.
34. Russell, D.G. and Prats, M., "Performance of Layered Reservoirs With Crossflow - Single Compressible Fluid Case," Soc. Pet. Eng. J. (March 1962) Trans., AIME, 53.
35. Katz, M.L. and Tek, M.R., "Theoretical Study of Pressure Distribution and Fluid Flux in Bounded Stratified Porous Systems with Crossflow," Soc. Pet. Eng. J. (March 1962) Trans., AIME, 68.
36. Wright, R.J., Dawe, R.A. and Wall, C.G., "Surfactant Slug Displacement Efficiency in Reservoirs Tracer Studies in 2-D Layered Models," Proc 1981 European Symp on EOR, Bournemouth, UK 161-178.
37. Wright, R.J., Wheat, M.R. and Dawe, R.A., "Slug Size and Mobility Requirements for Chemically Enhanced Oil Recovery Within Heterogeneous Reservoirs," Soc. Pet. Eng. J. (Feb. 1987) 92-102.
38. Ahmed, G., Castanier, L.M. and Brigham, W. E., "An Experimental Study of Waterflooding From a Two-Dimensional Layered Sand Model," Soc. Pet. Eng. J. (Feb. 1988) 45-54.
39. El-Khatib, N., "The Effect of Crossflow on Waterflooding of Stratified Reservoirs," Soc. Pet. Eng. J. (April 1985) 291-302.
40. Rapoport, L.A. and Leas, W.J., "Properties of Linear Waterfloods," AIME (1953) 139-148.

11. APPENDIX A

Table A.1

PRODUCTION HISTORY FOR RUN 1

Porosity, $\phi = 37.1\%$
 $k_{abs} = 23.7 \mu\text{m}^2$
 $k_{wor} = 3.5 \mu\text{m}^2$
 $k_{owr} = 16.5 \mu\text{m}^2$
 IOIP = 1612 ml
 $S_{oi} = 0.934$

Sample No.	Sample Vol, ml	Oil Vol, ml	Oil Cut, %	Fluid Prod., HCPV	Inj. Press, kPa	WOR	Cum Oil Rec., % IOIP
1	100	100.0	100.0	0.062	124.02	0.0	6.20
2	100	100.0	100.0	0.124	108.52	0.0	12.41
3	100	100.0	100.0	0.186	97.15	0.0	18.61
4	100	100.0	100.0	0.248	91.29	0.0	24.81
5	100	100.0	100.0	0.310	79.92	0.0	31.02
6	100	100.0	100.0	0.372	66.14	0.0	37.22
7	100	79.0	79.0	0.434	61.67	0.3	42.12
8	100	31.5	31.5	0.496	60.29	2.2	44.08
9	100	22.0	22.0	0.558	56.50	3.5	45.44
10	100	21.0	21.0	0.620	52.02	3.8	46.74
11	100	17.5	17.5	0.682	48.23	4.7	47.83
12	104	16.5	15.8	0.747	44.78	5.3	48.85
13	107	15.0	14.0	0.814	44.10	6.1	49.78
14	100	12.0	12.0	0.876	44.10	7.3	50.53
15	100	11.0	11.0	0.938	43.75	8.1	51.21
16	100	11.0	11.0	1.000	42.37	8.1	51.89
17	100	11.0	11.0	1.062	40.65	8.1	52.57
18	100	11.0	11.0	1.124	38.58	8.1	53.26
19	100	11.0	11.0	1.186	37.89	8.1	53.94
20	100	10.5	10.5	1.248	36.86	8.5	54.59
21	100	10.0	10.0	1.310	36.86	9.0	55.21
22	100	9.0	9.0	1.372	36.52	10.1	55.77
23	100	8.0	8.0	1.434	35.83	11.5	56.27
24	100	8.0	8.0	1.496	34.79	11.5	56.76
25	100	7.5	7.5	1.558	33.76	12.3	57.23
26	100	7.0	7.0	1.620	33.07	13.3	57.66
27	100	6.5	6.5	1.682	29.63	14.4	58.06
28	500	23.0	4.6	1.992	17.22	20.7	59.49
29	1000	30.0	3.0	2.613	9.99	32.3	61.35

Table A.2

PRODUCTION HISTORY FOR RUN 2

Porosity, $\phi = 37.1\%$
 $k_{abs} = 23.7 \mu\text{m}^2$
 $k_{wor} = 3.5 \mu\text{m}^2$
 $k_{owr} = 16.5 \mu\text{m}^2$
 IOIP = 1612 ml
 $S_{oi} = 0.934$

Sample No.	Sample Vol, ml	Oil Vol, ml	Oil Cut, %	Fluid Prod., HCPV	Inj. Press, kPa	WOR	Cum Oil Rec., % IOIP
1	100	100.0	100.0	0.062	173.97	0.0	6.20
2	100	100.0	100.0	0.124	141.24	0.0	12.41
3	100	100.0	100.0	0.186	119.20	0.0	18.61
4	100	100.0	100.0	0.248	101.97	0.0	24.81
5	100	100.0	100.0	0.310	87.85	0.0	31.02
6	100	86.0	86.0	0.372	72.69	0.2	36.35
7	100	58.0	58.0	0.434	59.94	0.7	39.95
8	100	41.0	41.0	0.496	59.25	1.4	42.49
9	100	30.0	30.0	0.558	58.56	2.3	44.35
10	100	24.0	24.0	0.620	53.40	3.2	45.84
11	100	21.0	21.0	0.682	48.57	3.8	47.15
12	100	19.0	19.0	0.744	45.13	4.3	48.33
13	100	17.0	17.0	0.806	44.78	4.9	49.38
14	101	16.0	15.8	0.869	44.44	5.3	50.37
15	100	14.5	14.5	0.931	42.37	5.9	51.27
16	100	13.0	13.0	0.993	39.96	6.7	52.08
17	100	12.0	12.0	1.056	35.14	7.3	52.82
18	100	11.0	11.0	1.118	34.45	8.1	53.50
19	100	10.0	10.0	1.180	33.76	9.0	54.13
20	100	10.0	10.0	1.242	32.73	9.0	54.75
21	100	9.5	9.5	1.304	31.69	9.5	55.33
22	100	8.0	8.0	1.366	31.00	11.5	55.83
23	500	35.0	7.0	1.676	30.66	13.3	58.00
24	500	30.0	6.0	1.986	29.28	15.7	59.86
25	1000	42.0	4.2	2.606	24.11	22.8	62.47
26	500	22.0	4.4	2.917	14.81	21.7	63.83

Table A.3
PRODUCTION HISTORY FOR RUN 3

Porosity, $\phi = 36.9\%$
 $k_{abs} = 21.4 \mu\text{m}^2$
 $k_{owr} = 16.0 \mu\text{m}^2$
 IOIP = 1200 ml
 $S_{oi} = 0.932$
 Emulsion Slug Size = $0.50PV_{bw}$

Sample No.	Sample Vol, ml	Oil Vol, ml	Oil Cut, %	Fluid Prod., HCPV	Inj. Press, kPa	WOR	Cum Oil Rec., % IOIP
1	100	27.0	27.0	0.083	33.76	2.7	2.25
2	100	14.5	14.5	0.167	42.37	5.9	3.46
3	100	15.0	15.0	0.250	49.95	5.7	4.71
4	100	45.0	45.0	0.333	42.72	1.2	8.46
5	100	61.5	61.5	0.417	38.24	0.6	13.58
6	100	39.0	39.0	0.500	27.22	1.6	16.83
7	100	18.0	18.0	0.583	22.74	4.6	18.33
8	100	7.0	7.0	0.667	22.39	13.0	18.92
9	100	5.0	5.0	0.750	21.70	19.0	19.33
10	500	8.0	1.6	1.167	21.36	62.0	20.00
11	1000	15.0	1.5	2.000	21.01	66.0	21.25

Table A.4
PRODUCTION HISTORY FOR RUN 4

Porosity, $\phi = 36.8\%$
 $k_{abs} = 18.7 \mu\text{m}^2$
 $k_{owf} = 17.2 \mu\text{m}^2$
 IOIP = 1200 ml
 $S_{oi} = 0.935$
 Emulsion Slug Size = $1.00PV_{bw}$

Sample No.	Sample Vol, ml	Oil Vol, ml	Oil Cut, %	Fluid Prod., HCPV	Inj. Press, kPa	WOR	Cum Oil Rec., % IOIP
1	100	37.5	37.5	0.083	34.11	1.7	3.12
2	100	14.0	14.0	0.167	44.44	6.1	4.29
3	100	13.0	13.0	0.250	57.88	6.7	5.37
4	100	35.0	35.0	0.333	58.56	1.9	8.29
5	100	62.5	62.5	0.417	50.30	0.6	13.50
6	100	58.0	58.0	0.500	42.03	0.7	18.33
7	100	32.0	32.0	0.583	38.93	2.1	21.00
8	100	10.0	10.0	0.667	32.38	9.0	21.83
9	100	5.0	5.0	0.750	32.04	19.0	22.25
10	300	12.0	4.0	1.000	31.69	24.0	23.25
11	200	4.0	2.0	1.167	31.69	49.0	23.58
12	1000	10.0	1.0	2.000	31.00	99.0	24.42

Table A.5
PRODUCTION HISTORY FOR RUN 5

Porosity, $\phi = 37.0\%$
 $k_{abs} = 21.9 \mu\text{m}^2$
 $k_{owr} = 18.6 \mu\text{m}^2$
 IOIP = 1200 ml
 $S_{oi} = 0.930$
 Emulsion Slug Size = $2.00PV_{bw}$

Sample No.	Sample Vol, ml	Oil Vol, ml	Oil Cut, %	Fluid Prod., HCPV	Inj. Press, kPa	WOR	Cum Oil Rec., % IOIP
1	100	62.0	62.0	0.083	20.67	0.6	5.17
2	100	31.5	31.5	0.167	30.32	2.2	7.79
3	100	25.5	25.5	0.250	30.66	2.9	9.92
4	100	21.5	21.5	0.333	31.69	3.6	11.71
5	100	20.5	20.5	0.417	31.69	3.9	13.42
6	100	35.0	35.0	0.500	28.59	1.9	16.33
7	100	35.0	35.0	0.583	27.22	1.9	19.25
8	100	24.0	24.0	0.667	26.18	3.2	21.25
9	100	10.0	10.0	0.750	21.70	9.0	22.08
10	100	3.5	3.5	0.833	21.01	27.6	22.37
11	100	3.0	3.0	0.917	20.67	32.3	22.62
12	100	2.5	2.5	1.000	19.98	39.0	22.83
13	100	2.5	2.5	1.083	18.95	39.0	23.04
14	100	2.0	2.0	1.167	18.26	49.0	23.21
15	1000	10.0	1.0	2.000	17.91	99.0	24.04
16	1000	10.0	1.0	2.833	16.54	99.0	24.87

Table A.6
PRODUCTION HISTORY FOR RUN 6

Porosity, $\phi = 37.0\%$
 $k_{abs} = 18.0 \mu\text{m}^2$
 $k_{owr} = 16.1 \mu\text{m}^2$
 IOIP = 1200 ml
 $S_{oi} = 0.930$
 Emulsion Slug Size = $0.75PV_{bw}$

Sample No.	Sample Vol, ml	Oil Vol, ml	Oil Cut, %	Fluid Prod., HCPV	Inj. Press, kPa	WOR	Cum Oil Rec., % IOIP
1	100	58.0	58.0	0.083	30.66	0.7	4.83
2	100	34.0	34.0	0.167	38.24	1.9	7.67
3	100	30.0	30.0	0.250	37.89	2.3	10.17
4	100	37.0	37.0	0.333	41.00	1.7	13.25
5	100	57.0	57.0	0.417	37.55	0.8	18.00
6	100	41.0	41.0	0.500	36.17	1.4	21.42
7	100	23.0	23.0	0.583	33.76	3.3	23.33
8	100	11.0	11.0	0.667	29.28	8.1	24.25
9	100	6.0	6.0	0.750	25.84	15.7	24.75
10	100	4.0	4.0	0.833	25.49	24.0	25.08
11	100	3.0	3.0	0.917	25.15	32.3	25.33
12	100	2.0	2.0	1.000	24.80	49.0	25.50
13	500	10.0	2.0	1.417	24.11	49.0	26.33

Table A.7

PRODUCTION HISTORY FOR RUN 7

Porosity, $\phi = 36.0\%$
 $k_{abs} = 18.0 \mu\text{m}^2$
 $k_{ovr} = 13.4 \mu\text{m}^2$
 IOIP = 1163 ml
 $S_{oi} = 0.926$

Sample No.	Sample Vol., ml	Oil Vol., ml	Oil Cut., %	Fluid Prod., HCPV	Inj. Press., kPa	WOR	Cum Oil Rec., % IOIP
1	50	26.0	52.0	0.043	27.56	0.9	2.24
2	55	14.0	25.4	0.090	26.87	2.9	3.44
3	50	10.0	20.0	0.133	26.18	4.0	4.30
4	53	11.0	20.7	0.179	27.22	3.8	5.25
5	50	10.0	20.0	0.222	28.59	4.0	6.10
6	50	10.0	20.0	0.265	30.32	4.0	6.96
7	100	22.0	22.0	0.351	30.66	3.5	8.86
8	100	26.0	26.0	0.437	31.69	2.8	11.09
9	100	28.0	28.0	0.523	31.35	2.6	13.50
10	100	31.0	31.0	0.609	30.66	2.2	16.16
11	100	33.0	33.0	0.695	30.32	2.0	19.00
12	100	32.0	32.0	0.781	29.63	2.1	21.75
13	100	33.0	33.0	0.867	28.59	2.0	24.59
14	100	33.0	33.0	0.953	27.56	2.0	27.43
15	100	35.0	35.0	1.039	26.53	1.9	30.44
16	100	37.0	37.0	1.125	25.15	1.7	33.62
17	100	35.0	35.0	1.211	24.46	1.9	36.63
18	100	30.0	30.0	1.297	22.05	2.3	39.21
19	100	20.0	20.0	1.383	20.67	4.0	40.93
20	100	16.5	16.5	1.469	18.60	5.1	42.35
21	100	15.0	15.0	1.555	17.91	5.7	43.64
22	100	15.0	15.0	1.641	17.23	5.7	44.93
23	100	12.0	12.0	1.727	16.19	7.3	45.96
24	80	7.0	8.7	1.795	15.16	10.4	46.56
25	101	6.0	5.9	1.882	14.12	15.8	47.08
26	140	8.5	6.1	2.003	14.12	15.5	47.81
27	100	6.0	6.0	2.089	14.12	15.7	48.32
28	100	6.0	6.0	2.174	13.78	15.7	48.84
29	100	5.0	5.0	2.260	13.78	19.0	49.27
30	100	5.0	5.0	2.346	14.12	19.0	49.70
31	100	4.5	4.5	2.432	13.78	21.2	50.09
32	100	3.0	3.0	2.518	13.44	32.3	50.34
33	100	2.0	2.0	2.604	12.40	49.0	50.52
34	100	2.0	2.0	2.690	12.40	49.0	50.69
35	100	1.0	1.0	2.776	11.37	99.0	50.77
36	100	0.5	0.5	2.862	11.71	199.0	50.82
37	100	0.5	0.5	2.948	11.37	199.0	50.86
38	500	2.0	0.4	3.378	11.02	249.0	51.03

Table A.8
PRODUCTION HISTORY FOR RUN 8

Porosity, $\phi = 35.7\%$
 $k_{abs} = 17.5 \mu\text{m}^2$
 $k_{owr} = 12.3 \mu\text{m}^2$
 IOIP = 1162 ml
 $S_{oi} = 0.933$
 Emulsion Slug Size = 1.00PV_{bw}

Sample No.	Sample Vol., ml	Oil Vol., ml	Oil Cut., %	Fluid Prod., HCPV	Inj. Press., kPa	WOR	Cum Oil Rec., % IOIP
1	100	34.0	34.0	0.086	62.35	1.9	2.93
2	100	6.5	6.5	0.172	84.40	14.4	3.49
3	100	60.5	60.5	0.258	80.96	0.7	8.69
4	104	85.0	81.7	0.348	68.90	0.2	16.01
5	100	55.0	55.0	0.434	46.51	0.8	20.74
6	100	28.5	28.5	0.520	42.03	2.5	23.19
7	100	22.0	22.0	0.606	38.24	3.5	25.09
8	100	9.0	9.0	0.692	38.24	10.1	25.86
9	101	6.5	6.4	0.779	40.31	14.5	26.42
10	100	5.0	5.0	0.865	40.31	19.0	26.85
11	250	10.0	4.0	1.080	42.03	24.0	27.71
12	500	10.0	2.0	1.510	37.89	49.0	28.57

Table A.9

PRODUCTION HISTORY FOR RUN 3

Porosity, $\phi = 36.0\%$
 $k_{abs} = 18.5 \mu\text{m}^2$
 $k_{owf} = 16.1 \mu\text{m}^2$
 IOIP = 1170 ml
 $S_{wi} = 0.932$
 Emulsion Slug Size = $1.00PV_{bw}$

Sample No.	Sample Vol, ml	Oil Vol, ml	Oil Cut, %	Fluid Prod., HCPV	Inj. Press, kPa	WOR	Cum Oil Rec., % IOIP
1	50	15.0	30.0	0.043	36.52	2.3	1.28
2	50	10.0	20.0	0.085	37.89	4.0	2.14
3	50	5.0	10.0	0.128	38.93	9.0	2.56
4	50	5.0	10.0	0.171	45.47	9.0	2.99
5	50	9.0	18.0	0.214	50.64	4.6	3.76
6	50	18.0	36.0	0.256	54.43	1.8	5.30
7	50	21.5	43.0	0.299	54.78	1.3	7.14
8	50	23.5	47.0	0.342	46.85	1.1	9.15
9	51	21.0	41.2	0.385	48.92	1.4	10.94
10	51	18.0	35.3	0.429	34.45	1.8	12.48
11	100	31.0	31.0	0.515	33.76	2.2	15.13
12	100	22.0	22.0	0.600	29.97	3.5	17.01
13	109	20.0	18.3	0.693	26.53	4.4	18.72
14	100	14.0	14.0	0.779	28.94	6.1	19.91
15	100	11.0	11.0	0.864	22.39	8.1	20.85
16	100	6.0	6.0	0.950	20.67	15.7	21.37
17	100	5.0	5.0	1.035	19.64	19.0	21.79
18	100	5.0	5.0	1.121	24.11	19.0	22.22
19	100	4.5	4.5	1.206	18.95	21.2	22.61
20	100	4.5	4.5	1.291	19.64	21.2	22.99
21	100	4.0	4.0	1.377	18.95	24.0	23.33
22	100	4.0	4.0	1.462	18.95	24.0	23.68
23	100	3.5	3.5	1.548	19.29	27.6	23.97
24	100	2.5	2.5	1.633	19.64	39.0	24.19
25	100	2.5	2.5	1.719	19.64	39.0	24.40

Table A.10

PRODUCTION HISTORY FOR RUN 10

Porosity, $\phi = 35.9\%$
 $k_{abs} = 18.5 \mu\text{m}^2$
 $k_{owr} = 15.7 \mu\text{m}^2$
 IOIP = 1165 ml
 $S_{oi} = 0.931$
 Emulsion Slug Size = $1.00PV_{bw}$

Sample No.	Sample Vol., ml	Oil Vol., ml	Oil Cut., %	Fluid Prod., HCPV	Inj. Press., kPa	WOR	Cum Oil Rec., % IOIP
1	39	3.5	9.0	0.033	36.17	10.1	0.30
2	70	9.5	13.6	0.094	41.34	6.4	1.12
3	96	10.5	10.9	0.176	39.96	8.1	2.02
4	72	22.5	31.2	0.238	36.17	2.2	3.95
5	76	28.0	36.8	0.303	32.73	1.7	6.35
6	97	29.0	29.9	0.386	29.28	2.3	8.84
7	126	26.0	20.6	0.494	25.15	3.8	11.07
8	128	25.0	19.5	0.604	22.05	4.1	13.22
9	132	20.0	15.2	0.718	23.43	5.6	14.94
10	104	6.0	5.8	0.807	22.05	16.3	15.45
11	182	5.0	2.7	0.963	21.70	35.4	15.88
12	144	5.5	3.8	1.087	21.70	25.2	16.35
13	104	5.0	4.8	1.176	21.36	19.8	16.78
14	93	3.0	3.2	1.256	21.36	30.0	17.04

Table A.11

PRODUCTION HISTORY FOR RUN 11

Porosity, $\phi = 37.1\%$
 $k_{abs} = 21.3 \mu\text{m}^2$
 $k_{owr} = 15.9 \mu\text{m}^2$
 IOIP = 1200 ml
 $S_{oi} = 0.927$

Sample No.	Sample Vol., ml	Oil Vol., ml	Oil Cut., %	Fluid Prod., HCPV	Inj. Press., kPa	WOR	Cum Oil Rec., % IOIP
1	70	29.0	41.4	0.058	42.03	1.4	2.42
2	50	15.0	30.0	0.100	48.57	2.3	3.67
3	50	10.0	20.0	0.142	63.73	4.0	4.50
4	50	9.0	18.0	0.183	72.34	4.6	5.25
5	50	12.0	24.0	0.225	79.23	3.2	6.25
6	50	22.0	44.0	0.267	83.71	1.3	8.08
7	50	31.0	62.0	0.308	88.54	0.6	10.67
8	50	38.0	76.0	0.350	91.64	0.3	13.83
9	50	39.0	78.0	0.392	98.53	0.3	17.08
10	50	38.0	76.0	0.433	105.07	0.3	20.25
11	100	75.0	75.0	0.517	111.27	0.3	26.50
12	100	76.0	76.0	0.600	115.06	0.3	32.83
13	100	76.0	76.0	0.683	115.06	0.3	39.17
14	100	85.0	85.0	0.767	121.26	0.2	46.25
15	250	220.0	88.0	0.975	126.78	0.1	64.58
16	500	490.0	98.0	1.392	127.46	0.0	105.42

Table A.12

PRODUCTION HISTORY FOR RUN 12

Porosity, $\phi = 36.3\%$ $k_{abs} = 20.0 \mu\text{m}^2$ $k_{owr} = 16.0 \mu\text{m}^2$

IOIP = 1180 ml

 $S_{oi} = 0.932$

Sample No.	Sample Vol, ml	Oil Vol, ml	Oil Cut, %	Fluid Prod., HCPV	Inj. Press, kPa	WOR	Cum Oil Rec., % IOIP
1	50	20.0	40.0	0.042	26.87	1.5	1.69
2	50	12.0	24.0	0.085	23.77	3.2	2.71
3	50	9.0	18.0	0.127	25.84	4.6	3.47
4	50	8.0	16.0	0.169	25.15	5.2	4.15
5	52	9.0	17.3	0.214	28.94	4.8	4.92
6	50	9.0	18.0	0.256	28.94	4.6	5.68
7	100	20.0	20.0	0.341	29.97	4.0	7.37
8	100	22.0	22.0	0.425	31.01	3.5	9.24
9	100	25.0	25.0	0.510	31.35	3.0	11.36
10	100	30.0	30.0	0.595	31.35	2.3	13.90
11	100	34.0	34.0	0.680	30.66	1.9	16.78
12	100	33.0	33.0	0.764	29.97	2.0	19.58
13	100	33.0	33.0	0.849	28.94	2.0	22.37
14	100	34.0	34.0	0.934	28.94	1.9	25.25
15	100	33.0	33.0	1.019	28.94	2.0	28.05
16	100	35.0	35.0	1.103	28.59	1.9	31.02
17	100	34.0	34.0	1.188	28.94	1.9	33.90
18	100	34.0	34.0	1.273	27.56	1.9	36.78
19	100	27.0	27.0	1.358	25.84	2.7	39.07
20	100	20.0	20.0	1.442	22.05	4.0	40.76
21	100	16.0	16.0	1.527	20.67	5.2	42.12
22	100	13.0	13.0	1.612	18.95	6.7	43.22
23	100	10.0	10.0	1.697	17.23	9.0	44.07
24	100	6.0	6.0	1.781	15.85	15.7	44.58
25	100	6.0	6.0	1.866	15.50	15.7	45.08
26	100	6.0	6.0	1.951	14.47	15.7	45.59
27	110	7.0	6.4	2.044	14.47	14.7	46.19
28	100	6.0	6.0	2.163	14.47	15.7	46.69
29	100	6.0	6.0	2.247	14.12	15.7	47.20
30	100	6.0	6.0	2.332	13.78	15.7	47.71
31	100	5.0	5.0	2.417	13.78	19.0	48.14
32	100	4.5	4.5	2.502	13.78	21.2	48.52
33	100	3.0	3.0	2.586	13.09	32.3	48.77
34	100	2.5	2.5	2.671	12.75	39.0	48.98

Table A.13

PRODUCTION HISTORY FOR RUN 13

Porosity, $\phi = 35.5\%$
 $k_{abs} = 18.2 \mu\text{m}^2$
 $k_{ovr} = 13.5 \mu\text{m}^2$
 IOIP = 1153 ml
 $S_{oi} = 0.931$
 Emulsion Slug Size = $1.00PV_{bw}$

Sample No.	Sample Vol., ml	Oil Vol., ml	Oil Cut., %	Fluid Prod., HCPV	Inj. Press., kPa	WOR	Cum Oil Rec., % IOIP
1	50	17.0	34.0	0.043	32.73	1.9	1.47
2	50	9.0	18.0	0.087	30.66	4.6	2.25
3	50	2.0	4.0	0.130	33.07	24.0	2.43
4	50	2.0	4.0	0.173	35.14	24.0	2.60
5	50	2.0	4.0	0.217	39.62	24.0	2.78
6	50	9.0	18.0	0.260	42.37	4.6	3.56
7	50	29.0	58.0	0.304	43.06	0.7	6.07
8	60	37.0	61.7	0.356	35.83	0.6	9.78
9	100	61.0	61.0	0.442	30.66	0.6	14.57
10	100	59.0	59.0	0.529	25.15	0.7	19.69
11	105	45.0	42.9	0.620	22.05	1.3	23.59
12	100	31.0	31.0	0.707	20.67	2.2	26.28
13	100	27.0	27.0	0.794	20.33	2.7	28.62
14	100	25.0	25.0	0.880	19.64	3.0	30.79
15	100	17.0	17.0	0.967	19.29	4.9	32.26
16	100	13.0	13.0	1.054	18.95	6.7	33.39
17	42	5.0	11.9	1.090	18.60	7.4	33.82
18	100	11.0	11.0	1.177	18.60	8.1	34.78
19	244	18.0	7.4	1.389	18.26	12.6	36.34
20	510	38.0	7.5	1.831	17.91	12.4	39.64
21	500	24.0	4.8	2.265	16.88	19.8	41.72
22	500	22.0	4.4	2.698	15.50	21.7	43.63
23	500	15.0	3.0	3.132	13.78	32.3	44.93

Table A.14
PRODUCTION HISTORY FOR RUN 14

Porosity, $\phi = 35.4\%$
 $k_{abs} = 17.8 \mu\text{m}^2$
 $k_{owr} = 13.2 \mu\text{m}^2$
 IOIP = 1150 ml
 $S_{oi} = 0.931$

Sample No.	Sample Vol., ml	Oil Vol., ml	Oil Cut., %	Fluid Prod., HCPV	Inj. Press., kPa	WOR	Cum Oil Rec., % IOIP
1	50	17.0	34.0	0.043	29.97	1.9	1.48
2	50	15.0	30.0	0.087	29.97	2.3	2.78
3	50	16.0	32.0	0.130	30.32	2.1	4.17
4	50	19.0	38.0	0.174	31.00	1.6	5.83
5	50	27.0	54.0	0.217	30.32	0.9	8.17
6	50	29.0	5	0.261	28.94	0.7	10.70
7	100	60.0	60.0	0.348	25.49	0.7	15.91
8	100	67.0	67.0	0.435	22.05	0.5	21.74
9	100	60.0	60.0	0.522	18.60	0.7	26.96
10	100	37.0	37.0	0.609	16.88	1.7	30.17
11	105	23.0	21.9	0.700	14.12	3.6	32.17
12	100	14.0	14.0	0.787	12.40	6.1	33.39
13	100	5.0	5.0	0.874	11.37	19.0	33.83
14	100	2.0	2.0	0.961	10.68	49.0	34.00
15	210	4.0	1.9	1.143	9.99	51.5	34.35

Table A.15

PRODUCTION HISTORY FOR RUN 15

Porosity, $\phi = 35.2\%$
 $k_{abs} = 18.5 \mu\text{m}^2$
 $k_{owr} = 16.7 \mu\text{m}^2$
 IOIP = 1150 ml
 $S_{oi} = 0.937$
 Emulsion Slug Size = $1.00PV_{bw}$

Sample No.	Sample Vol., ml	Oil Vol., ml	Oil Cut, %	Fluid Prod., HCPV	Inj. Press., kPa	WOR	Cum Oil Rec., % IOIP
1	50	22.0	44.0	0.043	33.42	1.3	1.91
2	52	12.0	23.1	0.089	37.55	3.3	2.96
3	50	9.0	18.0	0.132	40.65	4.6	3.74
4	50	8.0	16.0	0.176	41.34	5.2	4.43
5	51	10.0	19.6	0.220	43.06	4.1	5.30
6	50	20.0	40.0	0.263	44.78	1.5	7.04
7	50	30.0	60.0	0.307	41.34	0.7	9.65
8	100	62.0	62.0	0.394	38.24	0.6	15.04
9	100	62.0	62.0	0.481	31.69	0.6	20.43
10	100	50.0	50.0	0.568	26.18	1.0	24.78
11	100	33.0	33.0	0.655	23.08	2.0	27.65
12	100	25.0	25.0	0.742	20.67	3.0	29.83
13	100	22.0	22.0	0.829	19.29	3.5	31.74
14	100	18.0	18.0	0.916	18.95	4.6	33.30
15	104	18.0	17.3	1.006	16.88	4.8	34.87
16	108	18.0	16.7	1.100	15.50	5.0	36.43
17	100	16.0	16.0	1.187	13.78	5.2	37.83
18	100	14.0	14.0	1.274	13.78	6.1	39.04
19	100	12.0	12.0	1.361	13.09	7.3	40.09
20	100	11.0	11.0	1.448	12.40	8.1	41.04
21	100	10.0	10.0	1.535	12.40	9.0	41.91
22	100	8.0	8.0	1.622	11.02	11.5	42.61
23	100	8.0	8.0	1.709	11.02	11.5	43.30
24	100	7.0	7.0	1.796	10.68	13.3	43.91
25	100	7.0	7.0	1.883	10.68	13.3	44.52
26	500	25.0	5.0	2.317	10.33	19.0	46.70
27	500	20.0	4.0	2.752	8.27	24.0	48.43
28	500	15.0	3.0	3.187	7.92	32.3	49.74

Table A.16

PRODUCTION HISTORY FOR RUN 16

Porosity, $\phi = 35.7\%$
 $k_{abs} = 18.9 \mu\text{m}^2$
 $k_{owr} = 15.9 \mu\text{m}^2$
 IOIP = 1155 ml
 $S_{oi} = 0.928$
 Emulsion Slug Size = 1.00PV_{bw}

Sample No.	Sample Vol, ml	Oil Vol, ml	Oil Cut, %	Fluid Prod., HCPV	Inj. Press, kPa	WOR	Cum Oil Rec., % IOIP
1	50	26.0	52.0	0.043	23.08	0.9	2.25
2	50	15.0	30.0	0.087	27.56	2.3	3.55
3	60	12.0	20.0	0.139	30.66	4.0	4.59
4	50	10.0	20.0	0.182	32.04	4.0	5.45
5	50	12.0	24.0	0.225	34.45	3.2	6.49
6	50	28.0	56.0	0.268	33.76	0.8	8.92
7	50	31.0	62.0	0.312	32.04	0.6	11.60
8	100	62.0	62.0	0.398	28.59	0.6	16.97
9	100	58.0	58.0	0.485	24.46	0.7	21.99
10	100	54.0	54.0	0.571	22.74	0.9	26.67
11	100	36.0	36.0	0.658	18.60	1.8	29.78
12	100	29.0	29.0	0.745	15.50	2.4	32.29
13	100	24.0	24.0	0.831	14.47	3.2	34.37
14	100	21.0	21.0	0.918	13.78	3.8	36.19
15	100	20.0	20.0	1.004	14.12	4.0	37.92
16	100	16.0	16.0	1.091	13.44	5.2	39.31
17	100	15.0	15.0	1.177	14.12	5.7	40.61
18	100	13.0	13.0	1.264	14.12	6.7	41.73
19	100	12.5	12.5	1.351	13.78	7.0	42.81
20	100	17.0	17.0	1.437	11.71	4.9	44.29
21	100	13.5	13.5	1.524	11.37	6.4	45.45
22	100	11.0	11.0	1.610	11.02	8.1	46.41
23	100	11.0	11.0	1.697	11.02	8.1	47.36
24	100	10.0	10.0	1.784	10.33	9.0	48.23
25	100	10.0	10.0	1.870	10.33	9.0	49.09
26	100	10.0	10.0	1.957	10.33	9.0	49.96
27	500	55.0	11.0	2.390	10.33	8.1	54.72
28	500	45.0	9.0	2.823	9.65	10.1	58.61
29	500	40.0	8.0	3.255	8.61	11.5	62.08
30	500	30.0	6.0	3.688	8.27	15.7	64.68
31	500	15.0	3.0	4.121	8.27	32.3	65.97

Table A.17

PRODUCTION HISTORY FOR RUN 17

Porosity, $\phi = 35.6\%$
 $k_{abs} = 18.4 \mu\text{m}^2$
 $k_{owr} = 14.5 \mu\text{m}^2$
 IOIP = 1155 ml
 $S_{oi} = 0.930$
 Emulsion Slug Size = $1.00PV_{bw}$

Sample No.	Sample Vol, ml	Oil Vol, ml	Oil Cut, %	Fluid Prod., HCPV	Inj. Press, kPa	WOR	Cum Oil Rec., % IOIP
1	50	20.0	40.0	0.043	23.77	1.5	1.73
2	50	10.0	20.0	0.087	28.94	4.0	2.60
3	50	8.0	16.0	0.130	32.73	5.2	3.29
4	50	9.0	18.0	0.173	34.45	4.6	4.07
5	50	18.0	36.0	0.216	36.52	1.8	5.63
6	50	32.0	64.0	0.260	35.14	0.6	8.40
7	50	31.0	62.0	0.303	32.73	0.6	11.08
8	100	62.0	62.0	0.390	31.00	0.6	16.45
9	100	63.0	63.0	0.476	25.49	0.6	21.90
10	100	48.0	48.0	0.563	20.67	1.1	26.06
11	100	32.0	32.0	0.649	18.26	2.1	28.83
12	100	27.0	27.0	0.736	17.22	2.7	31.17
13	105	25.0	23.8	0.827	15.85	3.2	33.33
14	100	20.0	20.0	0.913	15.50	4.0	35.05
15	101	19.0	18.8	1.001	14.12	4.3	36.71
16	100	16.0	16.0	1.087	14.12	5.2	38.10
17	100	15.0	15.0	1.174	14.12	5.7	39.39
18	100	13.0	13.0	1.261	13.44	6.7	40.52
19	100	12.0	12.0	1.347	12.75	7.3	41.56
20	100	12.0	12.0	1.434	12.75	7.3	42.60
21	100	11.0	11.0	1.520	12.40	8.1	43.55
22	100	11.0	11.0	1.607	11.71	8.1	44.50
23	250	26.0	10.4	1.823	10.33	8.6	46.75
24	250	24.0	9.6	2.040	10.33	9.4	48.83
25	500	40.0	8.0	2.473	10.33	11.5	52.29
26	500	33.0	6.6	2.906	10.33	14.2	55.15
27	500	30.0	6.0	3.339	10.33	15.7	57.75
28	500	25.0	5.0	3.771	9.99	19.0	59.91
29	500	10.0	2.0	4.204	8.96	49.0	60.78
30	500	10.0	2.0	4.637	7.58	49.0	61.65

Table A.18

PRODUCTION HISTORY FOR RUN 18

Porosity, $\phi = 35.5\%$
 $k_{abs} = 19.3 \mu\text{m}^2$
 $k_{owr} = 16.1 \mu\text{m}^2$
 IOIP = 1155 ml
 $S_{oi} = 0.933$
 Emulsion Slug Size = $1.00PV_{bw}$

Sample No.	Sample Vol, ml	Oil Vol, ml	Oil Cut, %	Fluid Prod., HCPV	Inj. Press, kPa	WOR	Cum Oil Rec., % IOIP
1	50	20.0	40.0	0.043	22.05	1.5	1.73
2	50	14.0	28.0	0.087	26.87	2.6	2.94
3	50	10.0	20.0	0.130	29.28	4.0	3.81
4	50	12.0	24.0	0.173	31.00	3.2	4.85
5	50	16.0	32.0	0.216	32.73	2.1	6.23
6	55	30.0	54.5	0.264	33.07	0.8	8.83
7	50	31.0	62.0	0.307	31.69	0.6	11.52
8	100	61.0	61.0	0.394	29.63	0.6	16.80
9	100	59.0	59.0	0.481	25.84	0.7	21.90
10	100	50.0	50.0	0.567	23.77	1.0	26.23
11	100	35.0	35.0	0.654	22.39	1.9	29.26
12	100	28.0	28.0	0.740	20.67	2.6	31.69
13	100	24.0	24.0	0.827	20.33	3.2	33.77
14	100	21.0	21.0	0.913	18.95	3.8	35.58
15	100	20.0	20.0	1.000	18.60	4.0	37.32
16	100	18.0	18.0	1.087	17.91	4.6	38.87
17	105	16.0	15.2	1.177	16.88	5.6	40.26
18	100	14.0	14.0	1.264	16.88	6.1	41.47
19	100	13.0	13.0	1.351	15.50	6.7	42.60
20	100	12.0	12.0	1.437	15.16	7.3	43.64
21	100	12.0	12.0	1.524	15.50	7.3	44.68
22	100	11.0	11.0	1.610	14.81	8.1	45.63
23	100	11.0	11.0	1.697	14.81	8.1	46.58
24	100	10.0	10.0	1.784	14.47	9.0	47.45
25	100	10.0	10.0	1.870	14.47	9.0	48.31
26	100	10.0	10.0	1.957	14.47	9.0	49.18
27	500	40.0	8.0	2.390	14.12	11.5	52.64
28	500	35.0	7.0	2.823	14.12	13.3	55.67
29	500	30.0	6.0	3.255	14.12	15.7	58.27
30	500	20.0	4.0	3.688	14.12	24.0	60.00
31	500	10.0	2.0	4.121	14.12	49.0	60.87

Table A.19

PRODUCTION HISTORY FOR RUN 19

Porosity, $\phi = 35.3\%$
 $k_{abs} = 19.0 \mu\text{m}^2$
 $k_{owr} = 15.5 \mu\text{m}^2$
 IOIP = 1150 ml
 $S_{oi} = 0.934$
 Emulsion Slug Size = 1.00PV_{bw}

Sample No.	Sample Vol., ml	Oil Vol., ml	Oil Cut., %	Fluid Prod., HCPV	Inj. Press., kPa	WOR	Cum Oil Rec., % IOIP
1	50	22.0	44.0	0.043	22.39	1.3	1.91
2	50	9.0	18.0	0.087	29.63	4.6	2.70
3	50	7.0	14.0	0.130	33.07	6.1	3.30
4	50	10.0	20.0	0.174	33.76	4.0	4.17
5	50	16.0	32.0	0.217	35.48	2.1	5.57
6	50	28.0	56.0	0.261	33.76	0.8	8.00
7	55	32.0	58.2	0.309	32.73	0.7	10.78
8	100	62.0	62.0	0.396	29.28	0.6	16.17
9	100	61.0	61.0	0.483	24.80	0.6	21.48
10	100	45.0	45.0	0.570	22.39	1.2	25.39
11	100	30.0	30.0	0.657	21.70	2.3	28.00
12	100	26.0	26.0	0.743	20.33	2.8	30.26
13	100	25.0	25.0	0.830	19.29	3.0	32.43
14	100	20.0	20.0	0.917	18.95	4.0	34.17
15	100	20.0	20.0	1.004	18.95	4.0	35.91
16	100	15.0	15.0	1.091	18.60	5.7	37.22
17	100	15.0	15.0	1.178	18.26	5.7	38.52
18	100	12.0	12.0	1.265	16.54	7.3	39.57
19	100	12.0	12.0	1.352	16.19	7.3	40.61
20	100	11.0	11.0	1.439	15.50	8.1	41.57
21	100	11.0	11.0	1.526	15.16	8.1	42.52
22	100	10.0	10.0	1.613	15.16	9.0	43.39
23	250	25.0	10.0	1.830	15.16	9.0	45.57
24	250	20.0	8.0	2.048	14.81	11.5	47.30
25	500	30.0	6.0	2.483	14.47	15.7	49.91
26	500	30.0	6.0	2.917	14.81	15.7	52.52
27	500	20.0	4.0	3.352	14.47	24.0	54.26
28	500	15.0	3.0	3.787	14.47	32.3	55.57
29	500	10.0	2.0	4.222	14.12	49.0	56.43

Table A.20

PRODUCTION HISTORY FOR RUN 20

Porosity, $\phi = 35.7\%$
 $k_{abs} = 19.0 \mu\text{m}^2$
 $k_{owr} = 15.4 \mu\text{m}^2$
 IOIP = 1162 ml
 $S_{oi} = 0.933$

Sample No.	Sample Vol, ml	Oil Vol, ml	Oil Cut, %	Fluid Prod., HCPV	Inj. Press, kPa	WOR	Cum Oil Rec., % IOIP
1	50	15.0	30.0	0.043	26.53	2.3	1.29
2	50	10.0	20.0	0.086	26.87	4.0	2.15
3	50	8.0	16.0	0.129	27.90	5.2	2.84
4	50	7.0	14.0	0.172	29.28	6.1	3.44
5	50	9.0	18.0	0.215	29.28	4.6	4.22
6	50	10.0	20.0	0.258	30.32	4.0	5.08
7	100	20.0	20.0	0.344	30.66	4.0	6.80
8	100	23.0	23.0	0.430	30.66	3.3	8.78
9	100	25.0	25.0	0.516	30.32	3.0	10.93
10	100	31.0	31.0	0.602	29.28	2.2	13.60
11	100	31.0	31.0	0.688	28.94	2.2	16.26
12	100	30.0	30.0	0.774	28.25	2.3	18.85
13	100	30.0	30.0	0.861	26.53	2.3	21.43
14	100	33.0	33.0	0.947	24.80	2.0	24.27
15	100	32.0	32.0	1.033	24.46	2.1	27.02
16	100	33.0	33.0	1.119	21.70	2.0	29.86
17	100	32.0	32.0	1.205	21.36	2.1	32.62
18	100	31.0	31.0	1.291	17.91	2.2	35.28
19	100	23.0	23.0	1.377	17.91	3.3	37.26
20	100	18.0	18.0	1.463	17.23	4.6	38.81
21	100	14.0	14.0	1.549	16.54	6.1	40.02
22	100	13.0	13.0	1.635	15.50	6.7	41.14
23	100	12.0	12.0	1.721	14.81	7.3	42.17
24	100	9.0	9.0	1.807	14.47	10.1	42.94
25	100	8.0	8.0	1.893	14.12	11.5	43.63
26	100	8.0	8.0	1.979	14.12	11.5	44.32
27	100	6.0	6.0	2.065	13.44	15.7	44.84
28	100	5.0	5.0	2.151	13.44	19.0	45.27
29	100	5.0	5.0	2.237	13.44	19.0	45.70
30	250	10.0	4.0	2.453	12.06	24.0	46.56
31	250	10.0	4.0	2.668	11.71	24.0	47.42
32	500	15.0	3.0	3.098	11.02	32.3	48.71
33	500	10.0	2.0	3.528	11.02	49.0	49.57

Table A.21

PRODUCTION HISTORY FOR RUN 21

Porosity, $\phi = 35.9\%$ $k_{abs} = 19.5 \mu\text{m}^2$ $k_{owr} = 15.8 \mu\text{m}^2$

IOIP = 1550 ml

 $S_{oi} = 0.928$

Sample No.	Sample Vol, ml	Oil Vol, ml	Oil Cut, %	Fluid Prod., HCPV	Inj. Press, kPa	WOR	Cum Oil Rec., % IOIP
1	100	100.0	100.0	0.065	86.12	0.0	6.45
2	100	100.0	100.0	0.129	79.58	0.0	12.90
3	100	100.0	100.0	0.194	71.31	0.0	19.35
4	100	100.0	100.0	0.258	62.35	0.0	25.81
5	100	100.0	100.0	0.323	53.74	0.0	32.26
6	100	83.0	83.0	0.387	38.58	0.2	37.61
7	100	40.0	40.0	0.452	36.52	1.5	40.19
8	100	28.0	28.0	0.516	33.76	2.6	42.00
9	100	15.0	15.0	0.581	31.00	5.7	42.97
10	100	5.0	5.0	0.645	28.94	19.0	43.29
11	100	2.0	2.0	0.710	26.53	49.0	43.42
12	100	1.0	1.0	0.774	25.49	99.0	43.48
13	100	0.5	0.5	0.839	25.49	199.0	43.52
14	100	0.5	0.5	0.903	25.49	199.0	43.55
15	100	0.5	0.5	0.968	25.49	199.0	43.58
16	100	0.5	0.5	1.032	25.49	199.0	43.61

Table A.22

PRODUCTION HISTORY FOR RUN 22

Porosity, $\phi = 35.0\%$ $k_{abs} = 19.1 \mu\text{m}^2$ $k_{owr} = 15.3 \mu\text{m}^2$

IOIP = 1500 ml

 $S_{o1} = 0.922$

Sample No.	Sample Vol., ml	Oil Vol., ml	Oil Cut., %	Fluid Prod., HCPV	Inj. Press., kPa	WOR	Cum Oil Rec., % IOIP
1	100	100.0	100.0	0.067	88.19	0.0	6.67
2	100	100.0	100.0	0.133	77.86	0.0	13.33
3	100	100.0	100.0	0.200	69.93	0.0	20.00
4	100	100.0	100.0	0.267	66.49	0.0	26.67
5	100	100.0	100.0	0.333	52.71	0.0	33.33
6	100	100.0	100.0	0.400	44.10	0.0	40.00
7	100	72.0	72.0	0.467	37.89	0.4	44.80
8	100	36.0	36.0	0.533	33.76	1.8	47.20
9	100	30.0	30.0	0.600	32.73	2.3	49.20
10	100	19.0	19.0	0.667	31.69	4.3	50.47
11	100	11.0	11.0	0.733	31.35	8.1	51.20
12	100	10.0	10.0	0.800	29.63	9.0	51.87
13	104	10.0	9.6	0.869	29.28	9.4	52.53
14	100	10.0	10.0	0.936	28.94	9.0	53.20
15	100	8.0	8.0	1.003	28.59	11.5	53.73
16	100	7.0	7.0	1.069	28.25	13.3	54.20
17	100	6.0	6.0	1.136	25.15	15.7	54.60
18	250	12.0	4.8	1.303	24.80	19.8	55.40
19	250	12.0	4.8	1.469	23.43	19.8	56.20
20	500	25.0	5.0	1.803	23.08	19.0	57.87
21	500	20.0	4.0	2.136	23.08	24.0	59.20
22	500	15.0	3.0	2.469	23.08	32.3	60.20

Table A.23

PRODUCTION HISTORY FOR RUN 23

Porosity, $\phi = 35.1\%$
 $k_{abs} = 19.3 \mu\text{m}^2$
 $k_{owr} = 15.5 \mu\text{m}^2$
 IOIP = 1520 ml
 $S_{oi} = 0.931$

Sample No.	Sample Vol., ml	Oil Vol., ml	Oil Cut., %	Fluid Prod., HCPV	Inj. Press., kPa	WOR	Cum Oil Rec., % IOIP
1	100	100.0	100.0	0.066	99.22	0.0	6.58
2	100	100.0	100.0	0.132	86.81	0.0	13.16
3	100	100.0	100.0	0.197	76.13	0.0	19.74
4	100	100.0	100.0	0.263	66.49	0.0	26.32
5	100	100.0	100.0	0.329	56.84	0.0	32.89
6	100	100.0	100.0	0.395	47.20	0.0	39.47
7	100	76.0	76.0	0.461	38.24	0.3	44.47
8	100	38.0	38.0	0.526	34.79	1.6	46.97
9	100	32.0	32.0	0.592	33.42	2.1	49.08
10	100	29.0	29.0	0.658	33.42	2.4	50.99
11	102	27.0	26.5	0.725	32.38	2.8	52.76
12	100	25.0	25.0	0.791	32.04	3.0	54.41
13	107	22.0	20.6	0.861	30.66	3.9	55.86
14	100	20.0	20.0	0.927	29.63	4.0	57.17
15	100	17.0	17.0	0.993	29.28	4.9	58.29
16	100	15.0	15.0	1.059	28.25	5.7	59.28
17	100	15.0	15.0	1.124	27.22	5.7	60.26
18	100	12.0	12.0	1.190	26.53	7.3	61.05
19	100	11.0	11.0	1.256	25.84	8.1	61.78
20	100	10.0	10.0	1.322	25.15	9.0	62.43
21	100	9.0	9.0	1.387	24.11	10.1	63.03
22	100	9.0	9.0	1.453	23.08	10.1	63.62
23	500	40.0	8.0	1.782	23.08	11.5	66.25
24	500	35.0	7.0	2.111	22.39	13.3	68.55
25	500	25.0	5.0	2.440	22.05	19.0	70.20
26	500	20.0	4.0	2.769	22.05	24.0	71.51
27	500	15.0	3.0	3.098	22.05	32.3	72.50

Table A.24

PRODUCTION HISTORY FOR RUN 24

Porosity, $\phi = 35.8\%$
 $k_{abs} = 19.3 \mu\text{m}^2$
 $k_{owr} = 16.2 \mu\text{m}^2$
 IOIP = 1165 ml
 $S_{oi} = 0.933$
 Emulsion Slug Size = $1.00PV_{bw}$

Sample No.	Sample Vol, ml	Oil Vol, ml	Oil Cut, %	Fluid Prod., HCPV	Inj. Press, kPa	WOR	Cum Oil Rec., % IOIP
1	50	25.0	50.0	0.043	20.67	1.0	2.15
2	50	17.0	34.0	0.086	25.84	1.9	3.61
3	50	13.0	26.0	0.129	28.25	2.8	4.72
4	50	9.0	18.0	0.172	31.00	4.6	5.49
5	50	12.0	24.0	0.215	33.76	3.2	6.52
6	50	28.0	56.0	0.258	34.11	0.8	8.93
7	50	32.0	64.0	0.300	32.73	0.6	11.67
8	100	61.0	61.0	0.386	29.63	0.6	16.91
9	100	59.0	59.0	0.472	28.25	0.7	21.97
10	100	55.0	55.0	0.558	24.80	0.8	26.70
11	100	35.0	35.0	0.644	19.29	1.9	29.70
12	100	30.0	30.0	0.730	16.88	2.3	32.27
13	100	25.0	25.0	0.815	15.85	3.0	34.42
14	100	22.0	22.0	0.901	14.47	3.5	36.31
15	100	21.0	21.0	0.987	13.44	3.8	38.11
16	100	17.0	17.0	1.073	13.44	4.9	39.57
17	100	15.0	15.0	1.159	13.44	5.7	40.86
18	100	14.0	14.0	1.245	13.78	6.1	42.06
19	100	13.0	13.0	1.330	13.09	6.7	43.18
20	100	13.0	13.0	1.416	13.09	6.7	44.29
21	100	13.0	13.0	1.502	12.40	6.7	45.41
22	100	12.0	12.0	1.588	11.02	7.3	46.44
23	100	12.0	12.0	1.674	11.02	7.3	47.47
24	100	11.0	11.0	1.760	10.68	8.1	48.41
25	100	11.0	11.0	1.845	10.68	8.1	49.36
26	100	10.0	10.0	1.931	10.33	9.0	50.21
27	250	30.0	12.0	2.146	10.68	7.3	52.79
28	250	25.0	10.0	2.361	9.99	9.0	54.94
29	250	25.0	10.0	2.575	9.99	9.0	57.08
30	250	20.0	8.0	2.790	9.65	11.5	58.80
31	500	40.0	8.0	3.219	9.30	11.5	62.23
32	500	30.0	6.0	3.648	8.61	15.7	64.81
33	500	15.0	3.0	4.077	8.61	32.3	66.09

Table A.25

PRODUCTION HISTORY FOR RUN 25

Porosity, $\phi = 35.5\%$
 $k_{abs} = 19.0 \mu\text{m}^2$
 $k_{owr} = 15.4 \mu\text{m}^2$
 IOIP = 1155 ml
 $S_{oi} = 0.933$
 Emulsion Slug Size = $1.00PV_{bw}$

Sample No.	Sample Vol, ml	Oil Vol, ml	Oil Cut, %	Fluid Prod., HCPV	Inj. Press, kPa	WOR	Cum Oil Rec., % IOIP
1	50	22.0	44.0	0.043	22.74	1.3	1.90
2	50	15.0	30.0	0.087	27.22	2.3	3.20
3	50	11.0	22.0	0.130	30.66	3.5	4.16
4	50	12.0	24.0	0.173	31.69	3.2	5.19
5	50	16.0	32.0	0.216	34.11	2.1	6.58
6	50	29.0	58.0	0.260	33.07	0.7	9.09
7	50	32.0	64.0	0.303	31.35	0.6	11.86
8	100	62.0	62.0	0.390	30.66	0.6	17.23
9	100	60.0	60.0	0.476	29.28	0.7	22.42
10	100	53.0	53.0	0.563	24.80	0.9	27.01
11	100	34.0	34.0	0.649	23.43	1.9	29.96
12	100	27.0	27.0	0.736	22.39	2.7	32.29
13	100	25.0	25.0	0.823	19.64	3.0	34.46
14	100	20.0	20.0	0.909	18.95	4.0	36.19
15	100	20.0	20.0	0.996	18.26	4.0	37.92
16	100	19.0	19.0	1.082	17.91	4.3	39.57
17	105	16.0	15.2	1.173	16.88	5.6	40.95
18	100	15.0	15.0	1.260	16.54	5.7	42.25
19	100	13.0	13.0	1.346	15.50	6.7	43.38
20	100	12.0	12.0	1.433	15.85	7.3	44.42
21	100	11.0	11.0	1.519	15.16	8.1	45.37
22	100	10.0	10.0	1.606	14.81	9.0	46.23
23	100	10.0	10.0	1.693	14.47	9.0	47.10
24	100	9.0	9.0	1.779	14.12	10.1	47.88
25	100	9.0	9.0	1.866	14.12	10.1	48.66
26	100	9.0	9.0	1.952	13.78	10.1	49.44
27	250	20.0	8.0	2.169	13.73	11.5	51.17
28	250	20.0	8.0	2.385	13.44	11.5	52.90
29	250	15.0	6.0	2.602	13.78	15.7	54.20
30	250	15.0	6.0	2.818	13.44	15.7	55.50
31	500	26.0	5.2	3.251	13.44	18.2	57.75
32	500	20.0	4.0	3.684	13.44	24.0	59.48
33	500	10.0	2.0	4.117	13.44	49.0	60.35



National Library
of Canada

Bibliothèque nationale
du Canada

Canadian Theses Service Service des thèses canadiennes

Ottawa, Canada
K1A 0N4

NOTICE

The quality of this microform is heavily dependent upon the quality of the original thesis submitted for microfilming. Every effort has been made to ensure the highest quality of reproduction possible.

If pages are missing, contact the university which granted the degree.

Some pages may have indistinct print especially if the original pages were typed with a poor typewriter ribbon or if the university sent us an inferior photocopy.

Reproduction in full or in part of this microform is governed by the Canadian Copyright Act, R.S.C. 1970, c. C-30, and subsequent amendments.

AVIS

La qualité de cette microforme dépend grandement de la qualité de la thèse soumise au microfilmage. Nous avons tout fait pour assurer une qualité supérieure de reproduction.

S'il manque des pages, veuillez communiquer avec l'université qui a conféré le grade.

La qualité d'impression de certaines pages peut laisser à désirer, surtout si les pages originales ont été dactylographiées à l'aide d'un ruban usé ou si l'université nous a fait parvenir une photocopie de qualité inférieure.

La reproduction, même partielle, de cette microforme est soumise à la Loi canadienne sur le droit d'auteur, SRC 1970, c. C-30, et ses amendements subséquents.

UNIVERSITY OF ALBERTA

MOBILITY CONTROL BY
EMULSIONS UNDER BOTTOM WATER CONDITIONS

BY
KACHEONG YEUNG

A THESIS

SUBMITTED TO THE FACULTY OF GRADUATE STUDIES AND RESEARCH
IN PARTIAL FULFILLMENT OF THE REQUIREMENTS FOR THE DEGREE
OF MASTER OF SCIENCE
IN
PETROLEUM ENGINEERING

DEPARTMENT OF MINING, METALLURGICAL AND PETROLEUM
ENGINEERING

EDMONTON, ALBERTA

SPRING, 1991



National Library
of Canada

Bibliothèque nationale
du Canada

Canadian Theses Service Service des thèses canadiennes

Ottawa, Canada
K1A 0N4

The author has granted an irrevocable non-exclusive licence allowing the National Library of Canada to reproduce, loan, distribute or sell copies of his/her thesis by any means and in any form or format, making this thesis available to interested persons.

The author retains ownership of the copyright in his/her thesis. Neither the thesis nor substantial extracts from it may be printed or otherwise reproduced without his/her permission.

L'auteur a accordé une licence irrévocable et non exclusive permettant à la Bibliothèque nationale du Canada de reproduire, prêter, distribuer ou vendre des copies de sa thèse de quelque manière et sous quelque forme que ce soit pour mettre des exemplaires de cette thèse à la disposition des personnes intéressées.

L'auteur conserve la propriété du droit d'auteur qui protège sa thèse. Ni la thèse ni des extraits substantiels de celle-ci ne doivent être imprimés ou autrement reproduits sans son autorisation.

ISBN 0-315-66592-9

Canada

UNIVERSITY OF ALBERTA

RELEASE FORM

NAME OF AUTHOR: Kacheong Yeung

TITLE OF THESIS: Mobility Control by Emulsions Under Bottom Water Conditions

DEGREE FOR WHICH THESIS WAS PRESENTED : MASTER OF SCIENCE

YEAR THE DEGREE WAS GRANTED : SPRING, 1991

Permission is hereby granted to the UNIVERSITY OF ALBERTA LIBRARY to reproduce single copies of this thesis and to lend or sell such copies for private, scholarly or scientific research purposes only.

The author reserves other publication rights, and neither the thesis nor extensive extracts from it may be printed or otherwise reproduced without the author's written permission.

(SIGNED)

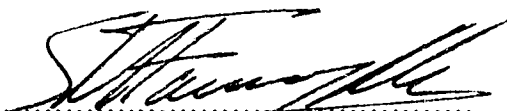
PERMANENT ADDRESS:

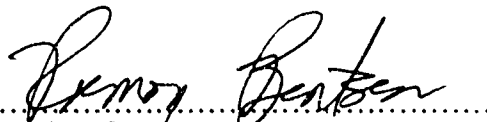
135A Pei Ho Street
2/F Sham Shui Po
Kowloon, Hong Kong

DATED :
Apr 12 1991

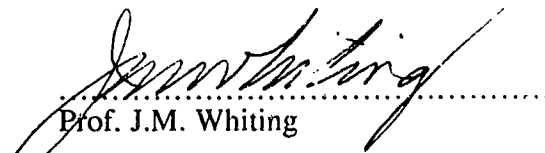
UNIVERSITY OF ALBERTA
FACULTY OF GRADUATE STUDIES AND RESEARCH


The undersigned certify that they have read and recommend to the Faculty of Graduate Studies and Research, for acceptance, a thesis entitled MOBILITY CONTROL BY EMULSIONS UNDER BOTTOM WATER CONDITIONS submitted by KACHEONG YEUNG in partial fulfillment of the requirements for the degree of MASTER OF SCIENCE in PETROLEUM ENGINEERING.


.....
Prof. S.M. Farouq Ali (Supervisor)


.....
Prof. R.G. Bentsen


.....
Prof. W.S. Tortike


.....
Prof. J.M. Whiting


.....
Prof. A. Chakma

DATED : *April 5, 1991*
.....

ABSTRACT

In many light or moderately viscous oil (viscosity 1 to 200 mPa.s) reservoirs in Alberta and Saskatchewan, a high water saturation zone of varying thickness and extent ("bottom water") occurs in communication with the oil zone above. As a result, the primary production period is short, and water coning occurs very early (6 to 12 months) in the life of the reservoir. Later, during the secondary recovery stage, such a zone can have an adverse effect on the waterflood efficiency. This research addresses the problem of waterflooding such reservoirs.

The research was directed towards reducing water mobility in the bottom water zone for more efficient oil displacement. Different surfactant concentrations were used to prepare 10% quality oil-in-water stable emulsions as blocking agents. Three displacement processes, the Emulsion-Slug Process (ESP), the Alternating-Water-Emulsion (AWE) Process and the Dynamic-Blocking Procedure (DBP), were used to improve vertical sweep efficiency. All of these methods consist of two modes: blocking and displacing. The differences among the processes lie in the application of the two modes. In the ESP, the blocking and displacing modes are used only once with the blocking agent injected first followed by a waterflood. In the AWE process, the two modes are used alternately. While in the DBP, the two modes are performed simultaneously.

A mathematical model, accounting for crossflow, for waterflooding a reservoir under bottom water conditions was developed to study water channelling quantitatively. From this model, given the reservoir descriptions, the amount of crossflow can be estimated. The model was used to analyze experimental data for all three processes. It is shown that the Dynamic-Blocking Procedure offers the possibility of controlling crossflow. Experiments conducted in this study showed that DBP led to nearly 15 percentile higher oil recovery than a conventional waterflood.

ACKNOWLEDGEMENTS

I wish to express my thanks to Dr. S.M. Farouq Ali for his supervision and encouragement throughout the course of this study.

I am also grateful to Dr. M.R. Islam for his suggestions regarding the experimental procedure during the early part of this study.

The assistance of the Petroleum Engineering technical staff is also greatly appreciated.

I would like to thank the Alberta Oil Sands Technology and Research Authority (AOSTRA) for providing the financial assistance necessary for conducting this study.

TABLE OF CONTENTS

CHAPTER	PAGE
1. INTRODUCTION	1
2. REVIEW OF THE LITERATURE.....	2
2.1 Waterflooding Bottom-Water Reservoirs.....	2
2.1.1 Viscous Water Injection.....	2
2.1.2 Polymer Injection	3
2.1.3 Emulsion Injection	4
2.2 Flow Mechanism of Emulsion in Porous Media.....	5
2.2.1 Experimental and Field Studies.....	5
2.2.2 Numerical Correlation Studies.....	8
2.3 Crossflow	9
2.3.1 Analytical and Experimental Studies.....	9
2.3.2 Numerical Studies.....	12
3. STATEMENT OF THE PROBLEM.....	14
4. DEVELOPMENT OF THE CROSSFLOW EQUATIONS	15
4.1 Introduction	15
4.2 Derivation of the Crossflow Equation	15
5. METHODS FOR IMPROVING WATERFLOOD PERFORMANCE.....	21
5.1 Introduction	21
5.2 The Problem	21
5.3 Emulsion-Slug Process (ESP).....	23
5.4 Alternating-Water-Emulsion (AWE) Process	24
5.5 Dynamic-Blocking Procedure (DBP)	26
6. EXPERIMENTAL APPARATUS AND PROCEDURE.....	28
6.1 Description of the Experimental Apparatus.....	28
6.2 Packing Procedure	28
6.3 Materials, Chemicals, and Fluids.....	30
7. PRESENTATION OF THE EXPERIMENTAL DATA.....	34

8. DISCUSSION OF THE RESULTS	74
8.1 Crossflow	74
8.1.1 The Effect of Injection Point on Crossflow.....	74
8.1.2 Verification of the Crossflow Equations	78
8.1.2.1 Zero Crossflow Case	78
8.1.2.2 Previous Linear Waterflood Studies	79
8.1.2.3 Previous Radial Waterflood Studies	81
8.1.3 The Region of Crossflow	86
8.2 Emulsion Flooding Under Bottom-Water Conditions	88
8.2.1 Effect of Slug Size on Oil Recovery in the Emulsion Slug Process	88
8.2.2 Effect of Surfactant Concentration of the Emulsion Slug on Oil Recovery.....	90
8.2.3 Effect of Injection Strategies on Recovery Under Bottom Water Conditions.....	91
8.2.3.1 Differences Between the Dynamic-Blocking Procedure (DBP) and Conventional Waterflooding.....	91
8.2.3.1.1 Conventional Waterflooding	91
8.2.3.1.2 Dynamic-Blocking Procedure.....	96
8.2.3.2 Experimental Results for the Injection Strategies.....	99
9. CONCLUSIONS.....	104
10. REFERENCES.....	105
11. APPENDIX A.....	108

LIST OF TABLES

TABLE		PAGE
6.1	Fluid Properties at 22°C	32
7.1	Summary of the Experimental Results	36
A.1	Production History for Run 1	109
A.2	Production History for Run 2	110
A.3	Production History for Run 3	111
A.4	Production History for Run 4	112
A.5	Production History for Run 5	113
A.6	Production History for Run 6	114
A.7	Production History for Run 7	115
A.8	Production History for Run 8	116
A.9	Production History for Run 9	117
A.10	Production History for Run 10	118
A.11	Production History for Run 11	119
A.12	Production History for Run 12	120
A.13	Production History for Run 13	121
A.14	Production History for Run 14	122
A.15	Production History for Run 15	123
A.16	Production History for Run 16	124
A.17	Production History for Run 17	125
A.18	Production History for Run 18	126
A.19	Production History for Run 19	127
A.20	Production History for Run 20	128
A.21	Production History for Run 21	129
A.22	Production History for Run 22	130

A.23	Production History for Run 23	131
A.24	Production History for Run 24	132
A.25	Production History for Run 25	133

LIST OF FIGURES

FIGURE	PAGE
6.1 Schematic of the Experimental Apparatus	29
6.2 The Effect of Concentration on Apparent Viscosity vs. Shear Rate	33
7.1 Summary Chart of all the Experiments	35
7.2 Production History for Run 1. Waterflooding a Homogeneous Pack (Injection Rate = 400 ml/hr)	37
7.3 Production History for Run 2. Waterflooding a Homogeneous Pack (Injection Rate = 600 ml/hr)	38
7.4 Production History for Run 3. Emulsion Flooding a Bottom-Water Reservoir Using the ESP (Emulsion Slug Size = $0.5 PV_{bw}$)	40
7.5 Production History for Run 4. Emulsion Flooding a Bottom-Water Reservoir Using the ESP (Emulsion Slug Size = $1.0 PV_{bw}$)	42
7.6 Production History for Run 5. Emulsion Flooding a Bottom-Water Reservoir Using the ESP (Emulsion Slug Size = $2.0 PV_{bw}$)	43
7.7 Production History for Run 6. Emulsion Flooding a Bottom-Water Reservoir Using the ESP (Emulsion Slug Size = $0.75 PV_{bw}$)	45
7.8 Production History for Run 7. Waterflooding a Bottom-Water Reservoir	47
7.9 Production History for Run 8. Emulsion Flooding a Bottom-Water Reservoir Using the ESP (Emulsion Slug Size = $1.0 PV_{bw}$)	48
7.10 Production History for Run 9. Emulsion Flooding a Bottom-Water Reservoir Using the AWE Process (Emulsion Slug Size = $1.0 PV_{bw}$)	50
7.11 Production History for Run 10. Emulsion Flooding a Bottom-Water Reservoir Using the DBP (Emulsion Slug Size = $1.0 PV_{bw}$)	52
7.12 Production History for Run 11. Oil Flooding a Bottom-Water Reservoir	53
7.13 Production History for Run 12. Waterflooding a Bottom-Water Reservoir in both the Oil and Water Zones	55
7.14 Production History for Run 13. Emulsion Flooding a Bottom-Water Reservoir Using the ESP (0.04% Surfactant Conc. Emulsion)	56
7.15 Production History for Run 14. Emulsion Flooding a Bottom-Water Reservoir Using the ESP (Surfactant Conc. 0.04%)	58

7.16	Production History for Run 15. Emulsion Flooding a Bottom-Water Reservoir Using the ESP (0.016% Surfactant Conc. Emulsion)	59
7.17	Production History for Run 16. Emulsion Flooding a Bottom-Water Reservoir Using the DBP (0.016% Surfactant Conc. Emulsion)	61
7.18	Production History for Run 17. Emulsion Flooding a Bottom-Water Reservoir Using the AWE Process (0.016% Surfactant Conc. Emulsion)	63
7.19	Production History for Run 18. Emulsion Flooding a Bottom-Water Reservoir Using the DBP (0.04% Surfactant Conc. Emulsion)	64
7.20	Production History for Run 19. Emulsion Flooding a Bottom-Water Reservoir Using the AWE Process (0.04% Surfactant Conc. Emulsion)	65
7.21	Production History for Run 20. Waterflooding a Homogeneous Pack (Inj. Rate = 400 ml/hr)	67
7.22	Production History for Run 21. Emulsion Flooding a Homogeneous Pack (0.4% Surfactant Conc. Emulsion)	68
7.23	Production History for Run 22. Emulsion Flooding a Homogeneous Pack (0.04% Surfactant Conc. Emulsion)	69
7.24	Production History for Run 23. Emulsion Flooding a Homogeneous Pack (0.016% Surfactant Conc. Emulsion)	70
7.25	Production History for Run 24. Emulsion Flooding a Bottom-Water Reservoir Using the ESP (0.016% Surfactant Conc. Emulsion)	72
7.26	Production History for Run 25. Emulsion Flooding a Bottom-Water Reservoir Using the ESP (0.04% Surfactant Conc. Emulsion)	73
8.1	The Effect of Injection Interval on Oil Recovery When Waterflooding a Bottom-Water Reservoir	75
8.2a	Crossflow as a Function of the Flood Front Position When Waterflooding the Oil Zone	77
8.2b	Crossflow as a Function of the Flood Front Position When Waterflooding Both the Oil and Water Zones	77
8.2c	Crossflow as a Function of the Flood Front Position When Waterflooding the Water Zone	77
8.3	Experimental Results of Oil Cut vs. Fluid Recovered from Islam ⁵	80
8.4	Crossflow as a Function of the Flood Front Position When Waterflooding in the Oil Zone in a Linear Equivalent Five-Spot Used by Barnes ³	85
8.5	The Effect of Displacing Fluid on Oil Recovery (Base Runs With Homogeneous Pack)	89

8.6	The Effect of Surfactant Concentration on the ESP	92
8.7	The Effect of Surfactant Concentration on the AWE Process	93
8.8	The Effect of Surfactant Concentration on the DBP	94
8.9	The Effect of the Injection Strategy on Oil Recovery Under Bottom-Water Conditions (0.016% Surfactant Emulsion)	100
8.10	The Effect of the Injection Strategy on Oil Recovery Under Bottom-Water Conditions (0.04% Surfactant Emulsion)	101
8.11	The Effect of the Injection Strategy on Oil Recovery Under Bottom-Water Conditions (0.4% Surfactant Emulsion)	102

NOMENCLATURE

Symbols

A_o	-	Cross-sectional area of the oil zone, m^2
A_w	-	Cross-sectional area of the bottom water zone, m^2
BT	-	Breakthrough
h	-	Height of model, m
HCPV	-	Hydrocarbon pore volume ($\phi S_{oi} V_{oil}$), fraction
h_o	-	Height of the oil zone, m
h_w	-	Height of the bottom water zone, m
k_{abs}	-	Absolute permeability, m^2
k_{eor}	-	Effective permeability to emulsion at irreducible oil saturation, m^2
k_o	-	Absolute permeability of the oil zone, m^2
k_{owr}	-	Effective permeability to oil at irreducible water saturation, m^2
k_w	-	Absolute permeability of the bottom water zone, m^2
k_{wor}	-	Effective permeability to water at residual oil saturation, m^2
IOIP	-	Initial oil-in-place, m^2
L	-	Length of model, m
M	-	Mobility ratio, fraction
M_{ac}	-	Fluid mobility in Zone a to fluid mobility in Zone c, fraction
M_{bd}	-	Fluid mobility in Zone b to fluid mobility in Zone d, fraction
PV	-	Pore volume, fraction
PV_{bw}	-	Pore volume of the bottom-water zone, fraction
PV_{oil}	-	Pore volume of the oil zone, fraction
q_a	-	Volumetric flow rate in the oil zone, m^3/s
q_b	-	Volumetric flow rate in the water zone, m^3/s
q_c	-	Volumetric crossflow flow rate between layers, m^3/s
q_o	-	Volumetric flow rate in the oil zone, m^3/s

- q_w - Volumetric flow rate in the water zone, m^3/s
- R_o - Resistance of the oil zone ($L\mu_o/A_ok_{or}$), $Pa.s/m^3$
- R_w - Resistance of the water zone($L\mu_w/A_wk_w$), $Pa.s/m^3$
- p - Pressure, Pa
- WOR - Water-oil-ratio, fraction
- X_f - Flood front distance from the injection end, fraction
- X_o - Flood front distance in the oil zone from the injection end, fraction
- X_w - Flood front distance in the bottom-water zone from the injection end, fraction

Subscripts

- bw - Bottom-water
- c - Crossflow
- e - Emulsion
- o - Oil
- vw - Viscous water
- w - Water

Greek Symbols

- μ - Viscosity, Pa.s
- ϕ - Porosity, fraction
- λ - Mobility, fraction
- α_1 - Term defined by Eq. (4.3)
- α_2 - Term defined by Eq. (4.4)
- α_3 - Term defined by Eq. (4.5)
- α_4 - Term defined by Eq. (4.6)

1. INTRODUCTION

Many light-to-medium oil reservoirs in Alberta and Saskatchewan contain some type of high water saturation zone ("bottom-water") underlying the oil reservoir. Waterflooding under such conditions is ineffective because of channelling of water through the bottom-water zone. However, in some cases, waterflooding such reservoirs may still be feasible and economically viable. While there is no doubt that some of the injected water bypasses the oil zone through the bottom-water zone, most of the injected water may still displace the oil, depending on the reservoir conditions. Therefore, a mechanistic understanding of oil displacement by a waterflood in the presence of a bottom-water zone is the basis for predicting recovery performance, and there is a need for developing a simple mathematical model to describe water channelling under bottom-water conditions. Given the reservoir description, the mathematical model should be able to estimate the amount of water channelling into the bottom-water zone.

A few techniques have been proposed to improve waterflood performance in layered reservoirs or under bottom-water conditions. Most of these are based upon the use of chemicals to plug the bottom-water zone near the injection well. However, none of the previous bottom-water studies accounted for crossflow effect when planning a chemical flood. Yet, the effect of crossflow plays a major role in waterflood performance in layered reservoirs. Thus, a systematic way of utilizing a chemical, in particular an emulsion, as a blocking agent under bottom-water conditions accounting for crossflow is required for efficient displacement of oil.

2. REVIEW OF THE LITERATURE

In a waterflood, water channelling from the injection to the producing wells, through the more permeable portions of the reservoir, results in low oil recovery. By reducing the water-oil mobility ratio in waterflooding, an increase in vertical sweep efficiency can be obtained¹. The problem of channelling is more severe in stratified reservoirs due to water channelling through the high permeability zones². In "bottom-water" reservoirs, the water channelling problem is more severe because the bottom layer may have a high water mobility. Many techniques have been proposed to improve waterflood performance in reservoirs under such conditions. Most of these are based upon the use of chemicals to plug the high water saturation zone near the injection well. In this chapter, previous work on this subject is briefly reviewed.

2.1 Waterflooding Bottom-Water Reservoirs

In the following sections, different strategies for waterflooding a bottom-water reservoir are discussed. Notice that none of the studies reported here treated the crossflow effect quantitatively.

2.1.1 Viscous Water Injection

The problem in recovering oil under bottom-water conditions was first recognized in the early sixties when Barnes³ suggested the use of a viscous water slug to improve waterflood efficiency in a reservoir partially invaded by bottom water. Viscous water in Barnes' study referred to water thickened by a chemical additive such that the viscosity of water was greater than 1.0 mPa.s. He argued that injecting a viscous water slug in bottom-water reservoirs would 1) reduce the flood life, 2) reduce lifting costs, and 3) increase ultimate recovery. He also pointed out that the larger the quantity and the higher the viscosity of the viscous slug injected into such a system, the greater the crossflow of oil ahead of the displacing front, thus leading to a higher oil rate during displacement. His visual model

studies showed that crossflow was most severe immediately ahead of the front and diminished to zero at the producing well. However, such a crossflow phenomenon was not described quantitatively in the study. Barnes' study was directed towards increasing the viscosity of water. Other chemical slugs that could reduce relative permeability to water were not considered.

2.1.2 Polymer Injection

The use of polymer as a mobility control agent in waterflooding was shown to be effective in the early sixties¹, when numerous field and model studies of the polymer flooding process were reported. Unlike the viscous water used by Barnes³, polymer has the ability to lower the mobility by reducing the relative permeability to water, as well as increasing its viscosity¹, so that the mobility ratio is improved.

Over two decades after Barnes' work, Zaidel⁴ looked at waterflooding bottom-water reservoirs with a polymer slug. His analytical model was based on the assumption of instantaneous gravitational phase separation along the vertical, i.e., the polymer solution did not enter the region with the residual oil saturation in a given section until it had filled the zone containing zero oil saturation. He concluded that a polymer with a mobility lower than that of water ($R = \frac{\text{mobility of water}}{\text{mobility of polymer}} > 1$, where R is the resistance factor)

improved oil recovery by increasing the flow resistance in the bottom-water zone, so that improved displacement in the oil zone would result. However, as the polymer mobility is lowered to a certain point ($R \geq 4$), the increase in resistance is primarily due to the oil bank formed in the bottom-water zone during the displacement. Thus, a polymer flood under bottom-water conditions can have both favourable and unfavourable manifestations: in the favourable sense, a high oil rate is obtained during the displacement; in the unfavourable sense, a certain amount of oil is lost to the bottom-water zone if the polymer mobility is too low. As a result, Zaidel suggested that a moderately low mobility polymer ($R = 2$ to 3)

would increase the oil rate during displacement while minimizing loss of oil to the water zone.

Shortly after Zaidel's theoretical work, Islam and Farouq Ali⁵⁻⁸ carried out an intensive experimental study on the use of various chemical slugs in waterfloods conducted under bottom-water conditions. The chemical slugs included polymer, emulsion, biopolymer gel, air, foam and carbon dioxide-activated silica gel. The variables examined were: slug size, permeability contrast, water-oil layer thickness ratio, oil viscosity, and injection rate of the mobility control agent. The study showed that polymer and emulsion performed better (i.e., high oil recovery and low WOR) than the other chemicals used. By comparing a polymer slug to a glycerine slug having the same viscosity, they showed that the reduction in the effective permeability to water by the polymer greatly improved oil recovery over that from the use of a glycerine slug. They claimed that a recovery improvement of 27% IOIP was due to the reduction in the effective permeability by adsorption and mechanical entrapment of the polymer.

2.1.3 Emulsion Injection

Based upon other studies carried out by Islam and Farouq Ali^{5,6,9,10} it was concluded that a 10% oil-in-water emulsion (200 ppm surfactant in the water phase) was most effective in blocking the bottom-water zone. A slug of one pore volume of the bottom-water zone was the minimum volume of emulsion required to create any blockage. However, a slug equal to 2.5 pore volumes of the bottom-water zone was found to be optimal and capable of reducing the bottom-water zone permeability permanently. Also, oil recovery was found to be insensitive to the thickness of the bottom-water zone when the bottom-water zone permeability was lower than that of the oil zone.

2.2 Flow Mechanism of Emulsion in Porous Media

In the following sections, the mechanism of flow of emulsions in porous media is briefly reviewed.

2.2.1 Experimental and Field Studies

An emulsion is a mixture of two immiscible liquids, one dispersed as droplets in the other, stabilized by an emulsifying agent¹¹. The flow behaviour of emulsions through tubes and unconsolidated synthetic porous media was investigated by Uzoigwe and Marsden¹². Newtonian behaviour was noticed even when the dispersed-phase concentration reached 50% (vol.), after which the emulsion exhibited non-Newtonian behaviour. The study treated the emulsion flow as that of a homogeneous liquid. No permeability reduction resulting from emulsion flow was observed.

Use of stable emulsions as mobility control agents for oil recovery processes was first introduced by McAuliffe¹³. In his study, he examined the transient permeability behaviour of dilute, stable emulsions. An oil-in-water emulsion was obtained by reacting asphaltic crude oil with a dilute solution of sodium hydroxide. Emulsions having different drop sizes were injected into a consolidated sandstone under a constant pressure. He suggested that for an emulsion to be most effective, the oil droplets in the emulsion should be slightly larger than the pore-throat constrictions in the porous medium. However, McAuliffe's results showed that significant permeability reduction occurred even when the emulsion drop sizes were very much smaller than the mean size of the pore constrictions. He argued that as oil-in-water emulsion was injected, a greater amount of emulsion entered the more permeable zones. As a result, flow became more restricted so that water began to flow into less permeable zones, resulting in greater vertical sweep efficiency. The emulsions reduced water permeability greatly, to a level of one to ten percent of the original permeability. He also observed that the permeability reduction caused by injecting an emulsion was retained even when the emulsion was followed by many pore volumes of water, which suggested a

permanent permeability reduction. One important finding was that flow of oil-in-water emulsions through porous media was non-Newtonian, regardless of the oil content of the emulsion.

McAuliffe also reported a field test of an oil-in-water emulsion flood¹⁴. A 14 percent oil-in-water emulsion of three percent pore volume of the affected area was injected followed by a cushion of fresh water of four percent pore volume after which saline water was injected. After emulsion treatment over a two-year period, increased oil production from the wells surrounding the emulsion-treated injectors, compared with little or no increase in oil production and increasing WOR's for wells surrounding the water injectors, was observed. It was concluded that the emulsion decreased channelling of the injected water, which increased the volumetric sweep efficiency. On the whole, 33,000 bbl of crude oil were emulsified and injected, and 55,000 bbl of additional oil were produced.

Johnson¹⁵ reviewed the caustic and emulsion flooding methods. He suggested that emulsion flooding was a natural extension of the caustic flooding emulsification and entrapment mechanisms. If the oil cannot be emulsified in situ, then other oil emulsions can be formed externally and injected. However, he pointed out that although the potential of emulsions for improving oil recovery was well established, the cost of oil for emulsification and injection was a serious deterrent to wider field use.

Soo and Radke¹⁶ reached the following conclusions from their study of a dilute, stable emulsion: 1) the permeability reduction was caused by oil drops captured on pore walls and in crevices as well as blocking of pores of throat sizes smaller than their own; and 2) the overall permeability reduction was determined by the volume of drops retained and how effective those drops were in restricting flow. As the drop size of the emulsion increased, the drop retention increased. However, for the same amount of oil drop volume retention, smaller sized drops were more effective in restricting flow. For the smaller drop-size

emulsion systems, the effect of drop size on retention dominated, and increasing the drop size resulted in an increased permeability reduction. On the other hand, for the larger drop-size emulsion systems, the effect of the drop size on restriction effectiveness dominated, and increasing the drop-size resulted in less transient permeability reduction.

Schmidt¹⁷ suggested using a dilute, stable emulsion to improve mobility control in EOR processes. He claimed that an oil-in-water emulsion provided microscopic mobility control through entrapment or local permeability reduction not through viscosity-ratio improvement. Schmidt concluded that mobility ratio improvement was achieved by small oil droplets irreversibly captured in the porous medium because of straining and interception, thereby lowering the local permeability to water.

French, Broz and Lorenz¹⁸ suggested the use of emulsions for mobility control in steamflooding. They observed that a reduction in permeability from emulsion plugging may not necessitate that the median droplet size equal to or exceeding the median pore throat diameter, and that competition from an ensemble of smaller droplets "crowding" a single pore throat would have the same effect in blocking a pore throat. French et al. concluded that injection of a small slug of oil-in-water emulsion prepared from oil and water available in a specific field caused a significant reduction in the permeability of core from that field.

Farouq Ali, Thomas and Khambharatana¹⁹ studied the flow of emulsions through porous media at elevated temperatures. In their work, thermal stability of emulsions was studied in order to assess the flow behaviour at elevated temperatures. Surfactant emulsions, carbon dioxide/water emulsions, sodium hydroxide (caustic) emulsions, acid emulsions and distilled water emulsions were passed through porous media to examine the changes in emulsion characteristics. The study showed that the flow of emulsions through porous media is a function of the drop-size distribution of the emulsion to pore-size distribution of

the porous medium ratio. Farouq Ali et al. concluded that for both oil-in-water and water-in-oil emulsions studied, the rheology of emulsions in the porous media is comparable to the rheology in a viscometer. Furthermore, emulsion mobility is governed by the flow velocity, an increase in which can cause shearing of the larger drops into smaller ones.

2.2.2 Numerical Correlation Studies

With the growing importance of emulsion flow through porous media, especially in mobility control, it is important to have a numerical model for accurate prediction of pressure drops due to emulsion flow. Currently, there are three theories available to describe emulsion flow through porous media: viz. the bulk viscosity²⁰, droplet retardation²¹, and filtration^{22,23} models.

The bulk viscosity model of Alvarado and Marsden²⁰ describes emulsion as a single phase, homogeneous fluid. The model does not allow interaction between drops and the pore walls; thus, no permeability reduction is predicted. According to the model, emulsion flow differs from Darcy flow only when the bulk emulsion viscosity varies with shear rate. Although this model is limited because it cannot predict transient permeability reduction behaviour, it is useful for emulsion flow computations in the case of high-concentration emulsions having small drop-size to pore-size ratios. The bulk viscosity model was further modified by Farouq Ali and Abou-Kassem²⁴⁻²⁶. The modified correlation was tested using the Alvarado and Marsden²⁰ experimental data for 11 consolidated cores involving 56 data points, obtaining accurate predictions: average absolute relative deviation of 2.4% with a maximum deviation of 14.3% from measured pressure drops.

The droplet retardation model of Devereux²¹, originally delineated by McAuliffe¹³, includes transient permeability reduction. In this model, the transient permeability behaviour was modeled based on oil droplets passing through pores of throat size smaller than their own diameters, so that they have to squeeze through the pore constrictions.

Thus, in the passage along the tortuous paths through the porous medium, these droplets overcome a capillary resistance force from each pore throat so that emulsion flow is retarded.

Soo and Radke^{22,23,27,28} proposed the filtration model for the flow of dilute, stable emulsions in porous media. They suggested that emulsion droplets are not merely retarded when they flow through porous media as describe by Devereux²¹; rather, they are actually captured. Soo and Radke claimed that this is the only plausible explanation as to why a permanent permeability reduction can occur. The filtration model predicts transient and steady state permeability reduction caused by an emulsion. They suggested that transient flow behaviour is characterized by three parameters: a filter coefficient, a flow-redistribution parameter and a flow-restriction parameter. The filter coefficient controls the sharpness of the emulsion front, while the flow-redistribution parameter dictates the steady-state retention, as well as the flow redistribution phenomenon, while the flow-restriction parameter describes the effectiveness of retained drops in reducing permeability.

2.3 Crossflow

When a stratified reservoir is being studied for waterflooding, failure to account for crossflow can lead to large errors in oil recovery predictions²⁹⁻³³. Under bottom-water conditions, this effect is aggravated due to the presence of the mobile water phase. Because of the complexity of the crossflow behaviour, analytical solutions are limited to two-layer reservoirs under specified conditions, while multi-layer reservoir studies are restricted to numerical solution only.

2.3.1 Analytical and Experimental Studies

Russell and Prats³⁴ were among the first researchers to investigate the performance of layered reservoirs with crossflow for a single, compressible fluid case. The system studied consisted of a centrally located well in a bounded cylindrical reservoir composed of two

layers of contrasting physical properties. The mathematical model showed that, except for early times, the performance of a two-layer reservoir with crossflow could be duplicated by that of an equivalent single-layer reservoir, having the same pore volume and same drainage and wellbore radii, and a flow capacity (kh , permeability-thickness product) equal to the sum of the flow capacities of the layers in the crossflow system.

Katz and Tek³⁵ studied the case of unsteady-state flow of single-phase, slightly compressible fluids during depletion of bounded two-layer porous systems. Both linear and radial systems were described mathematically. Katz and Tek suggested that performance of fluid flow with crossflow would lie between the upper bound (infinite vertical permeability, i.e., similar to single-layer reservoir discussed by Russell et al.³⁴), and the lower bound (zero vertical permeability, i.e., no crossflow between layers as in the layer-cake model). Furthermore, they concluded that the initial depletion performance of stratified systems was near the lower bound, and as time and the radius of drainage increased, the system performance tended towards the upper bound.

Warren and Cosgrove²⁹ approximated the effect of crossflow based on Dietz's theory. They claimed that the failure to use all available permeability data could lead to large errors in the prediction of the performance of a stratified reservoir. By assuming that the permeability could be characterized by a log-normal distribution, they concluded that the effect of crossflow in a stratified system could be appreciable, particularly at very favourable or very unfavourable mobility ratios.

Wright, Dawe, and Wall³⁶ investigated the basic flow mechanisms and dispersion of an immiscible chemical in layered reservoirs. The variables controlled were layer permeability ratios, fluid viscosity and flow rate. Based on the study, they concluded that crossflow increased the dispersion effect. Surfactant slugs would be susceptible to break down in layered reservoirs.

Lambeth and Dawe³³ studied the effect of viscous crossflow experimentally and theoretically. Experiments in layered formations utilized viscous fluids, designed to examine the crossflow behaviour. The analytical solution of a two-layer case was developed, assuming a linear pressure distribution in one layer while allowing the pressure in the other layer to vary with crossflow. Although this over-simplification is self-contradictory, the solution gave an indication of the magnitude of crossflow when one fluid displaces another fluid. The authors attempted to solve the case of non-linear flow in both layers. However, the solutions obtained did not satisfy the original material balance equations. Experimental study suggested that the viscous crossflow effects were rate independent.

Wright, Wheat, and Dawe³⁷ studied slug size and mobility requirements for chemically enhanced oil recovery within heterogeneous reservoirs. Using a modification of the analytical solution obtained by Lambeth and Dawe³³, the authors suggested that the criteria for the chemical slug disintegration caused by the effect of crossflow were more demanding than previously considered necessary for reservoirs with common heterogeneities. They claimed that a high-mobility slug would preferentially sweep the higher-conductivity layers, but a low-mobility slug would tend to be pushed by crossflow into the lower-conductivity layers. This mechanism must be considered when low-mobility slugs are used for waterflood conformance improvement.

Ahmed, Castanier, and Brigham³⁸ carried out an experimental study of waterflooding in a two-dimensional layered sand model. The effect of flow rate on oil recovery by waterflooding a three-layer sand visual model was studied. The authors reported that intermediate oil recovery during a waterflood in a stratified reservoir with vertical communication was sensitive to flow rate, oil viscosity, and interfacial tension (IFT). During the displacement, oil recovery was observed to increase when flow rate was

Decreased. Ahmed et al. concluded that oil recovery increased significantly when mobility ratio was reduced.

2.3.2 Numerical Studies

Due to the lack of analytical solutions for multi-layer reservoirs, only numerical solutions have been attempted to examine the effect of crossflow. Root and Skiba³⁰ were among the first researchers to investigate the crossflow effects during a waterflood in a stratified reservoir. The numerical study simulated one incompressible fluid displacing another incompressible fluid of the same density and viscosity. From this study, it was concluded that: 1) early breakthrough of displacing fluid could not be curtailed effectively by blocking access to it in the production and injection wells unless a high-permeability zone was completely isolated; and 2) when the adjacent strata were in communication, the single-zone production-injection method lost much of its effectiveness.

Goddin, Craig, Wilkes, and Tek³¹ reported a numerical study of waterflood performance in a stratified system with crossflow. Viscous and capillary crossflow was examined in a field-scale model of a two-layer, water-wet sandstone reservoir. The authors reported that maximum crossflow occurred in the vicinity of the flood front in the permeable layer, similar to the observation of Barnes³ in his visual model. It was concluded that viscous crossflow was a function of mobility ratio.

Silva and Farouq Ali³² developed a two-phase, three-dimensional reservoir simulator to study the effect of selective formation plugging in waterflooding a layered model. The authors concluded that partially plugging a high permeability layer was ineffective if the layers were in communication. They further concluded that reservoirs consisting of a bottom-water zone might be susceptible to efficient waterflooding.

El-Khatib³⁹ developed a mathematical model for waterflood simulation in linear stratified non-communicating layers, with no crossflow, and communicating layers with complete

crossflow (i.e., lower and upper bounds in Katz and Tek's study³⁵). The study showed that the effect of crossflow between layers increased the oil recovery at favourable mobility ratios and decreased it at unfavourable mobility ratios. El-Khatib concluded that crossflow increased the influence of mobility ratio in waterflood performance prediction.

3. STATEMENT OF THE PROBLEM

Two major observations can be made from the literature survey in the preceding section. First, waterflooding under bottom-water conditions is ineffective due to water channelling through the bottom-water zone; however, a lack of suitable fluid flow equations for layered formations may lead to conclusions that may not be valid. Second, injection of an emulsion as a blocking agent under bottom-water conditions has led to improved oil recovery^{5,6,9,10}; however, the mechanism of this process is still not fully understood.

The principal objectives of this study can be stated as follows:

- 1) To develop analytical expressions for crossflow occurring in a waterflood when bottom water is present, for several situations.
- 2) To compare the analytically calculated crossflow with the experimental values.
- 3) To carry out waterflood experiments in a two-dimensional model using three strategies involving emulsion injection: the Emulsion-Slug Process, Alternating-Water-Emulsion Process, and the Dynamic-Blocking Procedure.
- 4) To determine under what conditions emulsions are likely to improve waterflood performance.

4. DEVELOPMENT OF THE CROSSFLOW EQUATIONS

4.1 Introduction

The previous analytical solutions^{34,35} for layered reservoirs were obtained for a two-layer reservoir for single phase compressible fluid flow occurring during primary depletion. These solutions are, therefore, suitable only for the single-phase flow case. Lambeth and Dawe's³² solution for one fluid displacing another in a two-layer reservoir is unrealistic, because one of the major assumptions used in deriving their solution was that the pressure in the lower permeability layer was unaffected by crossflow. This assumption may be justified when the permeability contrast of the two layers is large. It may not be applicable under bottom-water conditions, where the magnitudes of the permeabilities of the layers are often of the same order. The following section presents the derivation of the crossflow equation without a linear pressure distribution with respect to distance assumption in either layer.

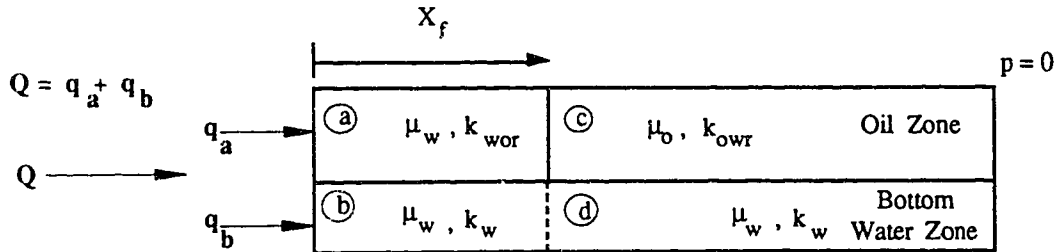
4.2 Derivation of the Crossflow Equation

In the following, an attempt is made to develop an expression for crossflow occurring while waterflooding a two-layer reservoir, the lower layer being a water zone. No assumption of linearity of pressure with distance is made.

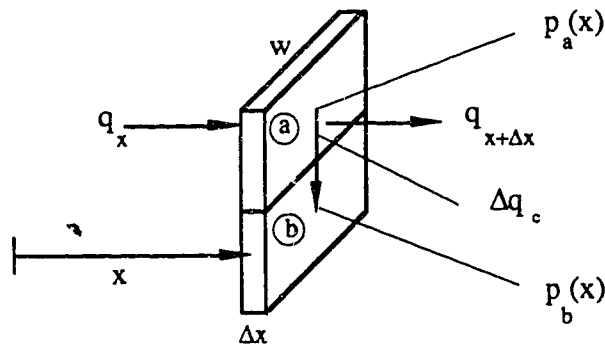
Consider a two-layer porous medium, the upper layer being the oil zone with a permeability k_{owr} , and the lower layer being the water zone with a permeability of k_w . Water is being injected at a total rate Q , of which q_a is entering the oil zone and q_b is entering the bottom-water zone. The following assumptions are made:

- 1) flow is steady state;
- 2) crossflow is vertical;
- 3) crossflow does not alter the mobility in either layer;
- 4) fluids are incompressible;
- 5) displacement is piston-like;

- 6) only oil is flowing ahead of the flood front in the oil zone;
- 7) only water is flowing behind the flood front; and
- 8) capillary and gravity forces are negligible.



Consider a vertical section of thickness Δx and width w , behind the flood front as shown below:



where q_x is the flow in Section a at a distance x from the injection end, $q_{x+\Delta x}$ is the flow in Section a at a distance $x+\Delta x$ from the injection end, and Δq_c is the vertical crossflow in the section. Applying a mass balance to water in Section a above gives

$$q_x - (q_{x+\Delta x} + \Delta q_c) = 0. \tag{4.1}$$

Using Darcy's equation and rearranging we obtain

$$\frac{A_s k_s}{\mu_s} \frac{\partial p_s}{\partial x} \Big|_{x+\Delta x} - \frac{A_s k_s}{\mu_s} \frac{\partial p_s}{\partial x} \Big|_x = \frac{2w\Delta x}{\frac{\mu_s h_s}{k_s} + \frac{\mu_b h_b}{k_b}} \cdot (p_s - p_b), \tag{4.2}$$

where p_a and p_b are the average pressures of the corresponding sections taken from each section center. (Note that the subscripts a, b, c and d are used for simplicity.) Taking the limit as Δx approaches zero, the following differential form of Eq. (4.2) results:

$$\frac{\partial^2 p_a}{\partial x^2} = \alpha_1 (p_a - p_b) \tag{4.3}$$

where $\alpha_1 = \frac{2}{h_a^2 (1 + M_{ab} \frac{h_b}{h_a})}$, and $M_{ab} = \frac{k_a/\mu_a}{k_b/\mu_b}$ is the ratio of the mobility of the fluid in

Section a to that in Section b. If a similar procedure is carried out for Sections b and a, c and d, and d and c, the following equations can be derived:

$$\frac{\partial^2 p_b}{\partial x^2} = \alpha_2 (p_b - p_a), \tag{4.4}$$

$$\frac{\partial^2 p_c}{\partial x^2} = \alpha_3 (p_c - p_d), \tag{4.5}$$

and
$$\frac{\partial^2 p_d}{\partial x^2} = \alpha_4 (p_d - p_c), \tag{4.6}$$

where $\alpha_2 = \frac{2}{h_b^2 (1 + M_{ba} \frac{h_a}{h_b})}$, $\alpha_3 = \frac{2}{h_c^2 (1 + M_{cd} \frac{h_d}{h_c})}$, $\alpha_4 = \frac{2}{h_d^2 (1 + M_{dc} \frac{h_c}{h_d})}$ and where the

M's are the mobility ratios for the corresponding sections. Solving Eqs. (4.3) and (4.4) simultaneously, and Eqs. (4.5) and (4.6) simultaneously, the following solutions result

$$p_a(x) = c_1 + c_2 x + c_3 \left(\frac{\alpha_1}{m}\right) \cdot \sinh(x\sqrt{m} + c_4), \tag{4.7}$$

$$p_b(x) = c_1 + c_2 x + c_3 \left(\frac{\alpha_1}{m} - 1\right) \cdot \sinh(x\sqrt{m} + c_4), \tag{4.8}$$

$$p_c(x) = c'_1 + c'_2 x + c'_3 \left(\frac{\alpha_3}{n}\right) \cdot \sinh(x\sqrt{n} + c'_4), \quad \dots\dots\dots(4.9)$$

and
$$p_d(x) = c'_1 + c'_2 x + c'_3 \left(\frac{\alpha_3}{n} - 1\right) \cdot \sinh(x\sqrt{n} + c'_4); \quad \dots\dots\dots(4.10)$$

where $m = \alpha_1 + \alpha_2$ and $n = \alpha_3 + \alpha_4$.

The following eight conditions are used to obtain the eight integration constants for the constant rate case:

1. $q = q_a$ at $x = 0$;
2. $q = q_b$ at $x = 0$;
3. $p_c = 0$ at $x = 1$;
4. $p_d = 0$ at $x = 1$;
5. $p_a = p_c$ at flood front X_f ;
6. $p_b = p_d$ at flood front X_f ;
7. $M_{ac} \frac{\partial p_a}{\partial x} = \frac{\partial p_c}{\partial x}$ at flood front X_f ; and
8. $M_{bd} \frac{\partial p_b}{\partial x} = \frac{\partial p_d}{\partial x}$ at flood front X_f .

It should be noted here that water influx into the oil and water zones is allowed to be arbitrary (i.e., q_a and q_b are independent variables). This is done for later application. It will be shown later that by forcing $q_b = 0$ has little effect on the displacement performance when crossflow exists, as was reported in previous studies^{30,32}. Normalized horizontal distance, x/L , where L is the length of the flow path, is used for the above conditions. Thus, by applying the first four conditions, and then the remaining conditions we get:

$$c_1 = \frac{q_b \mu_b}{A_b k_b} \frac{\alpha_1}{m} - \frac{q_a \mu_a}{A_a k_a} \left(\frac{\alpha_1}{m} - 1\right);$$

$$c_2 = \frac{q_a \mu_a}{A_a k_a} \left(\frac{\alpha_1}{m} - 1\right) - \frac{q_b \mu_b}{A_b k_b} \frac{\alpha_1}{m};$$

$$c_3 = \left(\frac{q_b \mu_b}{A_b k_b} - \frac{q_a \mu_a}{A_a k_a} \right) \frac{1}{\sqrt{m} \cdot \cosh(\sqrt{m})};$$

$$c_4 = -\sqrt{m};$$

$$c'_1 = -c'_2;$$

$$c'_2 = c_3 \left(\frac{M_{ac} M_{bd}}{M_{bd} - M_{ac}} \right) \left\{ \sqrt{m} \cosh(X_f \sqrt{m} - \sqrt{m}) - \frac{\sinh(X_f \sqrt{m} - \sqrt{m})}{\sqrt{n} \tanh(X_f \sqrt{n} - \sqrt{n})} \left(\frac{\alpha_3}{M_{ac}} + \frac{\alpha_4}{M_{bd}} \right) \right\};$$

$$c'_3 = c_3 \cdot \frac{\sinh(X_f \sqrt{m} - \sqrt{m})}{\sinh(X_f \sqrt{n} - \sqrt{n})}; \text{ and}$$

$$c'_4 = -\sqrt{n};$$

Now, vertical crossflow represented by Darcy's equation from the oil zone to the bottom-water zone behind the flood front is given by (note: crossflow is positive downwards):

$$q_c = \int_0^{x_f} dq_c = \frac{2wc_3}{\left(\frac{\mu_a h_a}{k_a} + \frac{\mu_b h_b}{k_b} \right)} \int_0^{x_f} \sinh(x\sqrt{m} - \sqrt{m}) dx. \quad \dots\dots\dots(4.11)$$

Integrating the above equation we obtain

$$q_c = \frac{2wc_3}{\left(\frac{\mu_a h_a}{k_a} + \frac{\mu_b h_b}{k_b} \right)} \cdot \left[\frac{\cosh(X_f \sqrt{m} - \sqrt{m}) - \cosh(\sqrt{m})}{\sqrt{m}} \right]. \quad \dots\dots\dots(4.12)$$

For crossflow ahead of the flood front, integrating from $x = X_f$ to $x = 1$ leads to

$$q_c = \frac{2wc'_3}{\left(\frac{\mu_c h_c}{k_c} + \frac{\mu_d h_d}{k_d} \right)} \cdot \left[\frac{1 - \cosh(X_f \sqrt{n} - \sqrt{n})}{\sqrt{n}} \right]. \quad \dots\dots\dots(4.13)$$

It should be noted that the only possible condition for zero crossflow between the oil and bottom-water zones is to make $c_3 = 0$, or simply

$$\frac{q_b \mu_b}{A_b k_b} - \frac{q_a \mu_a}{A_a k_a} = 0.$$

Thus, it can be seen that if flow occurs in only one of the layers (i.e., $q_a = 0$ or $q_b = 0$), crossflow is bound to take place. Also, in a vertical-front displacement, i.e., $q_a/A_a = q_b/A_b$, unless in a homogeneous reservoir ($k_a/\mu_a = k_b/\mu_b$), crossflow can never be zero.

5. METHODS FOR IMPROVING WATERFLOOD PERFORMANCE

5.1 Introduction

In this research, methods using a suitable emulsion as a blocking agent for improving the recovery of light and moderately viscous oils under bottom-water conditions are sought. Essentially the problem is that, when waterflooding a reservoir with a bottom-water zone underlying the oil zone, the injected water tends to bypass much of the oil zone, giving a low vertical sweep efficiency.

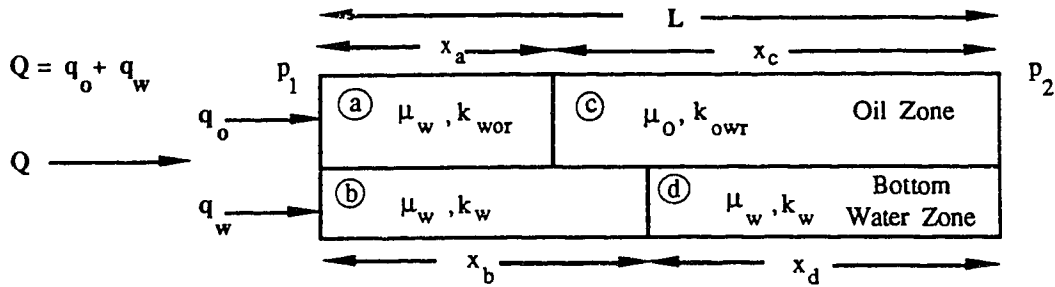
In this section, first the problem at hand is examined. Next, three approaches are proposed as possible solutions to the problem. These are referred to as the Emulsion-Slug Process (ESP), the Alternating-Water-Emulsion (AWE) process, and the Dynamic-Blocking Procedure (DBP). All of these methods consist of two modes: blocking and displacing. The differences among the processes lie in the application of the two modes. In the ESP, the blocking and displacing modes are used only once with the blocking agent injected first followed by a waterflood. In the AWE process, the two modes are used alternately. While in the DBP, the two modes are performed simultaneously.

5.2 The Problem

The problem of waterflooding an oil zone with an underlying water zone can be expressed mathematically, provided the following assumptions are met:

- 1) flow is steady state;
- 2) fluids are incompressible;
- 3) displacement is piston-like;
- 4) only oil is flowing ahead of the flood front in the oil zone;
- 5) only water is flowing behind the flood front;
- 6) capillary and gravity forces are negligible; and
- 7) no crossflow occurs between layers.

Consider a two-layer porous medium, the upper layer being the oil zone with a permeability k_{owr} , and the lower layer being the water zone with a permeability of k_w . Water is being injected at a total rate Q , of which q_o is entering the oil zone and q_w is entering the bottom-water zone.



With the above assumptions, one can write the following equations by using Darcy's law,

$$q_o = \frac{p_1 - p_2}{\frac{1}{A_o} \left(\frac{\mu_w x_a}{k_{wor}} + \frac{\mu_o x_c}{k_{owr}} \right)} \quad \dots\dots\dots(5.1)$$

$$q_w = \frac{p_1 - p_2}{\frac{1}{A_w} \left(\frac{\mu_w x_b}{k_w} + \frac{\mu_w x_d}{k_w} \right)} \quad \dots\dots\dots(5.2)$$

or,

$$q_o = \frac{p_1 - p_2}{R_o}; \quad \dots\dots\dots(5.3)$$

and
$$q_w = \frac{p_1 - p_2}{R_w}, \quad \dots\dots\dots(5.4)$$

where $R_o = \frac{1}{A_o} \left(\frac{\mu_w x_a}{k_{wor}} + \frac{\mu_o x_c}{k_{owr}} \right)$ and $R_w = \frac{1}{A_w} \left(\frac{\mu_w x_b}{k_w} + \frac{\mu_w x_d}{k_w} \right)$ are the flow resistances in the oil and bottom-water zones, respectively, and A_o and A_w are the cross-sectional areas of the oil and bottom-water zones, respectively.

Using Eqs. (5.1) and (5.2) with $A_o = A_w$, one can obtain the following equations:

For $x_a = x_b = 0$, and $x_c = x_d = L$,

$$\text{WOR} = \frac{q_w}{q_o} = \frac{k_w}{\mu_w} \frac{\mu_o}{k_{owr}}, \quad \dots\dots\dots(5.5)$$

where WOR is the ratio of the mobility of the fluid in the water zone to that in the oil zone. For most systems, the $\text{WOR} \gg 1$. In the experimental model used in this research, the WOR was about 60. This means that from the very beginning, the WOR will be at a highly unfavourable value. Thus, ways of impeding water flow in the bottom-water zone are essential for improving oil recovery by a waterflood.

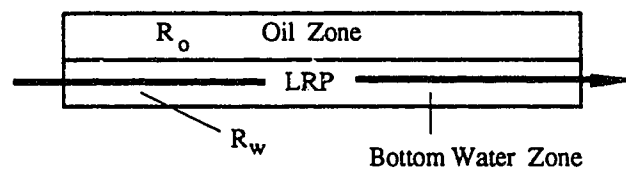
5.3 Emulsion-Slug Process (ESP) (considering the system as one unit)

The main objective of the three processes proposed above is to try to isolate the bottom-water zone when displacing oil by water. Emulsion is used as a blocking agent to increase the flow resistance of the bottom-water zone. In the Emulsion-Slug Process, the blocking mode is performed once at the beginning, followed by a waterflood. Under bottom-water conditions, the flow resistance of the oil zone is much higher than that of the bottom-water zone, i.e., $R_o \gg R_w$ as discussed above; thus, the WOR will be high at the beginning of the flood. The idea behind this approach is to inject emulsion into the bottom-water zone to increase R_w such that the bottom-water zone is partially isolated when followed by a waterflood. It should be noted that from the previous studies^{29,31}, partial blocking near the wellbore did not improve recovery performance when crossflow took place. As a result, a large slug of emulsion should be used so that most of the bottom-water zone is blocked (isolated) before the oil zone is waterflooded. However, the question arises: if emulsion is employed as a blocking agent, how can it block the bottom-water zone without blocking the oil zone when crossflow exists? This question applies even if the emulsion is injected only into the bottom-water zone, since the layers are in communication (this is analogous to the

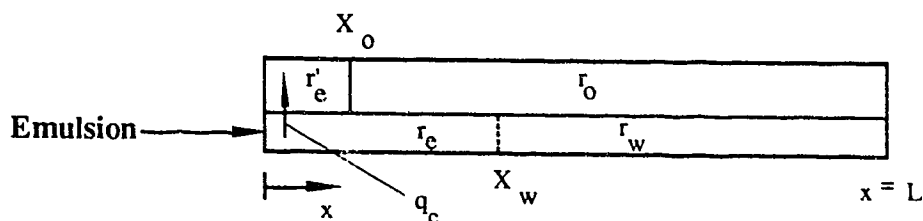
situation where injecting water only into the oil zone will not improve the displacement performance when crossflow exists^{29,31}). Although emulsion injection was shown to be effective in previous studies^{5,6,9}, the above question should be considered so that the blocking and displacing modes would perform more efficiently (the next two processes examine this question). Also, it should be noted that assuming emulsion does penetrate the bottom-water zone only, the water cut will be 100% during emulsion injection, which is not desirable.

5.4 Alternating-Water-Emulsion (AWE) Process (considering the model as many sub-units)

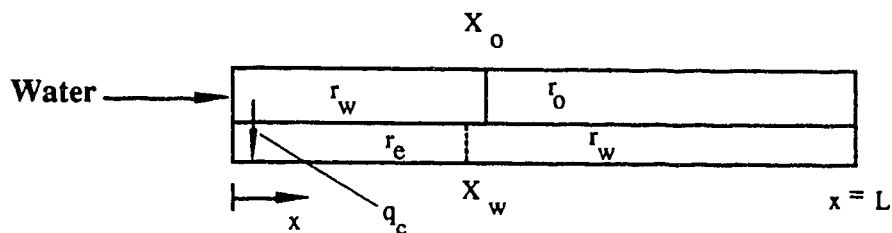
The Alternating-Water-Emulsion (AWE) process examines the question in Section 5.3 by considering the model as many sub-units. Consider a two-layer porous medium, the upper layer being the oil zone with a flow resistance R_o , and the lower layer being the water zone with a flow resistance R_w . The initial state before emulsion injection is illustrated below:



Any injected fluid travelling from an injector to a producer would take the path of least resistance. Thus the emulsion, which increases the resistance to flow as it advances, would flow directly into the bottom-water zone, since the least resistance path (LRP) is a straight line from the injector to the producer through the bottom-water zone as illustrated above, as $R_o \gg R_w$, where R_o and R_w are given by $R_o = L\mu_o/A_o k_{or}$ and $R_w = L\mu_w/A_w k_w$, respectively. Now, by injecting emulsion directly into the bottom-water zone, a point will be reached when the resistance of the bottom-water zone is equal in magnitude to that of the oil zone above, so that a large proportion of the injected emulsion invades the oil zone near the injection end instead of continuing to flow through the bottom-water zone, as illustrated below.



Here X_o is the emulsion flood front position in the oil zone, X_w is the emulsion flood front position in the bottom-water zone, and q_c is the emulsion crossflow. In the bottom-water zone, up to the emulsion flood front X_w , the resistance is $X_w r_e$ ($r_e = \mu_e / A_w k_{ewr}$, where the subscript "e" denotes the properties of the emulsion) and the corresponding resistance in the oil zone above is $X_o r'_e + (X_w - X_o) r_o$ (where $r'_e = \mu_e / A_o k_{oor}$ and $r_o = \mu_o / A_o k_{owr}$). When the conditions are such that the resistance of the bottom-water zone is higher than that of the oil zone above, i.e., $X_w r_e > X_o r'_e + (X_w - X_o) r_o$, then a large amount of injected emulsion is forced into the oil zone. Thus, at this point, a switch from the blocking to the displacing mode is needed, in order to minimize emulsion blockage of the oil zone. This stage is illustrated in the following diagram. (Note: the emulsion in the region $0 < X < X_o$ in the upper diagram is assumed to be small; thus, it is neglected in the following analysis.)



However, as water injection continues, the waterflood front will eventually advance to a point where water crossflow (channelling) into the bottom-water zone becomes prohibitive. At this point, a switch from the displacing to the blocking mode to further isolate the bottom-water zone is needed. This cycle is repeated as many times as necessary, and the resulting process is called the Alternating-Water-Emulsion Process.

It can be seen that by alternating between the blocking and displacing modes, the blocking of the oil zone by emulsion is much less than that in the Emulsion-Slug Process. However, the question arises: when to switch from the blocking mode to the displacing mode, and from the displacing mode to the blocking mode. To answer this question, the exact flow mechanism of emulsion under bottom-water conditions must be known. In other words, emulsion behaviour in both the oil and water layers must be known so that the amount of crossflow between the layers can be determined quantitatively. Only when all these factors are known, can the process be performed efficiently.

5.5 Dynamic-Blocking Procedure (DBP)

In order to eliminate some of the problems with the AWE process, such as finding the correct slug size, a knowledge of the flow mechanism of the blocking agents is needed. Thus, a new approach, which is called the Dynamic-Blocking Procedure (DBP), is considered. This approach results from taking the sub-units in the AWE process to be infinitesimally small.

Recall that the main concern in this research is to decrease water channelling by blocking the bottom-water zone effectively so that a waterflood (or mobility control agent, MCA) would advance in the oil zone. However, the blocking process is rendered difficult by the presence of crossflow between the layers in addition to the problems of stability and ageing of the blocking agent. Thus, if somehow the crossflow is minimized, the efficiency for both the displacing and blocking processes would be improved. Therefore, the factors determining viscous crossflow must be examined. Recall the crossflow equation behind the flood front,

$$q_c = \frac{2wc_3}{\left(\frac{\mu_a h_a}{k_a} + \frac{\mu_b h_b}{k_b}\right)} \cdot \left[\frac{\cosh(X_f \sqrt{m} - \sqrt{m}) - \cosh(\sqrt{m})}{\sqrt{m}} \right], \quad \dots\dots\dots(5.6)$$

where $c_3 = \left(\frac{q_b \mu_b}{A_b k_b} - \frac{q_a \mu_a}{A_a k_a} \right) \frac{1}{\sqrt{m} \cdot \cosh(\sqrt{m})}$. Consider the term $\left(\frac{q_b \mu_b}{A_b k_b} - \frac{q_a \mu_a}{A_a k_a} \right)$ in c_3 .

When only blocking agent is injected into the bottom-water zone, this term becomes $q_b \mu_b / A_b k_b$. It is evident that by injecting a displacement fluid into the oil zone, thus including the term $q_a \mu_a / A_a k_a$, the magnitude of upward crossflow is reduced, since

$\left(\frac{q_b \mu_b}{A_b k_b} \right) > \left(\frac{q_b \mu_b}{A_b k_b} - \frac{q_a \mu_a}{A_a k_a} \right)$, provided that $\frac{q_b \mu_b}{A_b k_b} > \frac{q_a \mu_a}{A_a k_a}$. Notice that if this is considered

from the displacement point of view (the displacement fluid being water) water channelling is reduced by the injection of a blocking agent into the bottom-water zone. Thus, depending on the fluids used and the rates at which they are injected, crossflow can be controlled in both magnitude and direction. It should be noted that the above crossflow equation applies to Newtonian fluids only, so that crossflow of a blocking agent such as an emulsion is applicable only approximately. However, the previous reasoning, i.e., by reducing the vertical pressure gradient, crossflow can be reduced, is still valid.

6. EXPERIMENTAL APPARATUS AND PROCEDURE

6.1 Description of the Experimental Apparatus

The experimental apparatus used in this research is shown in Fig. 6.1. It consisted of two constant-rate pumps and an aluminium coreholder with a rectangular cross-section. Two constant-rate pumps, a Jefri pump controlled by a PC, and an ISSCO pump, were used for fluid injection. In the experiments requiring simultaneous injection of two fluids, the ISSCO pump was used in conjunction with the Jefri pump. All other experiments used the Jefri pump only. The Jefri pump was connected to two cylinders containing floating pistons. This permitted a maximum volume of 1000 ml of fluid to be injected at a maximum rate of 1200 ml/hr. The Jefri pump was monitored by an IBM PC with a precision of 0.1 ml/hr. The ISSCO pump had a capacity of 500 ml of fluid to be injected at a maximum rate of 400 ml/hr. The pressure differentials across the length of the flow model were measured by a pressure transducer capable of sensing pressures up to 345 kPa (50 psi). The rectangular coreholder was made of aluminium. The inside dimensions of the coreholder were 122 cm (4 ft) length, 7.62 cm (3 in) depth, and 5.08 cm (2 in) width, designed for a maximum pressure of 2100 kPa when properly sealed. The injection well was specially designed to allow simultaneous injection of two different fluids. This well consisted of two concentric lengths of tubing: the inside tubing delivered the fluid to the bottom-water layer, while the fluid injected into the oil zone travelled in the annulus between the two tubes. The injection points were located at the middle of each layer, Points A and B in Fig. 6.1. A similar well was installed at the production end to simulate a vertical interface between the two fluids injected (i.e. to satisfy the boundary conditions of the crossflow equations).

6.2 Packing Procedure

The model was packed by the wet-packing method with 70-100 mesh glass beads, having an average density of 2.5 g/ml. The model was tamped with a rubber hammer during the

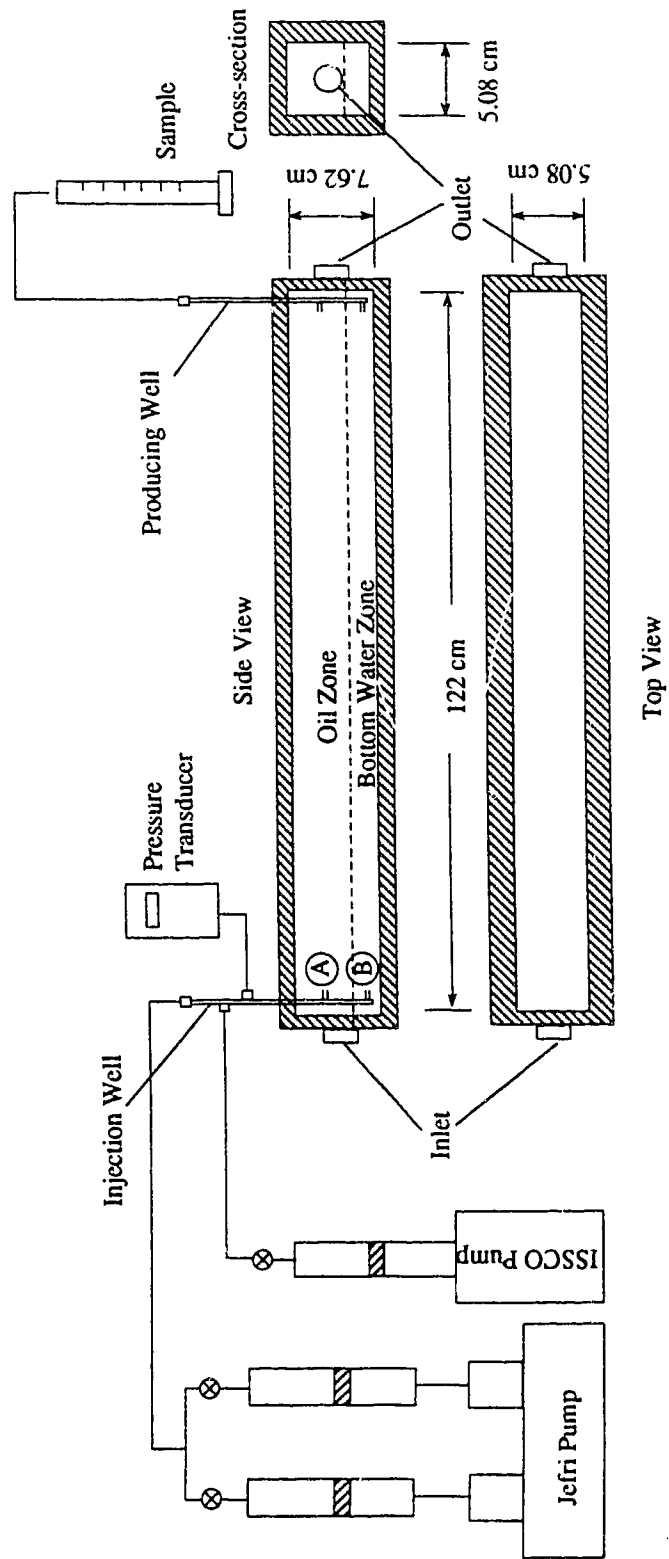


Fig. 6.1: Schematic of the Experimental Apparatus.

packing process. Once it was packed, air was driven through the bead pack for about 12 hours in order to remove the water used for packing. Then a vacuum was drawn overnight (about 24 hrs) to completely remove the water. The model was, then, connected to the pump and deionized water was pumped through. A material balance was performed to determine the pore volume of the bead pack. Subsequently, the absolute permeability of the bead pack was determined using Darcy's law for several flow rates.

At this point, an oil flood was conducted to establish the irreducible water saturation. This was done by injecting of about two pore volumes of oil, until no more mobile water was observed at the outlet. Subsequently, the permeability to oil at irreducible water saturation was determined using Darcy's law for several flow rates. The model was then opened from the side for packing the bottom-water layer. In order to establish an accurate height of the bottom-water layer, a special scraper was used to remove part of the oil bead pack. When the desired height was scraped off, the bottom-water layer was packed manually using the glass beads that were used for packing the oil zone; thus, the absolute permeability of the bottom-water layer was assumed to be the same as that of the oil layer.

The initial oil-in-place (IOIP) was calculated using the IOIP of the homogeneous pack before packing the bottom-water layer multiplied by the ratio of the height of the oil zone thickness to the model thickness. This method of obtaining the IOIP of the bottom-water layer was found to have less than 3% error when 4 checks were done by weighing the scraped-off oil layer to obtain the exact amount of the removed oil. Thus, all of the IOIP's of the bottom-water experiments were calculated using this method.

6.3 Materials, Chemicals, and Fluids

Glass beads of 70-100 mesh size were used for packing both the oil and bottom-water layers. MCT-10, supplied by Imperial Oil Ltd., was used as the oil phase and deionized

water was used for the water phase. The properties of oil and water phases can be found in Table 6.1.

Three different oil-in-water emulsions, having 10% volume dispersed (MCT-10 oil) quality, were used in the experiments as blocking agents. This amount of the dispersed phase was proven to be adequate in an earlier study⁵. Concentration of the surfactant (Stepanform HP-116, supplied by Stepan Company) was varied to obtain different emulsions (0.4%, 0.04% and 0.016% of the total volume). The stability of the emulsions was determined by visual observation of phase separation and apparent viscosity as a function of shear rate. All three emulsions were stable over a 24 hours time period; i.e., the emulsion exhibited a single phase after a 24 hours period, with no change in viscosity versus shear rate characteristics. All three emulsions had an average drop size of 2 μm . The viscosity versus shear rate behaviour of the emulsions is shown in Fig. 6.2.

TABLE 6.1: Fluid Properties at 22°C

Fluid	Viscosity (mPa.s)	Density (g/cm ³)
MCT-10 Oil	63.0	0.8709
Deionized Water	1.0	1.0

Interfacial tension between oil and water = 33.5 dyne/cm.

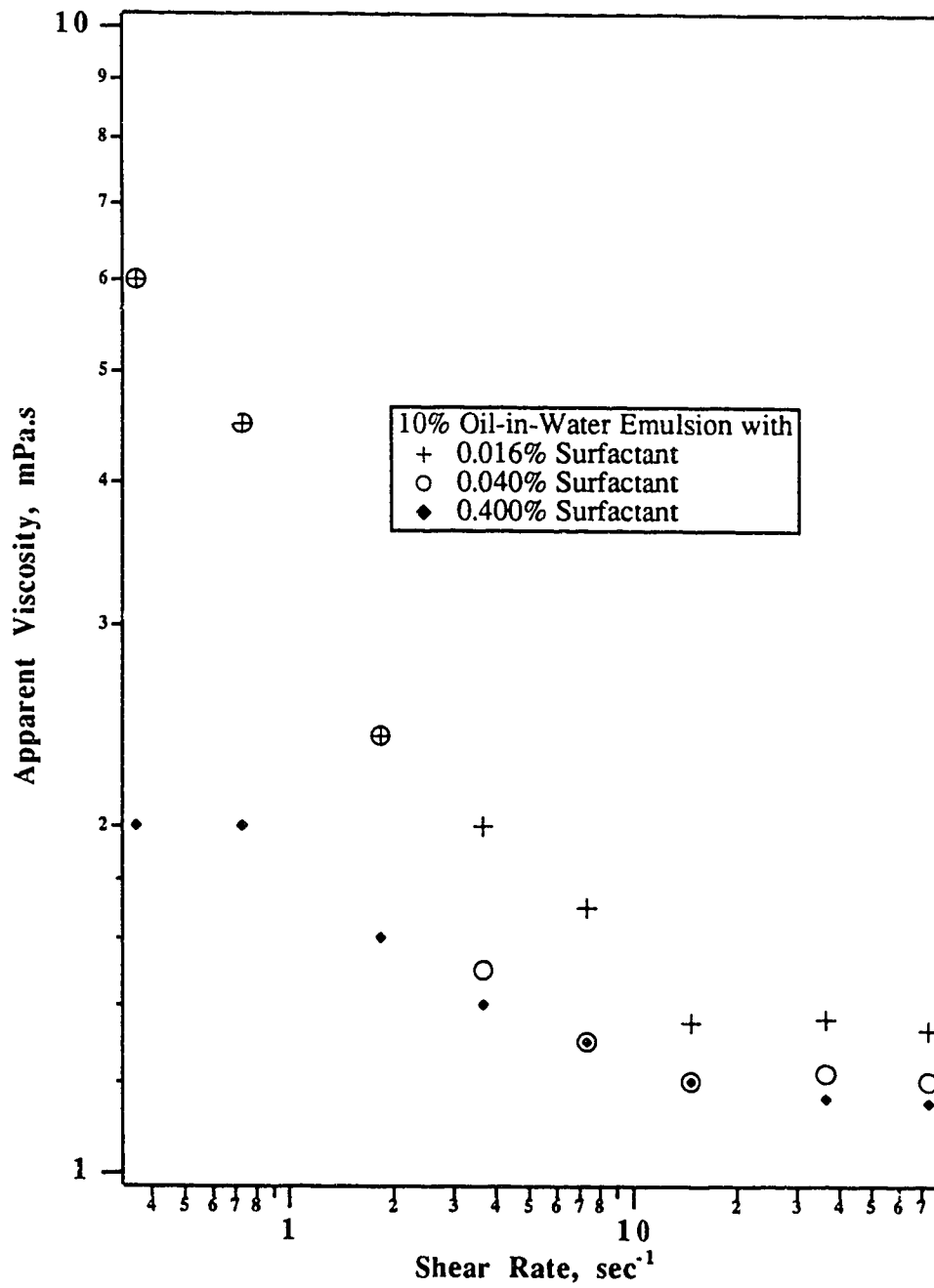


Fig. 6.2: The Effect of Concentration on Apparent Viscosity vs. Shear Rate.

7. PRESENTATION OF THE EXPERIMENTAL DATA

A total of 25 experiments was conducted to study waterflooding and various injection strategies with the use of emulsions under bottom-water conditions. The presentation of the experiments is in chronological order. A summary chart of the runs is given in Fig. 7.1 for classification of the types of runs conducted. Results of all the experiments are summarized in Table 7.1. Data for each experiment is also presented in tabular form in Appendix A.

Runs 1 and 2: Waterfloods at Different Injection Rates

Runs 1 and 2 were carried out at different water injection rates in a homogeneous pack (viz. no bottom-water). This was done to study the waterflood performance in the absence of the bottom-water layer, and to estimate the effective permeability to water at residual oil saturation, k_{wor} , for later analysis. These runs served as base runs since the effect would be comparable to completely blocking the bottom-water layer, if present. In Run 1, an injection rate of 400 ml/hr was used. Water breakthrough occurred after 0.391 HCPV of fluid production. Figure 7.2 shows the production history for this run. Notice that after water breakthrough, the oil cut dropped sharply.

In Run 2, an injection rate of 600 ml/hr was used. Water breakthrough occurred at 0.332 HCPV of fluid production. Figure 7.3 shows the production history of this run. Again, after water breakthrough, the oil cut dropped sharply. Figures 7.2 and 7.3 show that the production histories for Runs 1 and 2 are very similar. Thus, it is concluded that the injection rate does not play a significant role over the range considered.

Effect of Emulsion Slug Size

Run 3: Bottom-Water Run with Emulsion-Slug Process (0.4% Surfactant Conc. Emulsion)
 $h_o/h_{bw} = 3$, $k_o/k_{bw} = 1$, Slug Size = $0.5 PV_{bw}$

Run 3 was conducted to study the effect of the Emulsion-Slug Process with a small emulsion slug size. An oil-to-bottom-water layer thickness ratio (h_o/h_{bw}) of 3:1 was used in

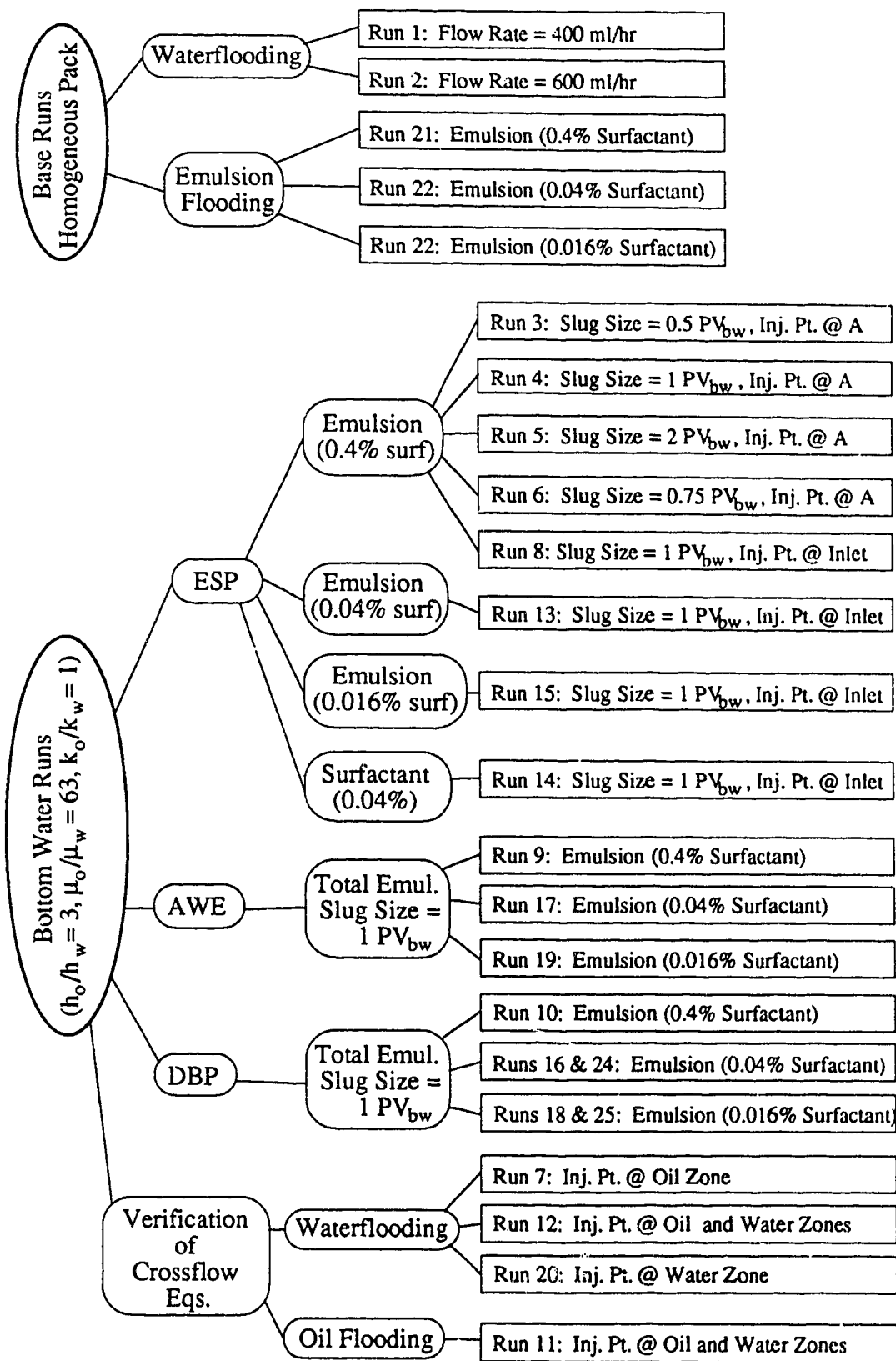


Fig. 7.1: Summary Chart of all the Experiments.

TABLE 7.1: Summary of the Experimental Results

Run No.	Process	Blocking Agent	Slug Size PVbw	ko (μm^2)	Porosity ϕ	Soi	IOIP (cm ³)	Recovery @ WOR=20
1	BASE	N/A	N/A	23.7	0.371	0.934	1612	59.5
2	BASE	N/A	N/A	23.7	0.371	0.934	1612	62.5
3	ESP	Emulsion (0.4%)	0.5	21.4	0.369	0.932	1200	20.0
4	ESP	Emulsion (0.4%)	1	18.7	0.368	0.935	1200	23.3
5	ESP	Emulsion (0.4%)	2	21.9	0.370	0.930	1200	22.4
6	ESP	Emulsion (0.4%)	0.75	18.0	0.370	0.930	1200	25.1
7	WF	N/A	N/A	18.0	0.360	0.926	1163	50.1
8	ESP	Emulsion (0.4%)	1	17.5	0.357	0.933	1162	27.7
9	AWE	Emulsion (0.4%)	1	18.5	0.360	0.932	1170	22.6
10	DBP	Emulsion (0.4%)	1	18.5	0.359	0.931	1165	17.0
11	OF	N/A	N/A	21.3	0.371	0.927	1200	N/A
12	WF	N/A	N/A	20.0	0.363	0.932	1180	48.5
13	ESP	Emulsion (0.04%)	1	18.2	0.355	0.931	1153	43.6
14	ESP	Surfactant (0.04%)	1	17.8	0.354	0.931	1150	34.0
15	ESP	Emulsion (0.016%)	1	18.5	0.352	0.937	1150	48.4
16	DBP	Emulsion (0.016%)	1	18.9	0.357	0.928	1155	66.0
17	AWE	Emulsion (0.016%)	1	18.4	0.356	0.930	1155	60.8
18	DBP	Emulsion (0.04%)	1	19.3	0.355	0.933	1155	60.0
19	AWE	Emulsion (0.04%)	1	19.0	0.353	0.934	1150	54.3
20	WF	N/A	N/A	19.0	0.357	0.933	1162	46.6
21	BASE	Emulsion (0.4%)	N/A	19.5	0.359	0.928	1150	43.4
22	BASE	Emulsion (0.04%)	N/A	19.1	0.350	0.922	1500	59.2
23	BASE	Emulsion (0.016%)	N/A	19.3	0.351	0.931	1520	71.5
24	DBP	Emulsion (0.016%)	1	19.3	0.358	0.933	1165	66.1
25	DBP	Emulsion (0.04%)	1	19.0	0.355	0.933	1150	59.5

AWE - Alternating-Water-Emulsion Process

BASE - Base Run

DBP - Dynamic-Blocking Procedure

ESP - Emulsion-Slug Process

N/A - Not Applicable

OF - Oil Flood

WF - Waterflood

For all experiments:

ho/hw = 3,

Injection Rate = 400 ml/hr except for Run 2 which was 600 ml/hr.

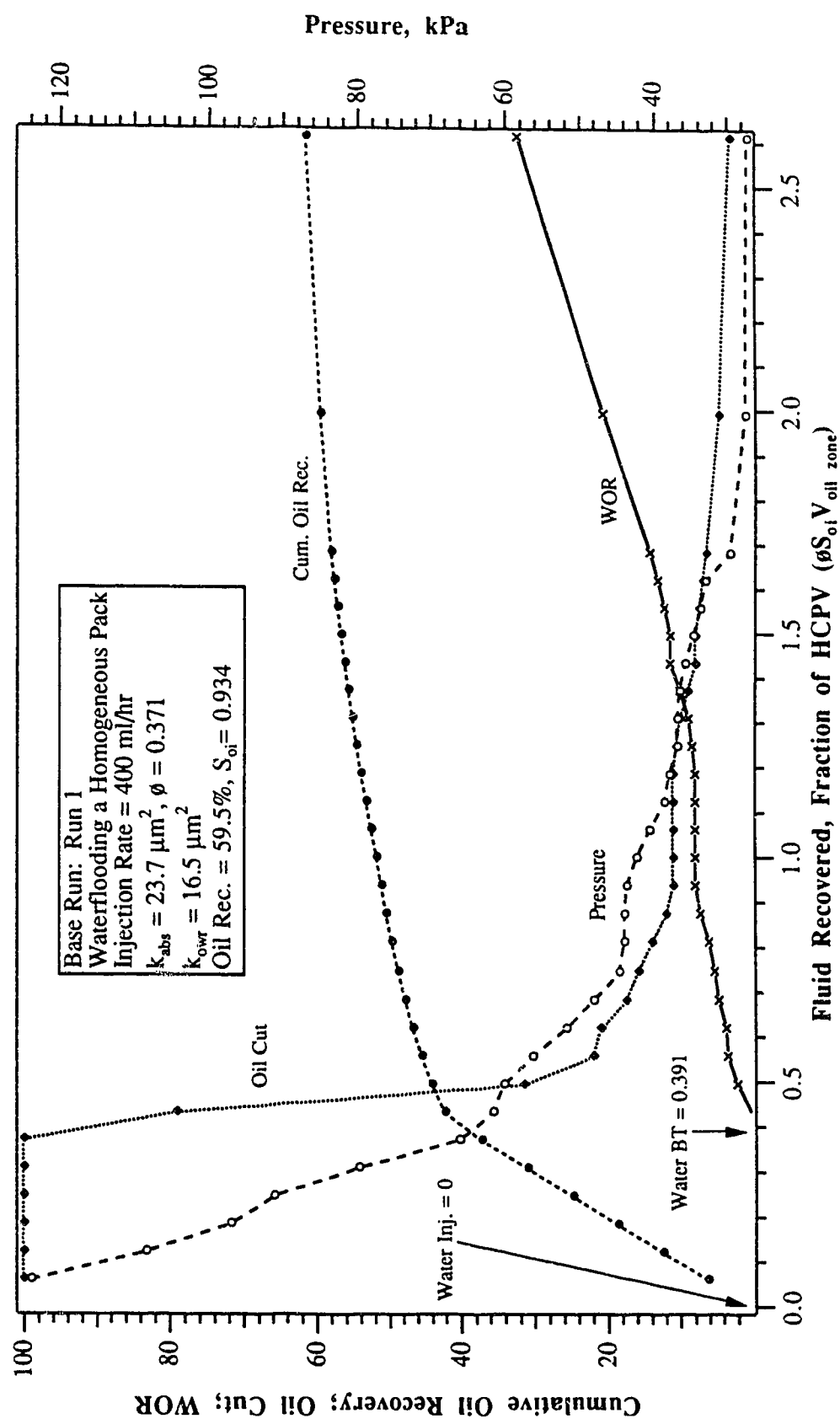


Fig. 7.2: Production History for Run 1. Waterflooding a Homogeneous Pack (Inj. Rate = 400 ml/hr).

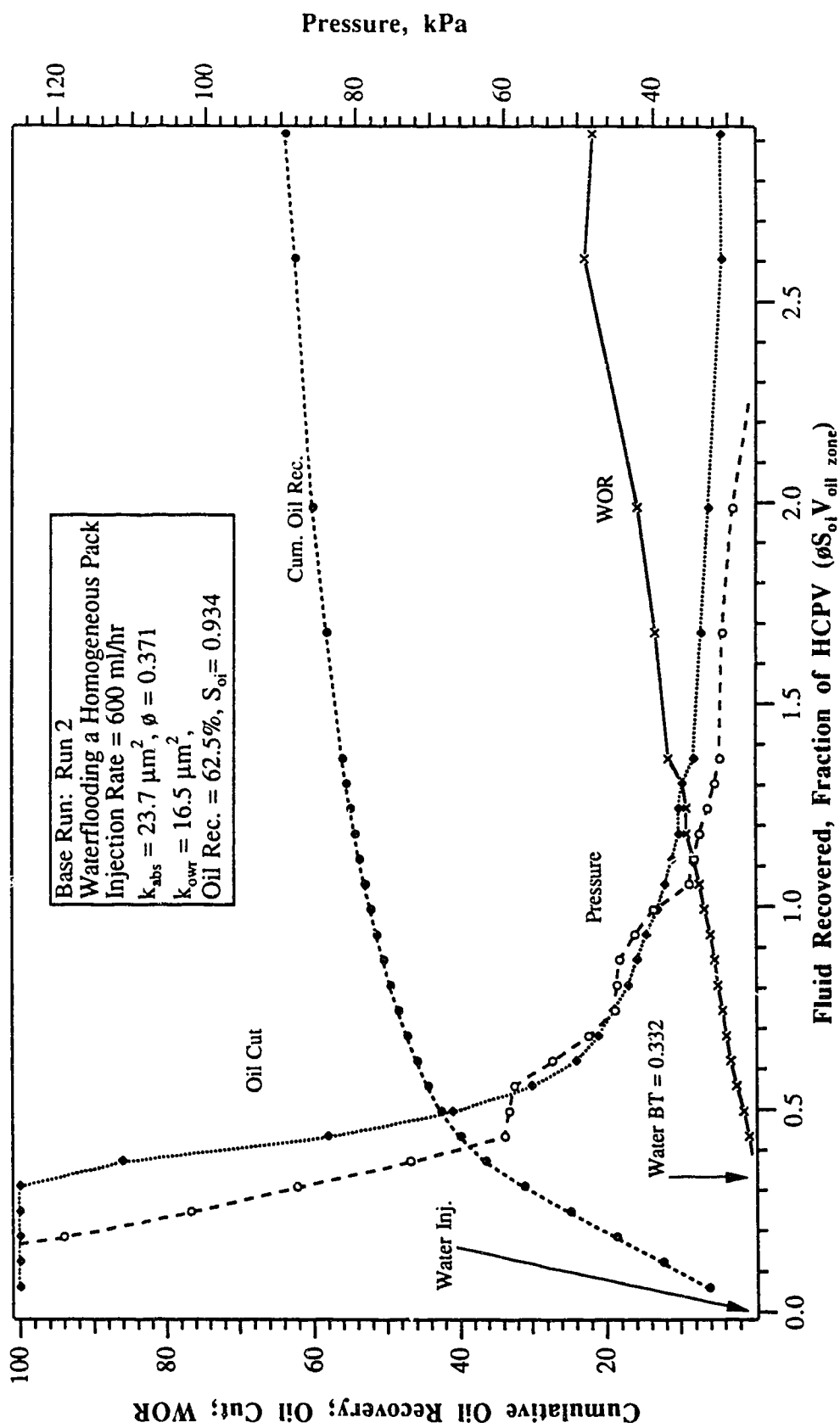


Fig. 7.3: Production History for Run 2. Waterflooding a Homogeneous Pack (Inj. Rate = 600 ml/hr).

the experiment. Absolute permeabilities of both zones were equal ($k_o/k_{bw} = 1$). The injection and production wells were located at a depth of 50% of the oil zone. Both the emulsion and the water were injected through the injection well, Point A in Fig. 6.1. In this run, a $0.5 PV_{bw}$ (bottom-water pore volume) of emulsion was injected at the beginning of the run at a rate of 400 ml/hr, followed by water injection at the same rate. Notice that $0.5 PV_{bw}$ is equivalent to a volume of 0.18 HCPV.

Water breakthrough occurred after 0.0083 HCPV (10 ml) of fluid production, indicating that the emulsion was going into the bottom-water zone. Figure 7.4 shows the production history of this run. Notice that the oil cut decreased rapidly to less than 15%, while the pressure increased to the maximum permissible value. This rapid drop in oil cut indicates that the emulsion was blocking the bottom-water zone. After emulsion breakthrough at 0.225 HCPV of fluid production, the oil cut increased from 14% to a maximum of 60% and then dropped rapidly to a low value. This indicates that the emulsion slug had only partially blocked the water layer and as a result of the partial block, the injected water bypassed the oil zone. This resulted in a low ultimate oil recovery: only 20% of IOIP was recovered. (Note: ultimate oil recovery is defined as that obtained at a producing WOR equal to or greater than 20.)

Run 4: Bottom-Water Run with Emulsion-Slug Process (0.4% Surfactant Conc. Emulsion)
 $h_o/h_{bw} = 3$, $k_o/k_{bw} = 1$, Slug Size = $1.0 PV_{bw}$

A larger emulsion slug size was used in Run 4, $1.0 PV_{bw}$. In this run, the ratio of the height and permeability as well as the depth of the injection well were kept the same ($h_o/h_{bw} = 3:1$, $k_o/k_{bw} = 1$, well penetration equal to 50%). The only variable was the emulsion slug size. This time an emulsion slug size of $1.0 PV_{bw}$ was used.

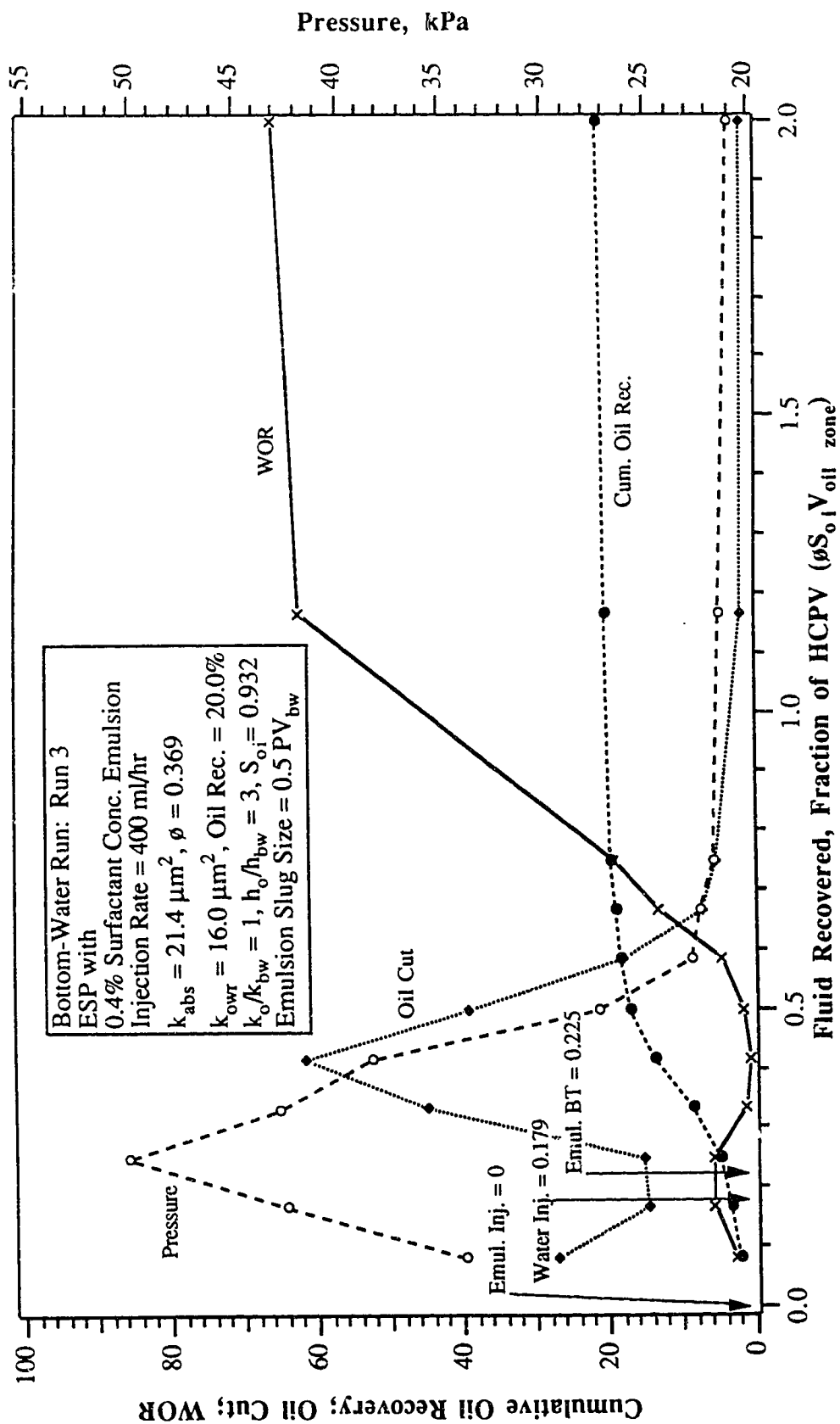


Fig. 7.4: Production History for Run 3. Emulsion Flooding a Bottom-Water Reservoir Using the ESP (Emulsion Slug Size = $0.5 PV_{bw}$).

The emulsion was again injected through the injection well at a rate of 400 ml/hr at the start of the run. Figure 7.5 shows the production history of this run. Water breakthrough occurred early at 0.014 HCPV of fluid production, and initial oil cut dropped to 13%, which indicated that the injected fluid was going into the bottom-water zone. The rapid increase in the injection pressure indicated that the emulsion was blocking the bottom-water. After emulsion breakthrough at 0.252 HCPV of fluid production, the oil cut increased to a maximum of 62.5%. Unlike Run 3, this time the oil cut did not drop sharply; instead, it remained high for a while, before dropping to a low value. Because of this larger slug size, a high oil cut was sustained for a longer period of time, which gave a better ultimate oil recovery of 23.3% IOIP.

Run 5: Bottom-Water Run with Emulsion-Slug Process (0.4% Surfactant Conc. Emulsion)
 $h_o/h_{bw} = 3$, $k_o/k_{bw} = 1$, Slug Size = 2.0 PV_{bw}

Run 5 was conducted to investigate further the effect of slug size on recovery. Once again, all parameters except the slug size were kept constant. A 2.0 PV_{bw} emulsion slug was used. The production history is shown in Figure 7.6. Unlike Runs 3 and 4, initial oil cut did not drop to a very low value; it declined to 20.5%. Early water breakthrough at 0.013 HCPV of fluid production, and rising pressure during the initial period indicated that the emulsion was starting to block off the bottom-water layer. After emulsion breakthrough at 0.279 HCPV of fluid production, the oil cut which was still decreasing, started to increase and peaked at 0.50 HCPV of fluid production. This maximum value was less than that for the previous runs, but was sustained for a longer period.

Since a larger slug size was used, it was expected that a higher ultimate recovery would be obtained. Contrary to expectations, the ultimate recovery - 22.4% IOIP - was less than that for Run 4 (23.3% of IOIP for a 1.0 PV_{bw} emulsion slug). Because the ultimate oil recovery for the two runs was very close, it was assumed that the optimal emulsion slug size had

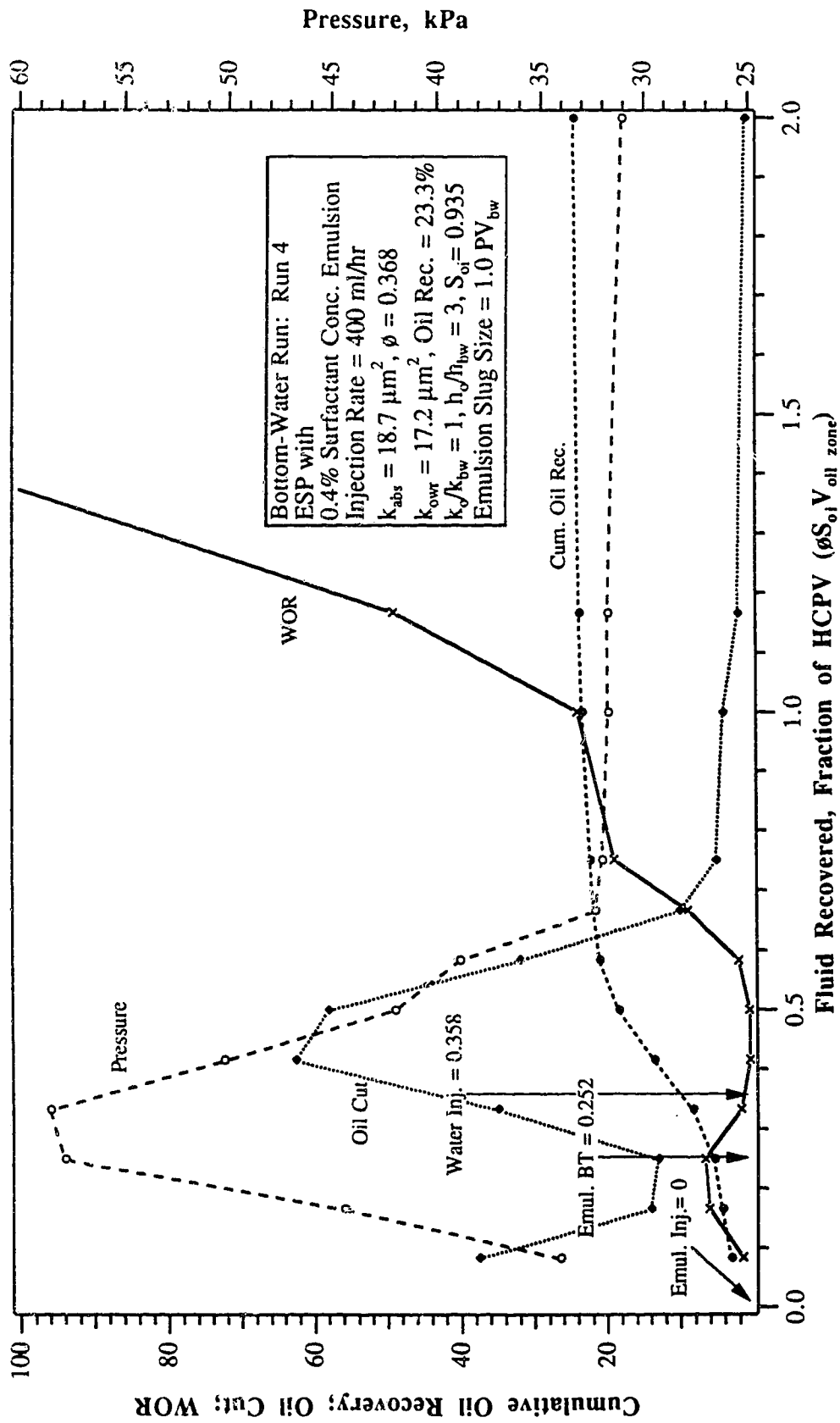


Fig. 7.3. Production History for Run 4. Emulsion Flooding a Bottom-Water Reservoir Using the ESP (Emulsion Slug Size = 1.0 PV_{bw}).

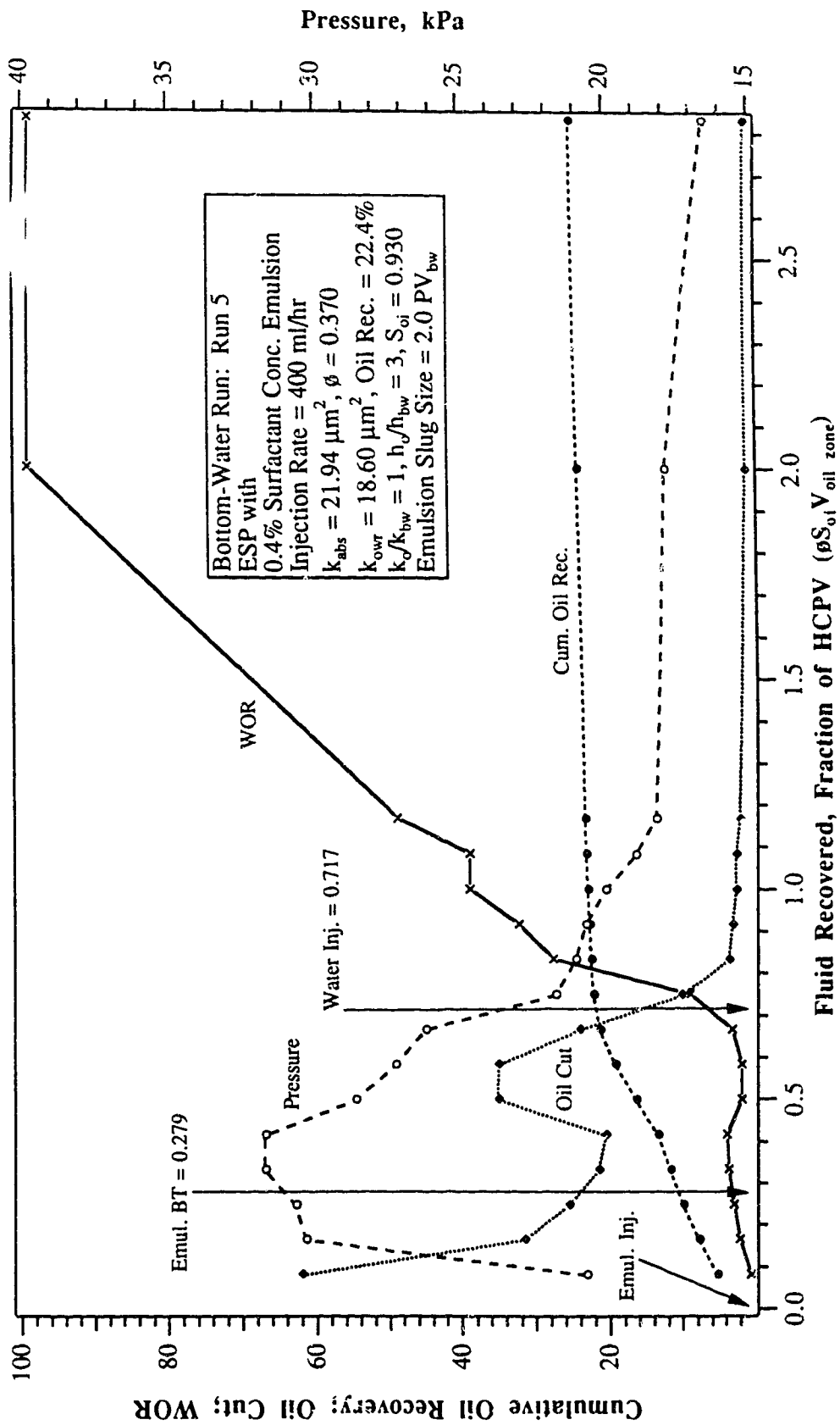


Fig. 7.6: Production History for Run 5. Emulsion Flooding a Bottom-Water Reservoir Using the ESP (Emulsion Slug Size = 2.0 PV_{bw}).

been reached (i.e., a larger emulsion slug size would not recover any additional oil). It appeared that the optimal slug size was approximately $1.0 PV_{bw}$.

Run 6: Bottom-Water Run with Emulsion-Slug Process (0.4% Surfactant Conc. Emulsion)
 $h_o/h_{bw} = 3$, $k_o/k_{bw} = 1$, Slug Size = $0.75 PV_{bw}$

This run was designed to pinpoint the optimal slug size for the emulsion. From Runs 3 and 4, it was found that a slug size greater than $1.0 PV_{bw}$ would not help to recover more oil. As before, all parameters except for the slug size were kept constant. Figure 7.7 shows the production history of this run. The emulsion slug was injected through the injection well at a rate of 400 ml/hr, followed by a waterflood at the same rate. Water breakthrough was at 0.014 HCPV of fluid production, indicating that the emulsion was entering the bottom-water zone. An increase in pressure before emulsion breakthrough indicated that the emulsion was blocking the bottom-water zone. This time, however, the initial oil cut dropped to only 30%. After emulsion breakthrough at 0.246 HCPV of fluid production, the oil cut increased to a maximum of 57%. This run followed a trend similar to that of Run 3, except for the minimum oil cut value, which was twice that in Run 3. Because of the comparatively higher initial oil cut, this run gave the highest ultimate oil recovery (25.1% of IOIP) of all the runs with bottom-water. However, this figure is only slightly higher than 23.3%, obtained when an emulsion slug size of $1 PV_{bw}$ was used in Run 4.

Run 7: Bottom-Water Run with Waterflood in the Oil Zone
 $h_o/h_{bw} = 3$, $k_o/k_{bw} = 1$

This run had the same parameters as all previous runs with bottom-water, the only difference being that no emulsion was used. This was done in order to see waterflood performance under bottom-water conditions ($h_o/h_{bw} = 3$, $k_o/k_{bw} = 1$, and well penetration = 50% of oil-zone thickness). With the previous runs in view, it was expected that the waterflood performance without the help of a blocking agent would be very poor. However, an ultimate oil recovery of 50.1% of IOIP was obtained, which is far more than

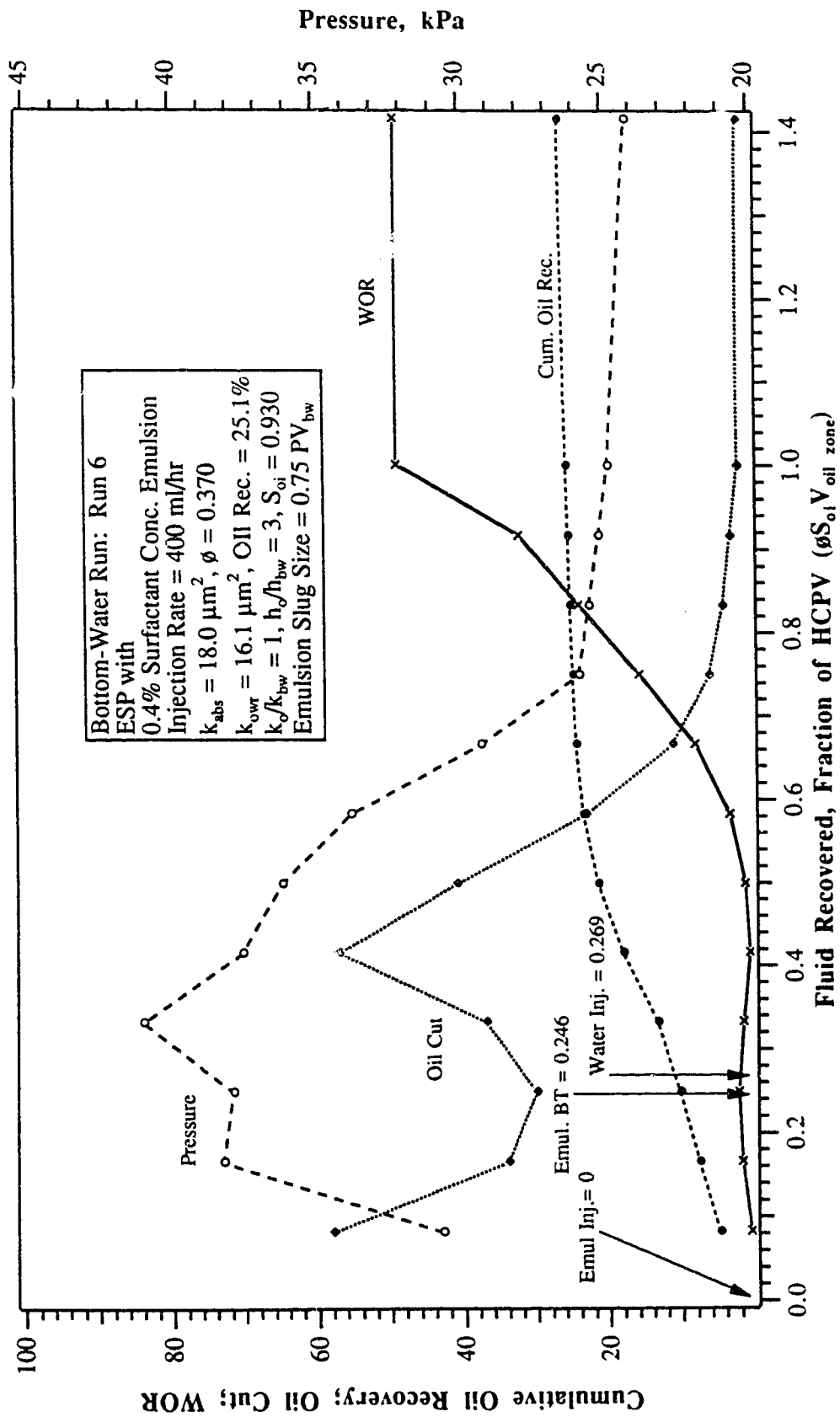


Fig. 7.7: Production History for Run 6. Emulsion Flooding a Bottom-Water Reservoir Using the ESP (Emulsion Slug Size = 0.75 PV_{bw}).

expected. Figure 7.8 shows the production history of this run. Notice that the pressure did not rise to as high a value as in previous runs, but was sustained at close to the maximum value for a longer time. The oil cut dropped very rapidly to 20%, and then increased slowly to a maximum of 37%. However, since this oil cut remained at an average of 33.2% for a period of 0.767 HCPV of fluid production, oil recovery was almost 40% before the decline started.

Run 8: Bottom-Water Run with Emulsion-Slug Process (0.4% Surfactant Conc. Emulsion)
 $h_o/h_{bw} = 3$, $k_o/k_{bw} = 1$, Slug Size = $1.0 PV_{bw}$

The reason for carrying out Run 8 was to see if the emulsion injection point influenced oil recovery. Run 8, in essence, duplicated the conditions of Run 4, except that the emulsion injection point was the end inlet, instead of the injection well (see Fig. 6.1). This end inlet was located at the centre of the injection end. Because the end inlet was designed to pack the model and to measure k_{abs} only, a semi-permeable metal plate was installed, which acted as a smooth wall to the model, while covering the injection end. (Note: the injection Point B in Fig. 6.1 had not been installed at the time of the experiment; therefore, the end inlet was used instead.)

Comparing Run 8 (Fig. 7.9) with other emulsion floods (especially Run 4), two differences are to be noted in this run. They are 1) the faster response time, and 2) a higher oil cut. First, it took only 0.172 HCPV of injected emulsion before the oil cut started to increase. This value is much less compared to that for other runs (0.25 HCPV in Run 4). Second, the oil cut increased to 81.7% (62.5% in Run 4, which was the highest among the other runs). With these two changes, the ultimate oil recovery was 27.7% of IOIP, which is 4.4% percentiles higher than the recovery for Run 4, which is credited to a more favourable emulsion injection position. Thus, it can be seen that the point of emulsion injection has an effect on oil recovery under bottom-water conditions. However, the difference is still too small for it to be conclusive.

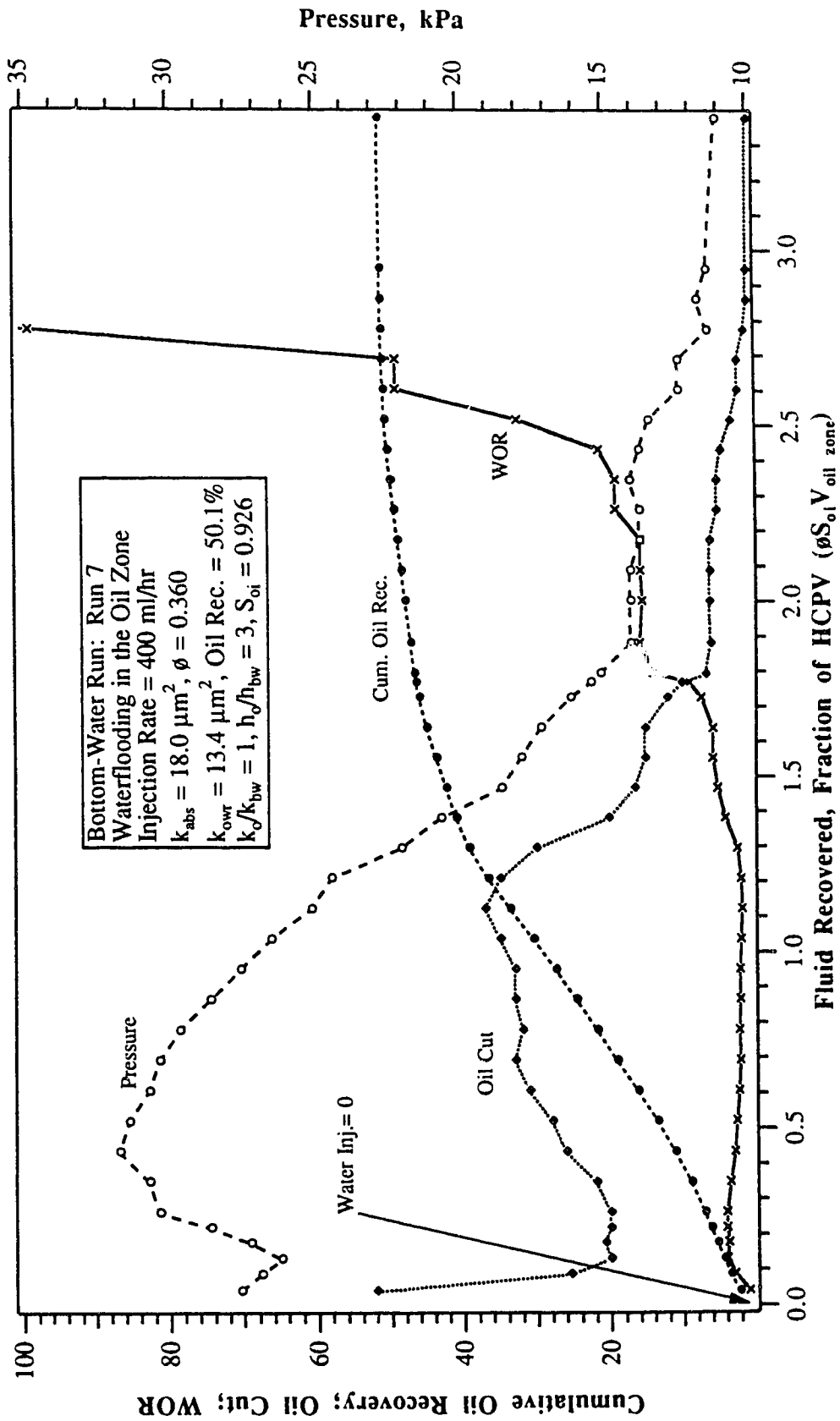


Fig. 7.8: Production History for Run 7. Waterflooding a Bottom-Water Reservoir.

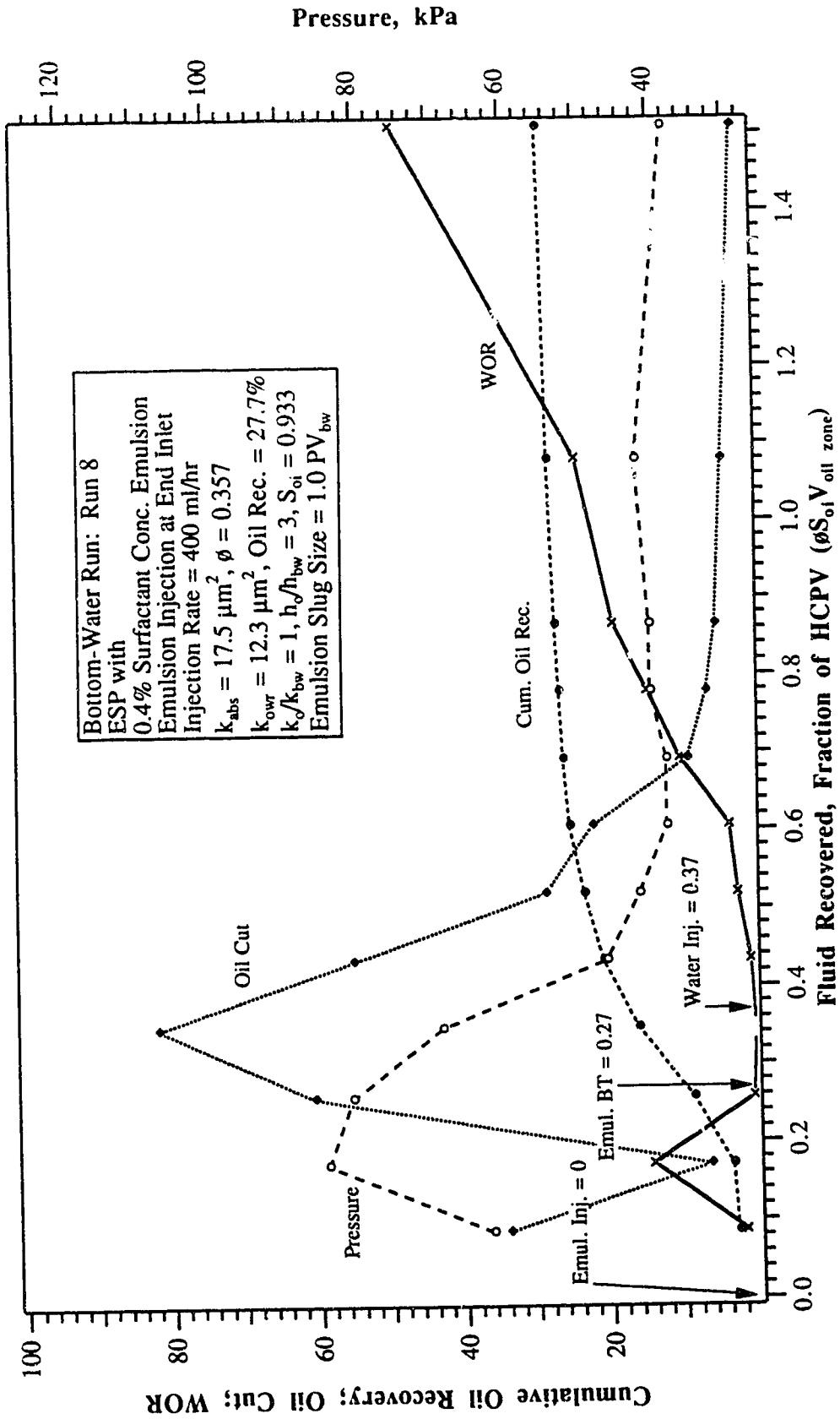


Fig. 7.9: Production History for Run 8. Emulsion Flooding a Bottom-Water Reservoir Using the ESP (Emulsion Slug Size = $1.0 PV_{bw}$)

Run 9: Bottom-Water Run with AWE Process (0.4% Surfactant Conc. Emulsion)
 $h_o/h_{bw} = 3$, $k_o/k_{bw} = 1$, Slug Size = $1.0 PV_{bw}$ (= $4 \times 0.25 PV_{bw}$)

Run 9 was conducted to study the effect of the AWE process. An oil-to-bottom-water layer thickness ratio (h_o/h_{bw}) of 3:1 was used in the experiment. Absolute permeabilities of both zones were equal ($k_o/k_{bw} = 1$). The $1.0 PV_{bw}$ emulsion slug was divided into four batches to block the water zone. Similarly, the drive water was divided into four batches, each of which had a size of $0.25 PV$ of the oil zone. Unlike the previous runs with a single injection point, this run was conducted with a special well that allowed emulsion injection in the water zone and water injection in the oil zone, as described in the previous section. The run was started by injecting a $0.25 PV_{bw}$ emulsion slug into the water zone, followed by a $0.25 PV_{oil}$ water slug into the oil zone. The whole process was repeated by injecting the emulsion and water alternately. The production history is shown in Fig. 7.10.

The production history of this run is similar to that of the previous single slug runs. Water breakthrough occurred after 0.01 HCPV of fluid production, indicating that the emulsion was going into the bottom-water zone. Notice how the oil cut decreased rapidly to less than 10%, while the pressure increased to a maximum. This rapid drop indicates that the emulsion was blocking the bottom-water zone. The only difference between this run and the previous runs is that the pressure increased shortly after each emulsion injection. However, there was not a noticeable increase in the oil cut corresponding to the pressure increment. The highest oil cut was 47.0%. The ultimate oil recovery was 22.6% of IOIP, which is similar to that for Run 4 with a single emulsion slug, 23.3% of IOIP.

Run 10: Bottom-Water Run with Dynamic-Blocking Procedure
 (0.4% Surfactant Conc. Emulsion) $h_o/h_{bw} = 3$, $k_o/k_{bw} = 1$, Slug Size = $1.0 PV_{bw}$

Because Run 9 did not show an improvement in oil recovery over Run 4, where a single slug was employed, the simultaneous injection of emulsion and water was investigated in this run. Given the same amount of emulsion, $1.0 PV_{bw}$, the single slug is an extreme case

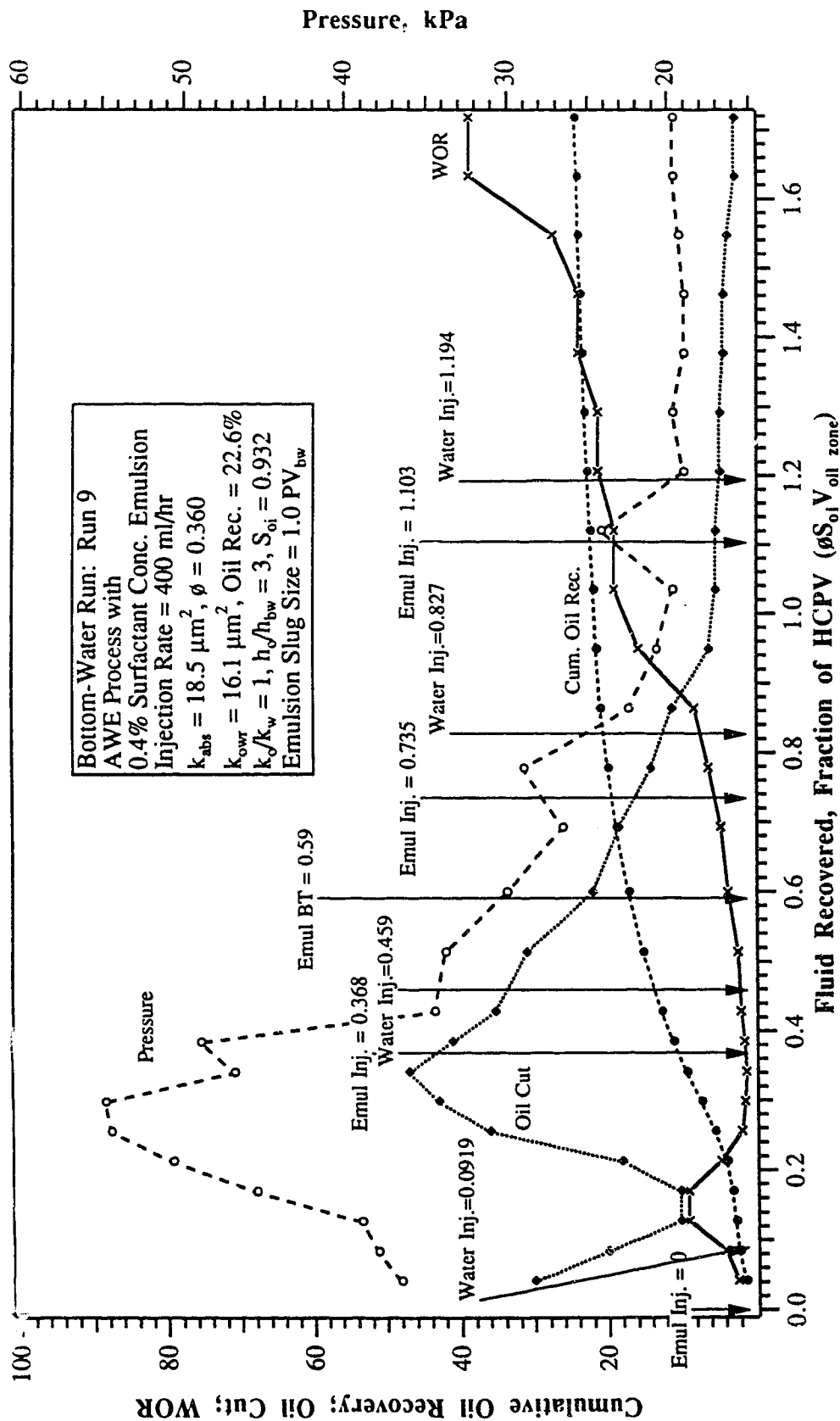


Fig. 7.10: Production History for Run 9. Emulsion Flooding a Bottom-Water Reservoir Using the AWE Process (Emulsion Slug Size = 1.0 PV_{bw}).

of the AWE process because it employs only one slug. (On the other hand, as the number of slugs increases, in the limit it is equivalent to injecting the emulsion and water simultaneously into the water and the oil zones, respectively.) The production history for this run is shown in Fig. 7.11.

The oil cut peaked at 36.8%, and then dropped sharply. Because of the low oil cut obtained during production, the ultimate oil recovery was low: 17.0% of IOIP. This value is the lowest among all the previous runs with bottom-water.

Runs 11 and 12: Oil Flooding and Waterflooding a Bottom-Water Formation

Run 11 was carried out to examine the effect of injection fluid on oil recovery under bottom-water conditions. In this run, the same in-place oil was injected into both oil and bottom-water zones. To simulate a vertical front displacement, the respective volumetric injection rates for the zones were proportional to the cross-sectional area of each zone. Figure 7.12 shows the production history for Run 11. Notice that after 0.35 HCPV of fluid production, an oil cut of 76% was attained. However, despite the fact that the mobility ratios were favourable in both oil and bottom-water zones, the oil cut decreased for a period of 0.18 HCPV of fluid production to less than 20%, before it started to increase. Thus, it seems that the low oil rate during initial production of a bottom-water reservoir is unavoidable. When a high oil cut of 76% was reached, this value was sustained for a period of 0.37 HCPV of fluid production before the oil cut started to increase due to production of injected oil. Thus, it appears that there is a pseudostable region where the oil cut is approximately constant for a Newtonian fluid flooding a bottom-water formation. A similar pseudostable region was observed in Run 7.

Run 12 was carried out to further investigate this region. This run employed the exact injection strategy and experimental set-up as that of Run 11, the only difference being that water was injected instead of oil. Also, Run 12 is similar to Run 7 except that water

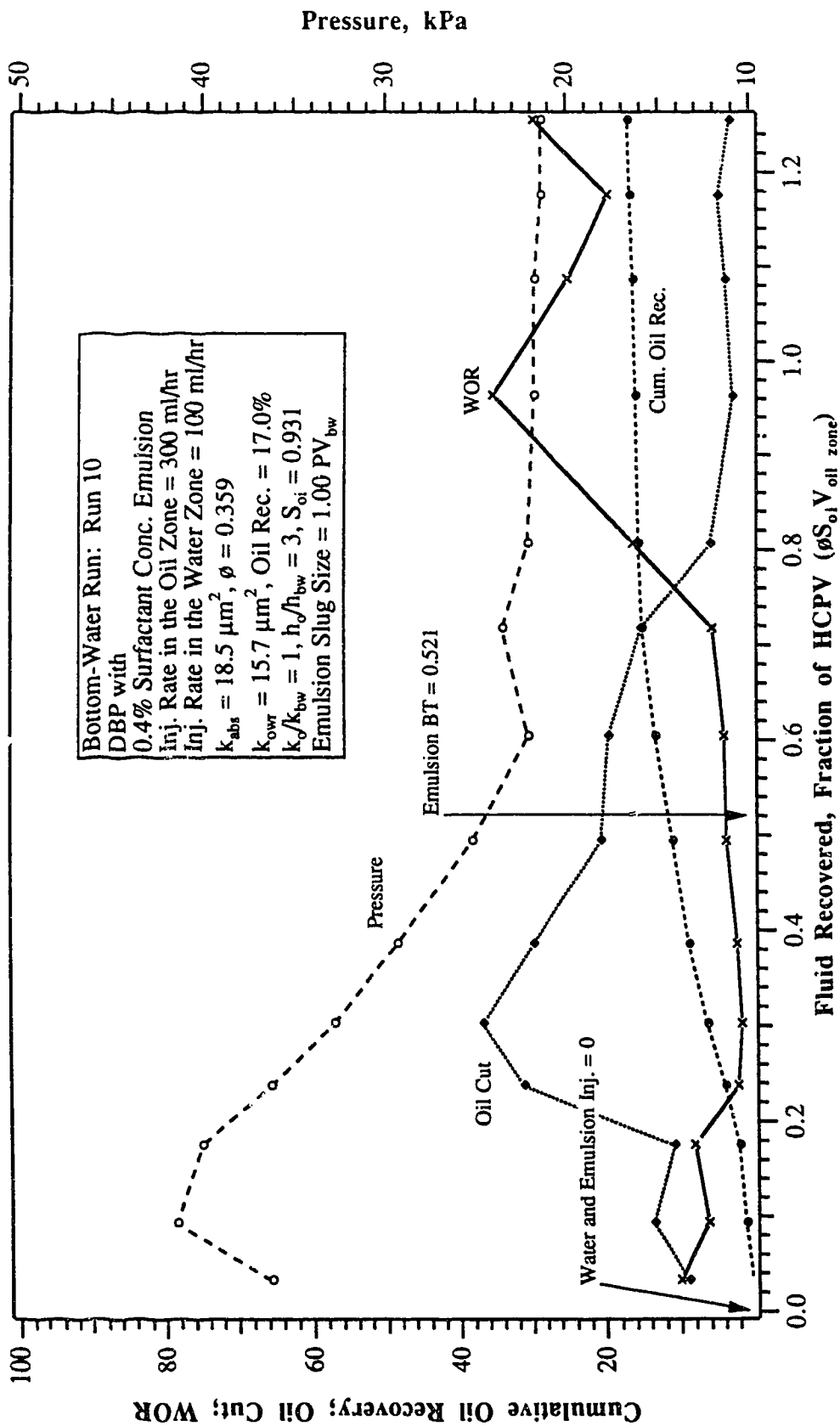


Fig. 7.11: Production History for Run 10. Emulsion Flooding a Bottom-Water Reservoir Using the DBP (Emulsion Slug Size = 1.0 PV_{bw}).

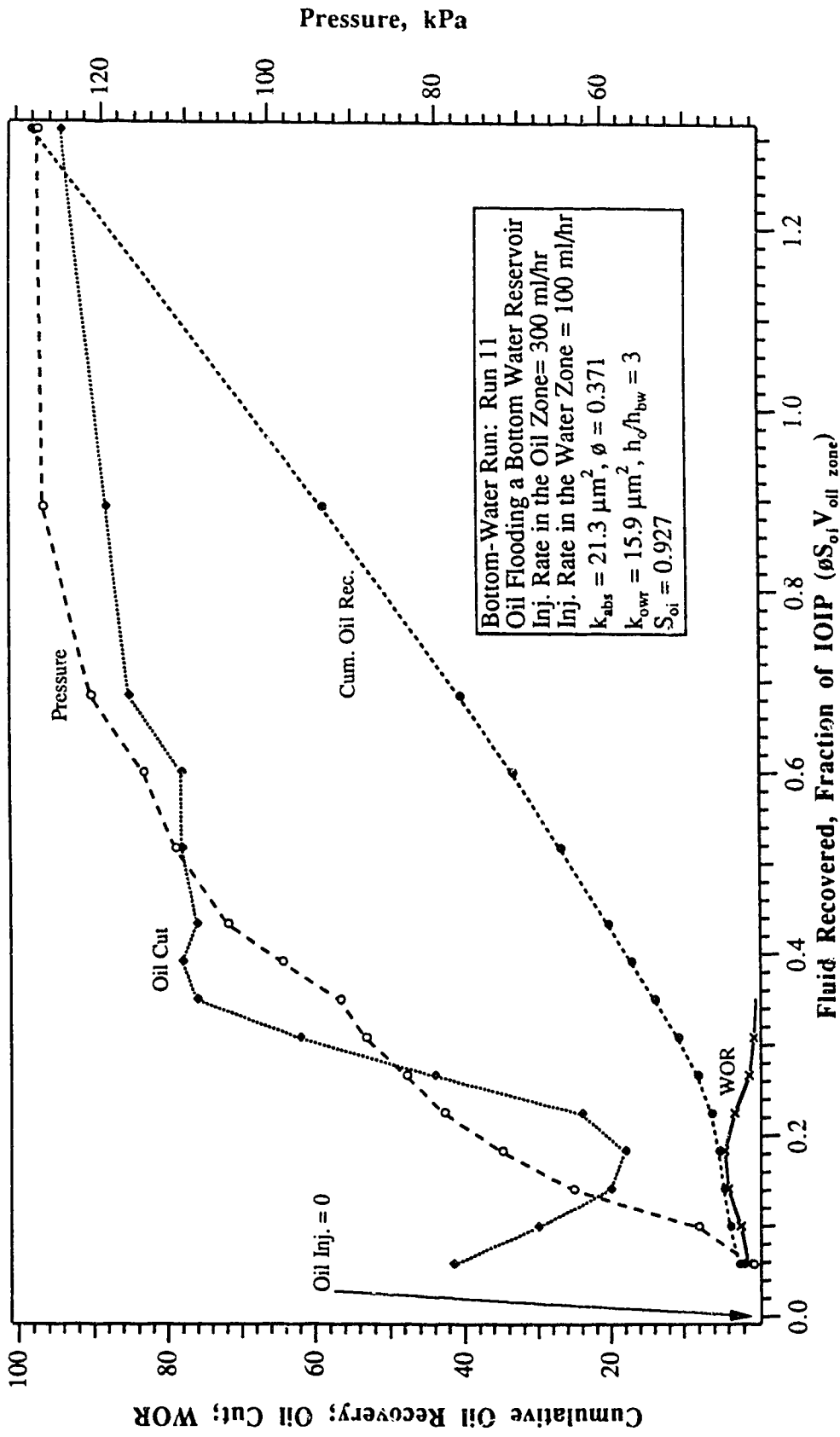


Fig. 7.12: Production History for Run 11. Oil Flooding a Bottom-Water Reservoir.

injection in Run 12 was conducted in both layers. From the production history in Fig. 7.13, it can be seen that the oil cut curve had a trend similar to that of Run 7. Notice that an oil cut of 33.3% for a period of 0.76 HCPV of fluid production was obtained. Thus, 25.3% of IOIP was recovered during this pseudostable period. When the WOR was over 20, an ultimate oil recovery of 48.5% IOIP was obtained as compared to 50.1% for Run 7.

Run 13: Bottom-Water Run with Emulsion-Slug Process
(0.04% Surfactant Conc. Emulsion) $h_o/h_{bw} = 3$, $k_o/k_{bw} = 1$, Slug Size = 1.0 PV_{bw}

This experiment was carried out to examine the effect of a lower surfactant concentration emulsion on oil recovery under bottom-water conditions. Run 13, in essence, duplicated the conditions of Run 8, except that the surfactant concentration of the emulsion was lowered to 0.04% from 0.4%. The viscosity versus shear rate relationship of this emulsion can be found in Fig. 6.2. The end inlet was used for emulsion injection even though injection Point B was available. This was done to single out the variable of a lower surfactant concentration emulsion in this run with Run 8.

The production history in Fig. 7.14 shows that all curves exhibit trends similar to those in Run 8 except that the oil cut was sustained at a high value of 60% for a period of 0.27 HCPV of fluid production, giving over 16% IOIP recovery. Also, the oil cut did not drop as rapidly as in Run 8; as a result, an oil recovery of 43.6% was obtained when the WOR reached 20. Thus, by lowering the surfactant concentration by a factor of 10, using the Emulsion-Slug Process, the ultimate oil recovery was improved by 15.9 percentiles.

Run 14: Bottom-Water Run with Emulsion-Slug Process (0.04% Surfactant Solution)
 $h_o/h_{bw} = 3$, $k_o/k_{bw} = 1$, Slug Size = 1.0 PV_{bw}

Run 14 had the same injection strategy and experimental set-up as that of Run 13; the only difference being that 0.04% surfactant was injected instead of emulsion (i.e., the 10% oil was removed from the emulsion used in Run 13). Thus, this run examined whether the

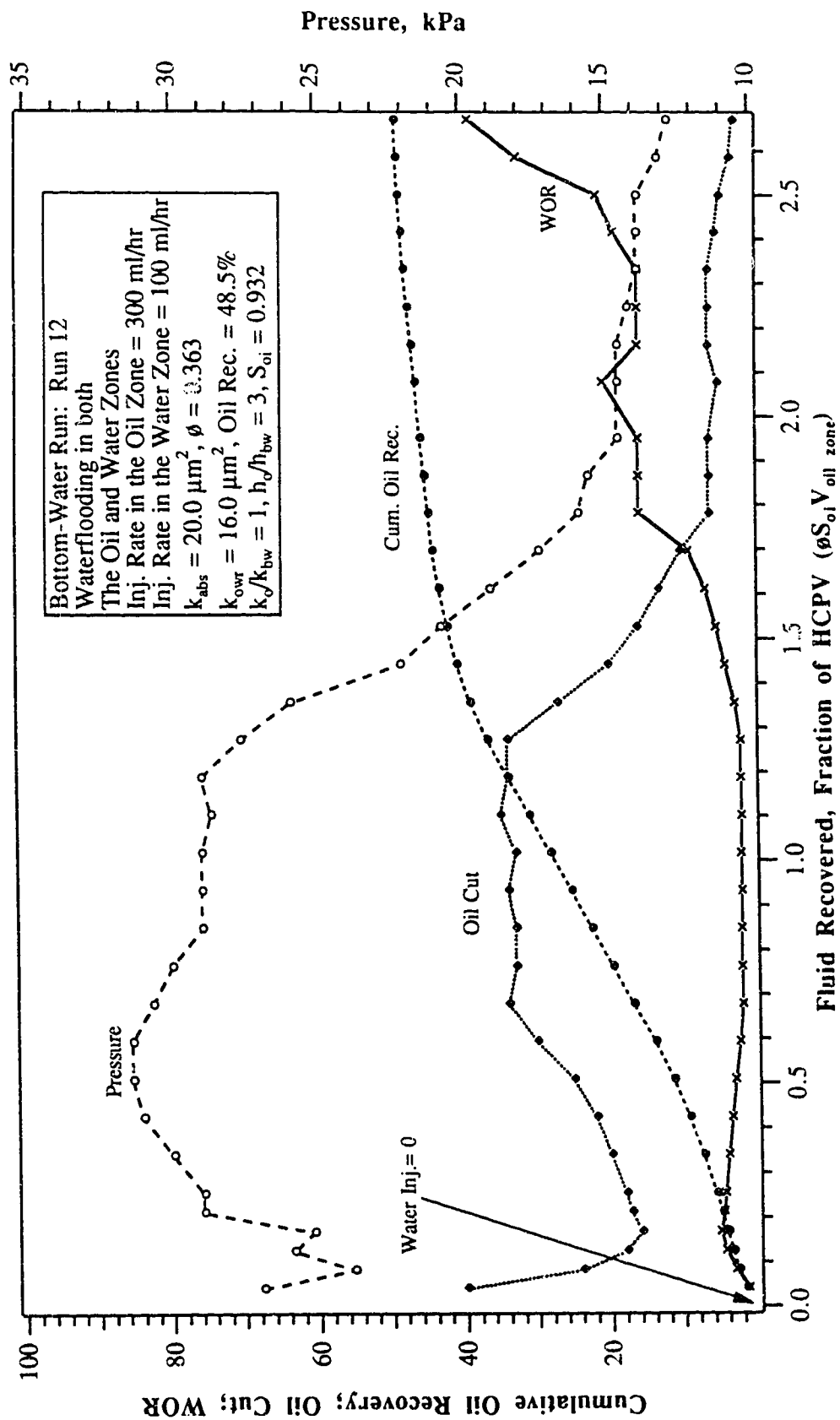


Fig. 7.13: Production History for Run 12. Waterflooding a Bottom-Water Reservoir in both the Oil and Water Zones.

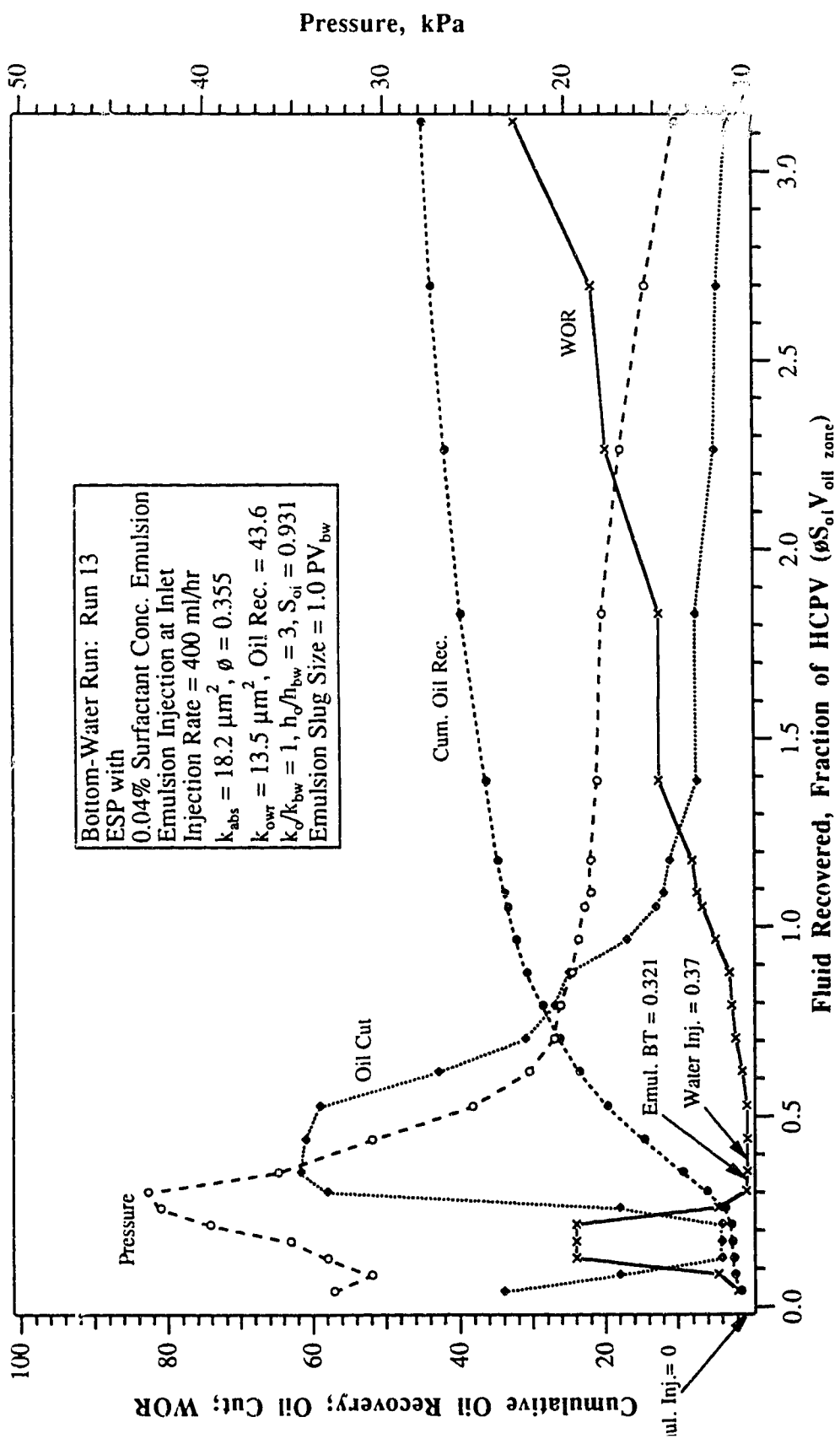


Fig. 7.14: Production History for Run 13. Emulsion Flooding a Bottom-Water Reservoir Using the ESP (0.04% Surfactant Conc. Emulsion).

10% of oil in the emulsion was needed. Note that 10% oil in a 1 PV_{bw} is less than 4% IOIP under the conditions studied.

The production history plot in Fig. 7.15 shows that the injection of surfactant gave an oil cut similar to that in Run 13. However, after the oil cut reached a maximum of 67%; it declined much more rapidly as compared to the case of an emulsion slug. Thus, surfactant showed very little, if any, blockage in the bottom-water zone after a maximum oil cut was reached. As a result, an ultimate oil recovery of 34% IOIP was achieved. Thus, by emulsifying less than 4% IOIP oil to prepare an emulsion slug, as in Run 13, an extra 9.6% IOIP was recovered.

Run 15: Bottom-Water Run with Emulsion-Slug Process
(0.016% Surfactant Conc. Emulsion) $h_o/h_{bw} = 3$, $k_o/k_{bw} = 1$, Slug Size = 1.0 PV_{bw}

This experiment was carried out to investigate further the effect of a lower surfactant concentration emulsion on oil recovery under bottom-water conditions. In this run, a surfactant concentration of 0.016% was used to make a 10% oil-in-water emulsion. This was the minimum concentration needed to obtain a stable emulsion; also, this concentration was used in a previous study⁵ for making a stable emulsion. Run 15, in essence, duplicated the conditions of Runs 8 and 13, except that the surfactant concentration was lowered to 0.016%. The viscosity versus shear rate relationship for this emulsion can be found in Fig. 6.2. Again, the end inlet was used for emulsion injection so that this run could be compared with Runs 8 and 13.

It can be seen from the production history in Fig. 7.16 that all curves exhibit trends similar to those of Runs 8 and 13. As in Run 13, oil cut was sustained at a high average value of 58% for a period of 0.30 HCPV of fluid production, giving over 17% IOIP recovery. Also, the oil cut did not drop as rapidly as in Run 8; as a result, an oil recovery of 48.4% was obtained when the WOR reached 20. Thus, by lowering the surfactant concentration

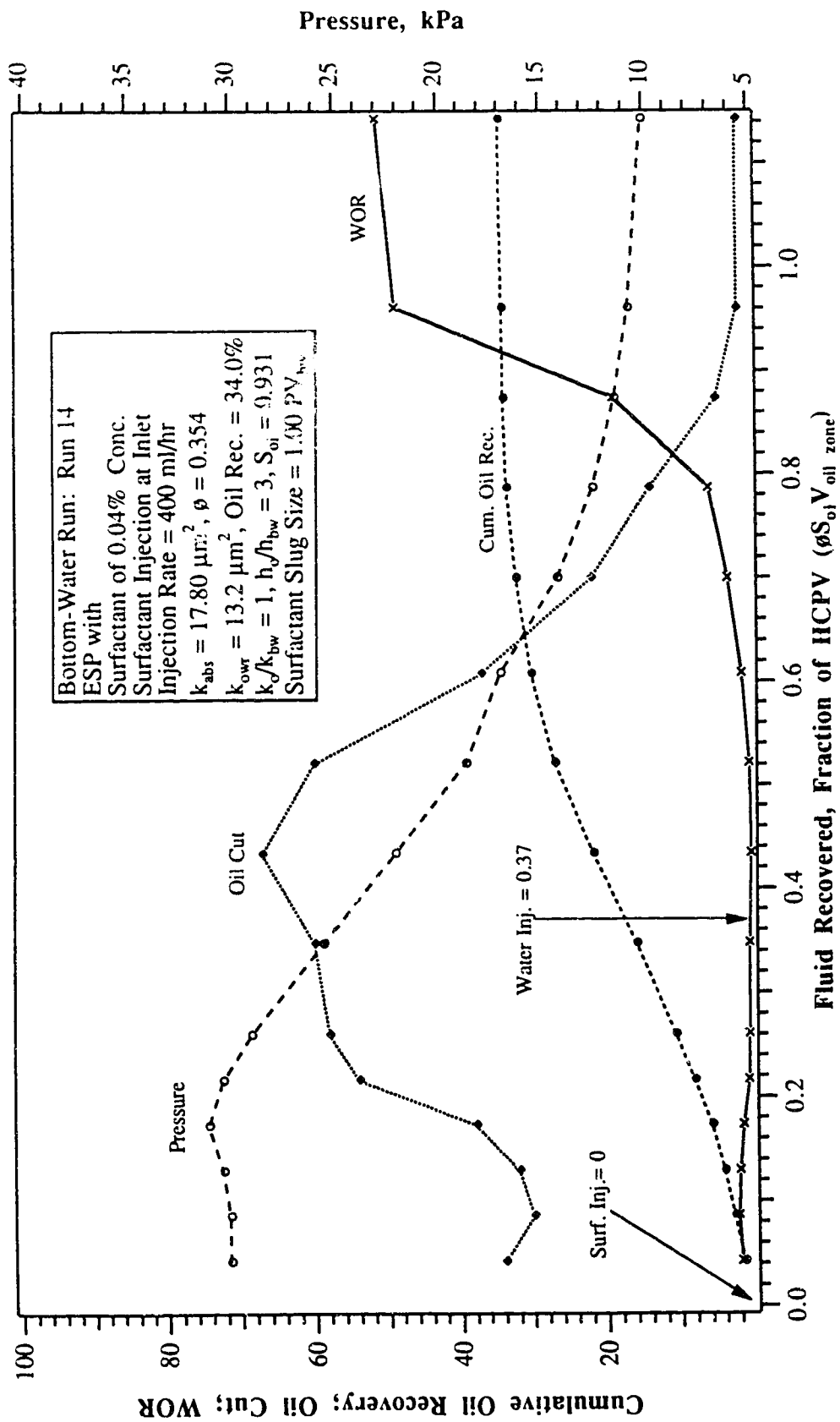


Fig. 7.15: Production History for Run 14. Surfactant Flooding a Bottom-Water Reservoir Using the ESP (Surfactant Conc. 0.04%).

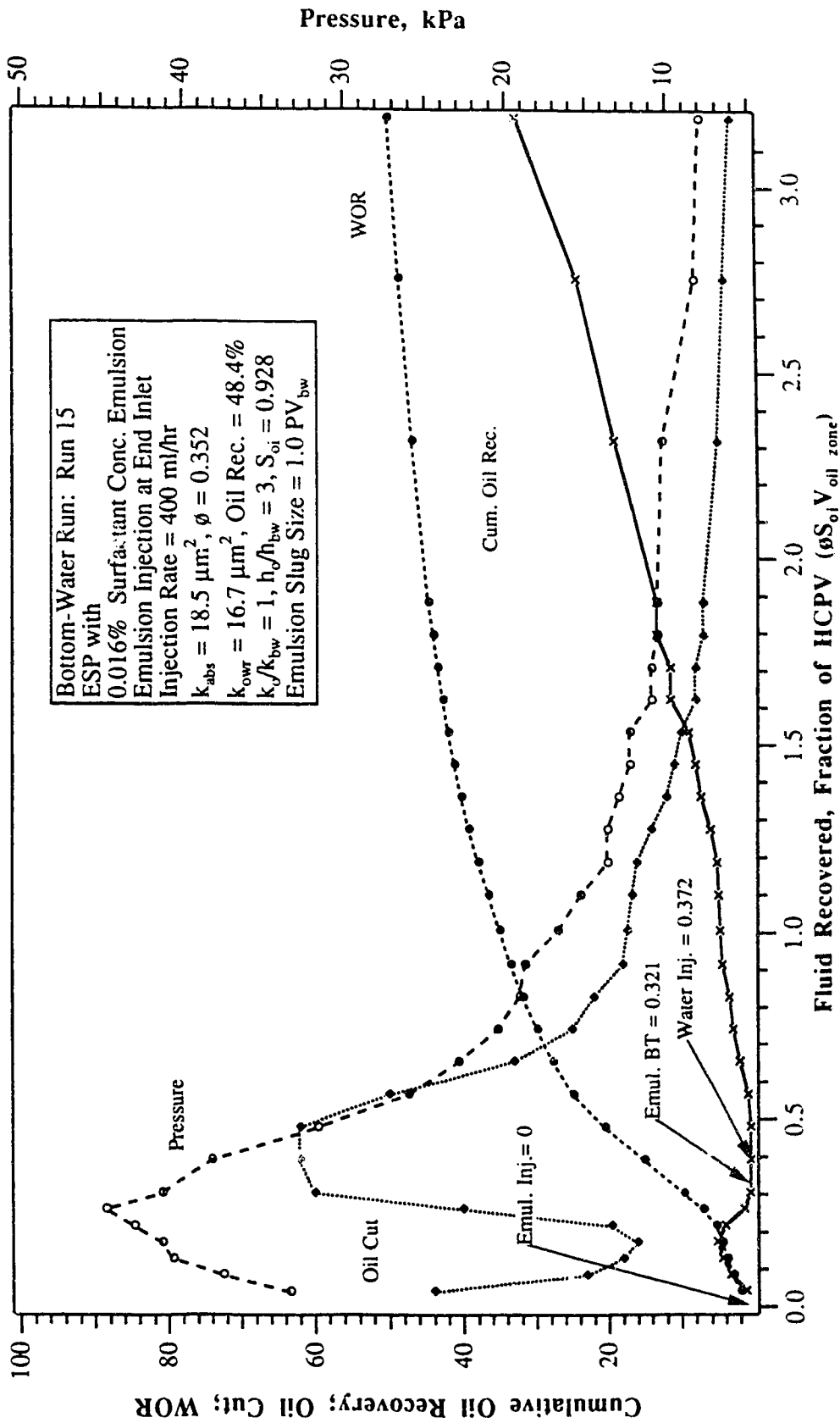


Fig. 7.16: Production History for Run 15. Emulsion Flooding a Bottom-Water Reservoir Using the ESP (0.016% Surfactant Conc. Emulsion).

further to 0.016%, using the Emulsion-Slug Process, the ultimate oil recovery was improved by 20.7% and 4.8% over Runs 8 and 13, respectively.

Runs 16 and 17: Effect of Injection Strategy on Bottom-Water Runs Using 0.016% Surfactant Conc. Emulsion ($h_o/h_{bw} = 3$, $k_o/k_{bw} = 1$, Slug Size = $1.0 PV_{bw}$)

To examine the effect of injection strategy on oil recovery under bottom-water conditions, Runs 16 and 17 were conducted using the Dynamic-Blocking Procedure, DBP, and the Alternate-Water-Emulsion, AWE, process. In these runs, the experimental set-up and the emulsion used in Run 15 were kept unchanged to examine the effect of injection strategy. In the DBP injection method, water and emulsion are injected simultaneously into the oil and bottom-water zones, respectively. The injection rates are proportional to the cross-sectional areas to simulate a vertical front displacement. On the other hand, in the AWE process, water and emulsion are injected alternately into the oil and bottom-water zones, respectively. The $1.0 PV_{bw}$ emulsion slug was divided into four batches to block the water zone. Similarly, the drive water was divided into four batches, each of which had a size of 0.25 PV of the oil zone.

The production history for Run 16 (Fig. 7.17) shows that the oil cut curve had a trend similar to that of Run 15 employing the Emulsion-Slug Process. However, the oil cut declined much more slowly in this run. This suggested that the blocking process of the emulsion lasted for a longer time period when the DBP method was used. As a result, an ultimate oil recovery of 66% IOIP was obtained in Run 16, as compared to 48.4% IOIP in Run 15. Comparing this run with Run 10, which utilized the same experimental set-up and injection strategy but a higher surfactant concentration emulsion, the result was quite different: an ultimate oil recovery of 17% IOIP for Run 10 as compared to 66% for Run 16. Thus, it was concluded that the DBP injection strategy is strongly affected by the blocking agent used.

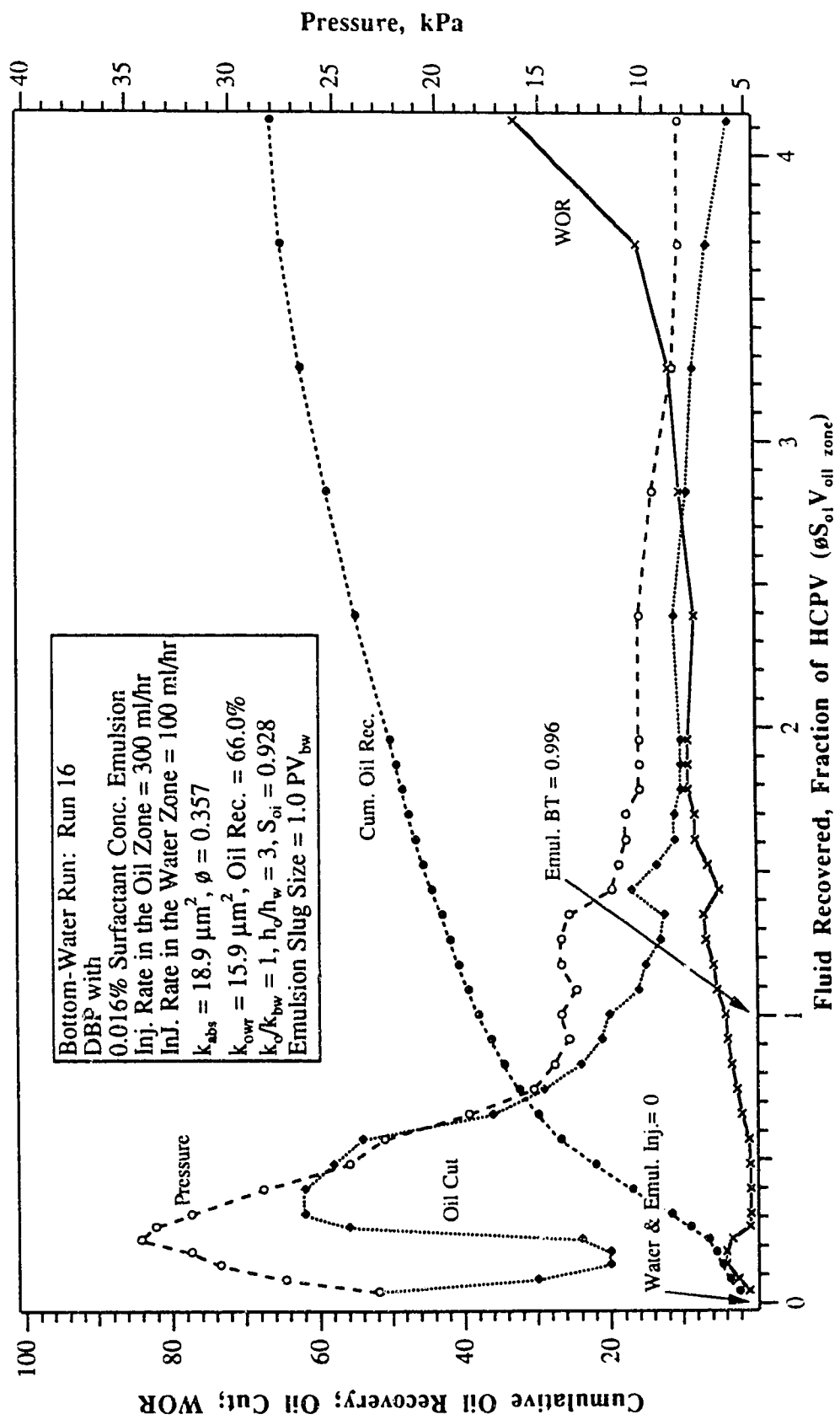


Fig. 7.17: Production History for Run 16. Emulsion Flooding a Bottom-Water Reservoir Using the DBP (0.016% Surfactant Conc. Emulsion).

Similarly for the AWE process, the production history for which is shown in Fig. 7.18, it can be seen that the oil cut curve had a trend similar to that of Runs 15 and 16. The oil cut declined much more slowly than that in Run 15, but it was similar to that in Run 16. As a result, an ultimate oil recovery of 60.8% IOIP was obtained in Run 17. Comparing this run with Run 9, which utilized an identical experimental set-up and injection strategy but a higher surfactant concentration emulsion, the result was quite different: an ultimate oil recovery of 22.6% IOIP for Run 9 as compared to 60.8% for Run 17. Thus, it was concluded that the AWE injection strategy is also strongly affected by the blocking agent used.

Runs 18 and 19: Effect of Injection Strategy on Bottom-Water Runs Using 0.04%
Surfactant Conc. Emulsion ($h_o/h_{bw} = 3$, $k_o/k_{bw} = 1$, Slug Size = $1.0 PV_{bw}$)

To examine the effect of surfactant concentration in emulsion on injection strategies under bottom-water conditions, Runs 18 and 19 were conducted using the Dynamic-Blocking Procedure, DBP, and the Alternate-Water-Emulsion, AWE, process. Runs 18 and 19, in essence, duplicated Runs 16 and 17, respectively, the only difference being that a slightly higher surfactant concentration emulsion was used: 0.04%.

The production histories for Runs 18 and 19, plotted in Figs. 7.19 and 7.20, show that the oil-cut curves had a trend similar to those of Runs 16 and 17, respectively. The only difference in Runs 18 and 19 with a higher surfactant concentration was that the oil cut for these runs was slightly lower than that in Runs 16 and 17, respectively. As a result, ultimate oil recovery was lower for these runs: an ultimate oil recovery of 60% IOIP for Run 18 and 54.3% IOIP for Run 19. Comparing these runs with Runs 16 and 17 (ultimate oil recovery of 66% IOIP and 60.8% IOIP, respectively), it was concluded that both the DBP and AWE injection strategies are governed by the blocking agent used.

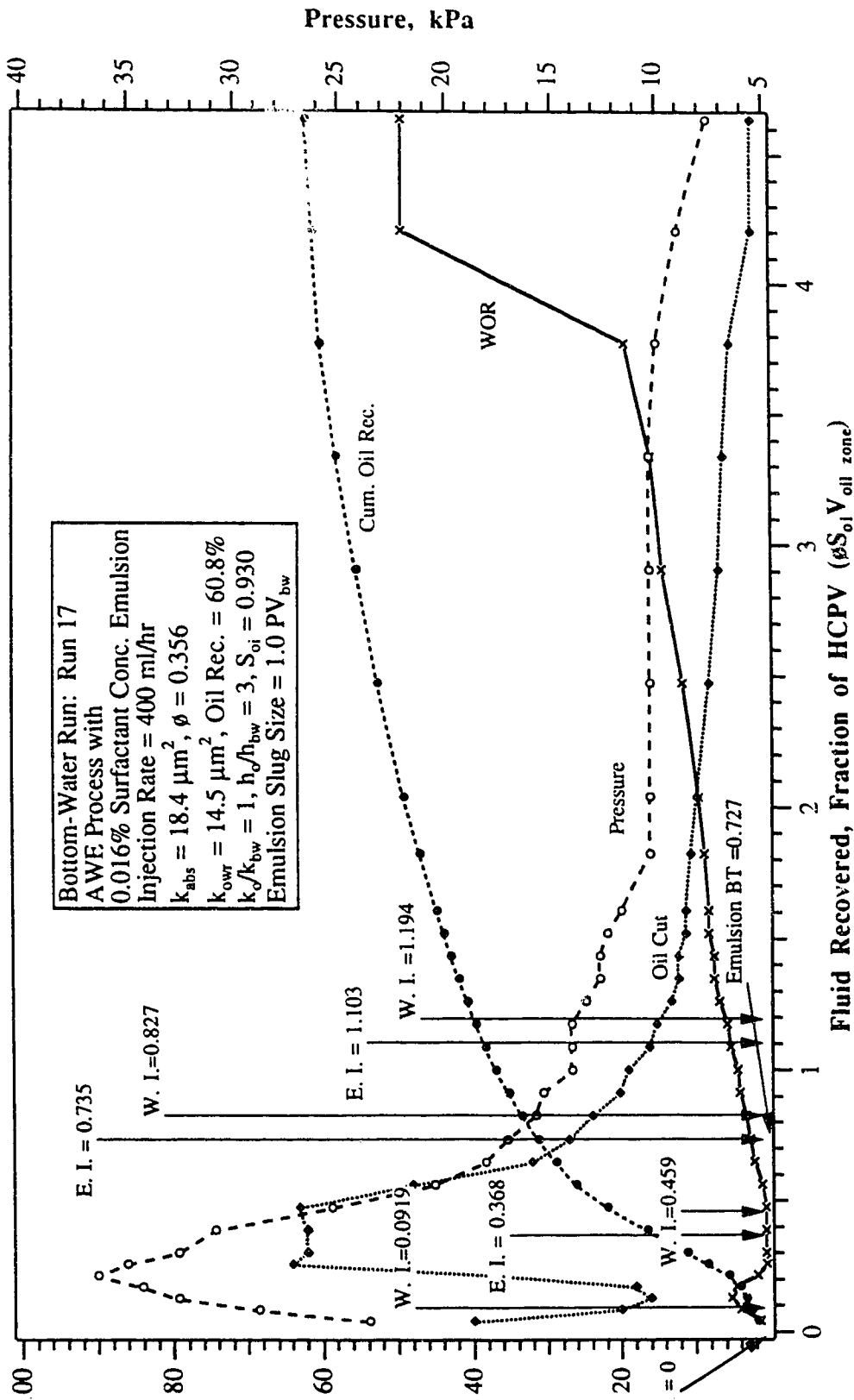


Fig. 7.18: Production History for Run 17. Emulsion Flooding a Bottom-Water Reservoir Using the AWE Process (0.016% Surfactant Conc. Emulsion).

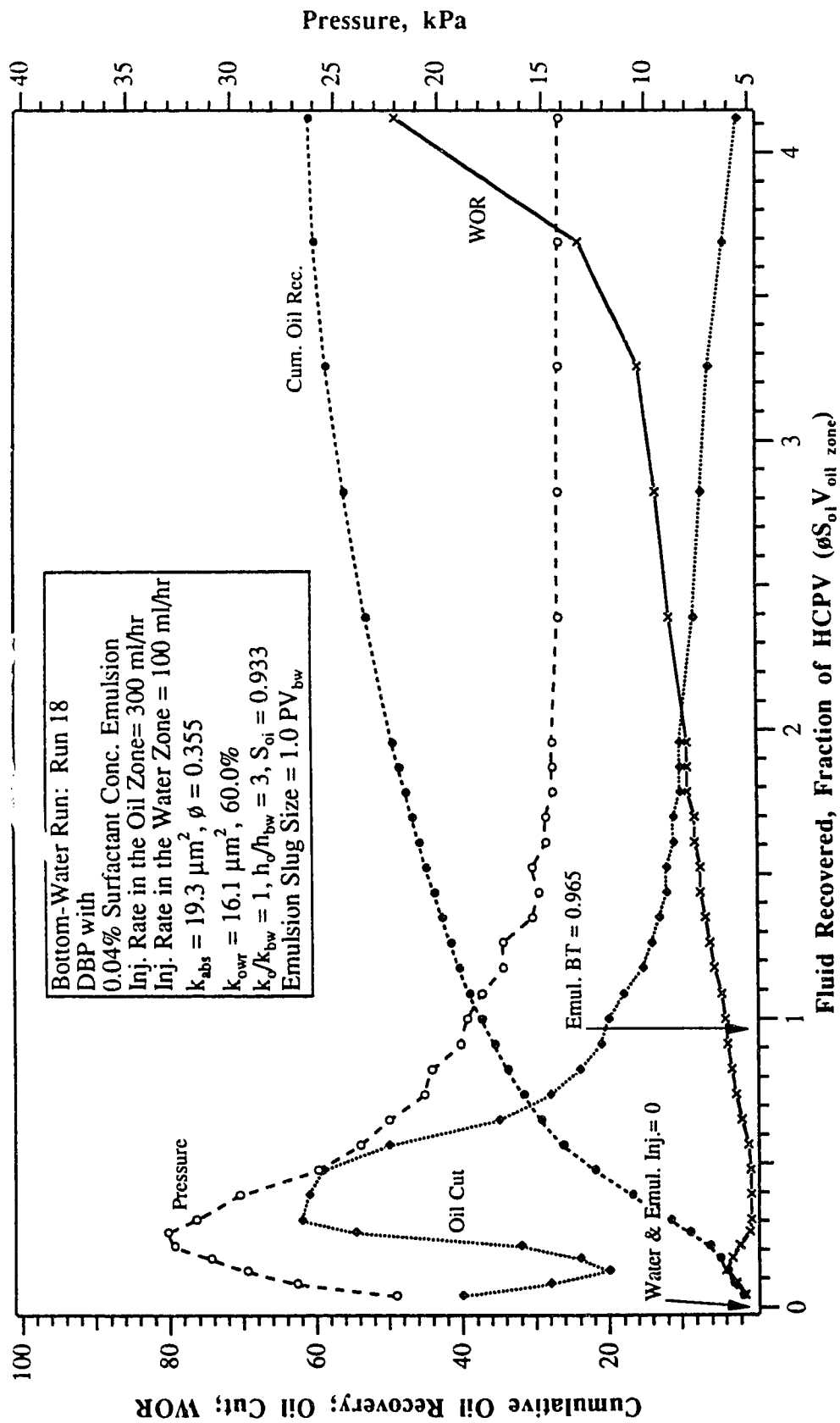


Fig. 7.19: Production History for Run 18. Emulsion Flooding a Bottom-Water Reservoir Using the DBP (0.04% Surfactant Conc. Emulsion)

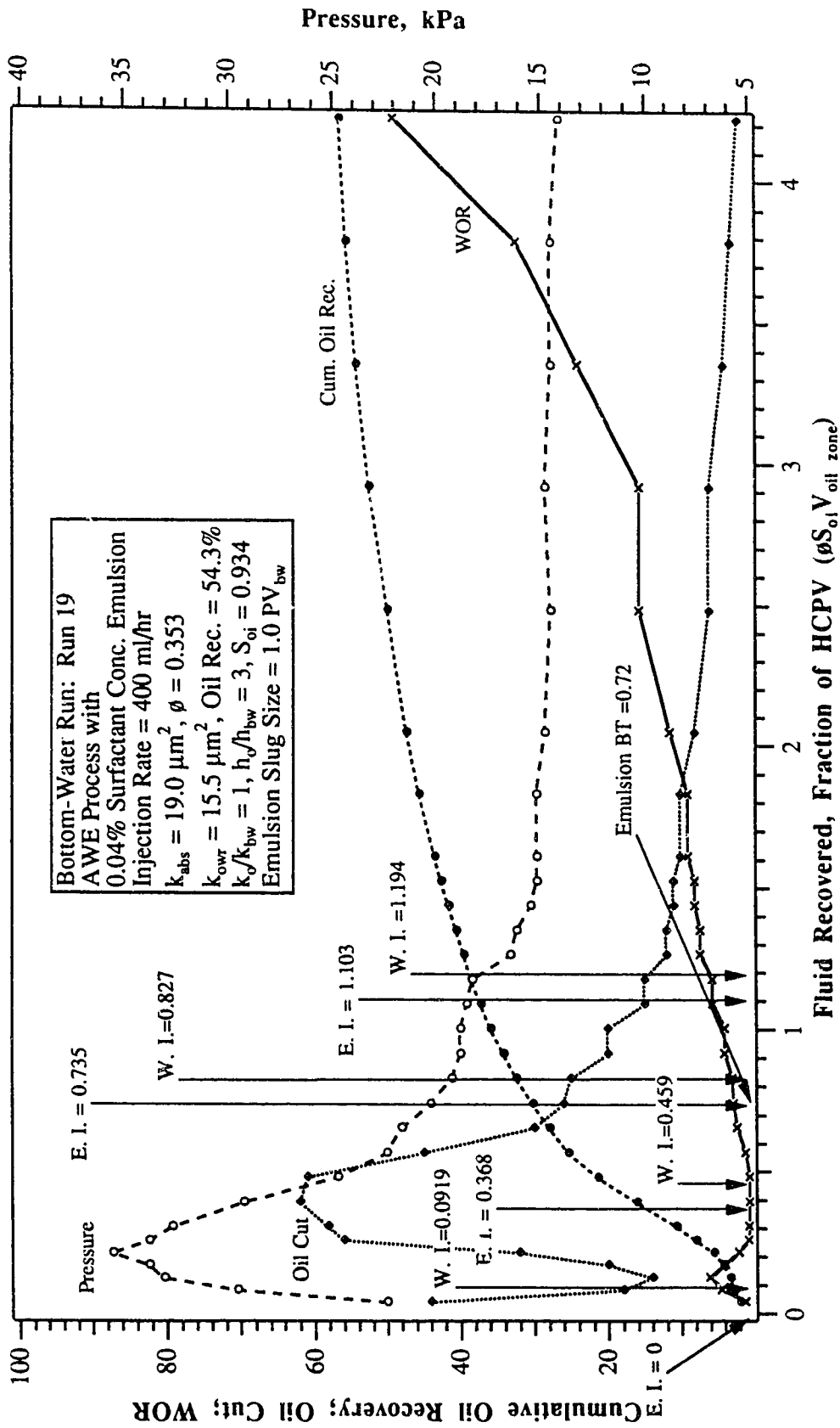


Fig. 7.20: Production History for Run 19. Emulsion Flooding a Bottom-Water Reservoir Using the AWE Process (0.04% Surfactant Conc. Emulsion).

Run 20: Bottom-Water Run with Waterflooding in the Bottom-Water Zone
 $h_o/h_{bw} = 3, k_o/k_{bw} = 1$

This run employed the same parameters as all previous runs with bottom-water. It was conducted to further examine waterflooding performance under bottom-water conditions ($h_o/h_{bw} = 3, k_o/k_{bw} = 1$, and well penetration = 50% of bottom-water zone thickness, Point B in Fig. 6.2). This run employed the same experimental set-up as that of Runs 7 and 12, except that the waterflood was carried out in the bottom-water zone to examine the effect of the point of injection under bottom-water conditions. Figure 7.21 shows the production history of this run. Notice that the oil cut was not greatly affected by the unfavourable injection point location. In fact, a trend similar to that of Runs 7 and 12 was observed. Initially, the oil cut dropped very rapidly to 14%, and then increased slowly to an approximately constant value of 31.4% for a period of 0.77 HCPV of fluid production; oil recovery was over 35% IOIP before the decline started. The ultimate oil recovery was less than that for Runs 7 and 12 (50.1% IOIP and 48.5% IOIP, respectively). Nevertheless, 46.6% IOIP was recovered when the WOR reached 20.

Base Runs: Emulsion Flooding in the Absence of Bottom-Water Layer

Runs 21, 22 and 23: Emulsion Floods with Different Surfactant Concentrations

Runs 21, 22 and 23 were conducted to examine the effect of different emulsions (same quality but with different surfactant concentrations) on oil recovery in a homogeneous pack. The three different emulsions used in previous bottom-water runs were employed in these runs. Emulsions were made using the same amount 10% (vol.) of oil content with different surfactant concentrations: 0.4%, 0.04% and 0.016% for Runs 21, 22 and 23, respectively. Figures 7.22, 7.23 and 7.24 show the production histories of these runs. From Fig. 7.22, it can be seen that the emulsion with 0.4% surfactant concentration had an early emulsion breakthrough at 0.368 HCPV of fluid production. After emulsion

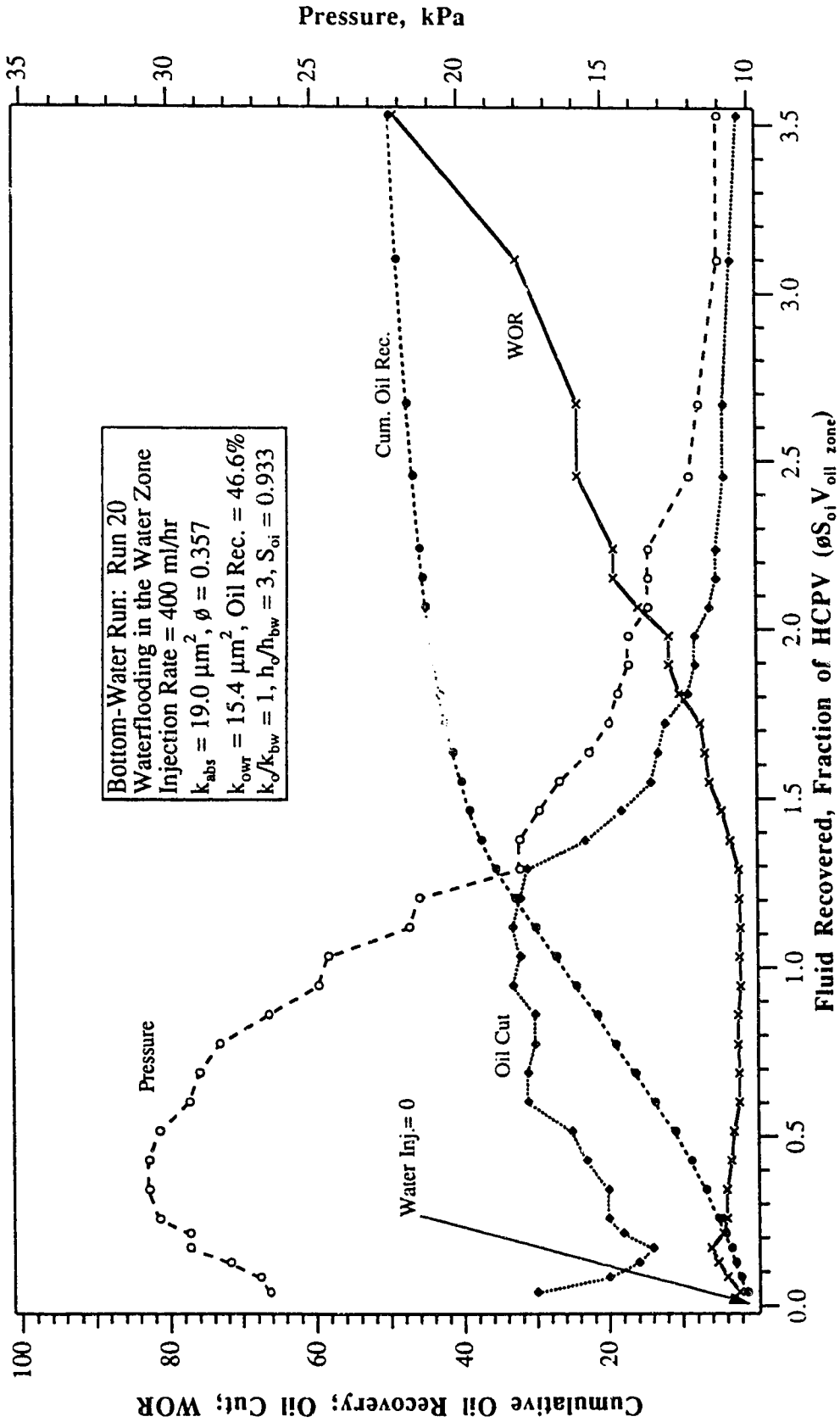


Fig. 7.21: Production History for Run 20. Waterflooding a Bottom-Water Reservoir.

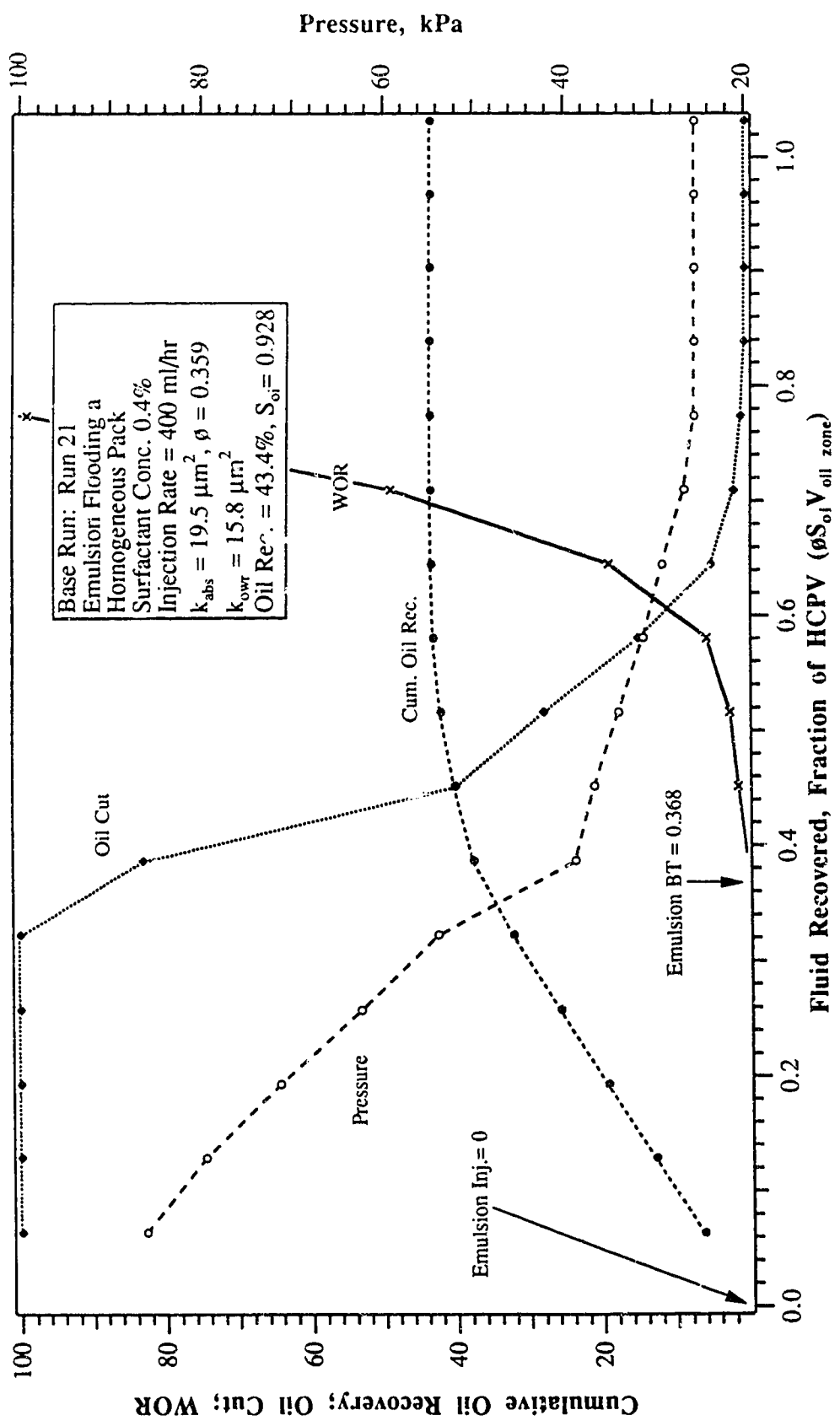


Fig. 7.22: Production History for Run 21. Emulsion Flooding a Homogeneous Pack (0.4% Surfactant Conc. Emulsion).

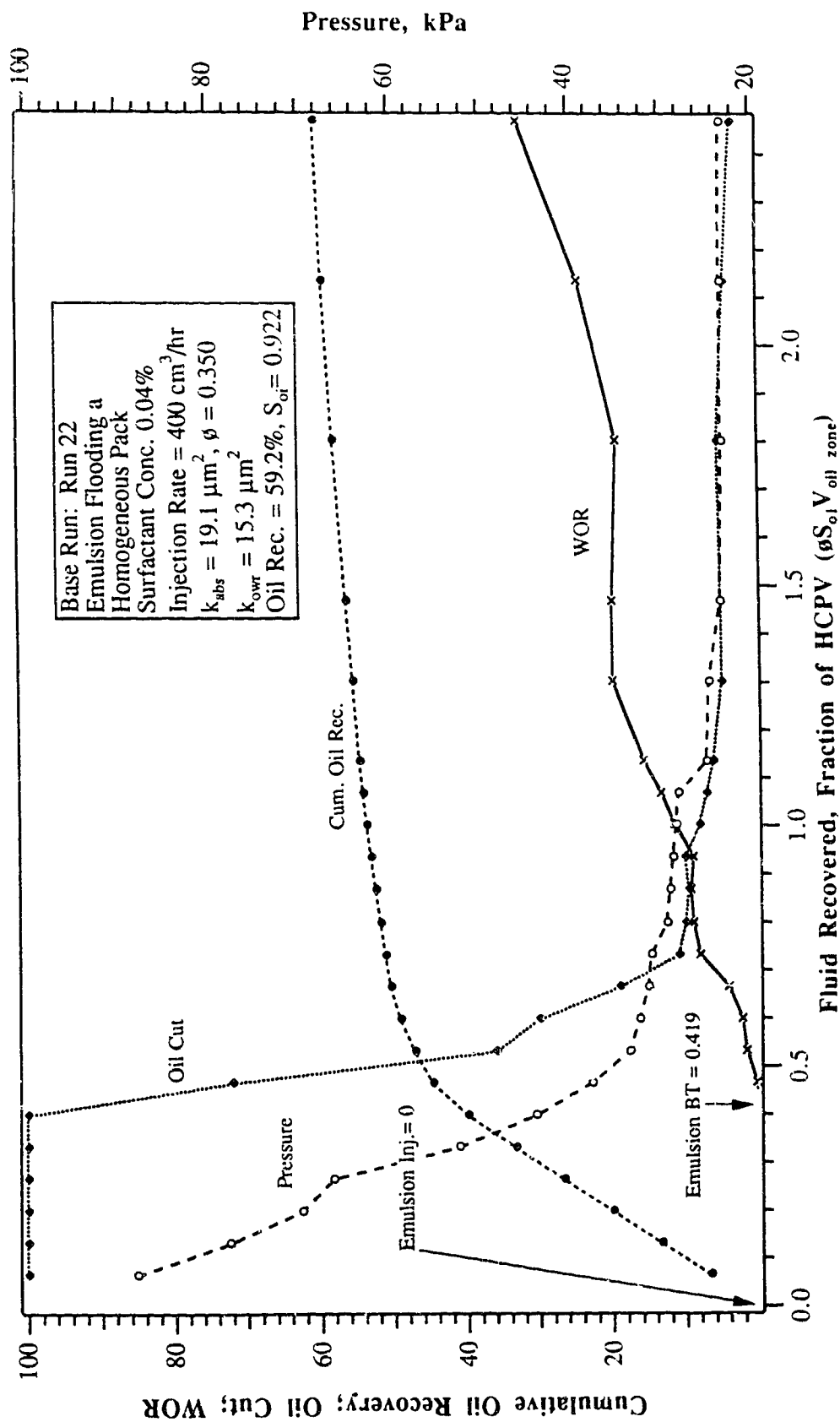


Fig. 7.23: Production History for Run 22. Emulsion Flooding a Homogeneous Pack (0.04% Surfactant Conc. Emulsion).

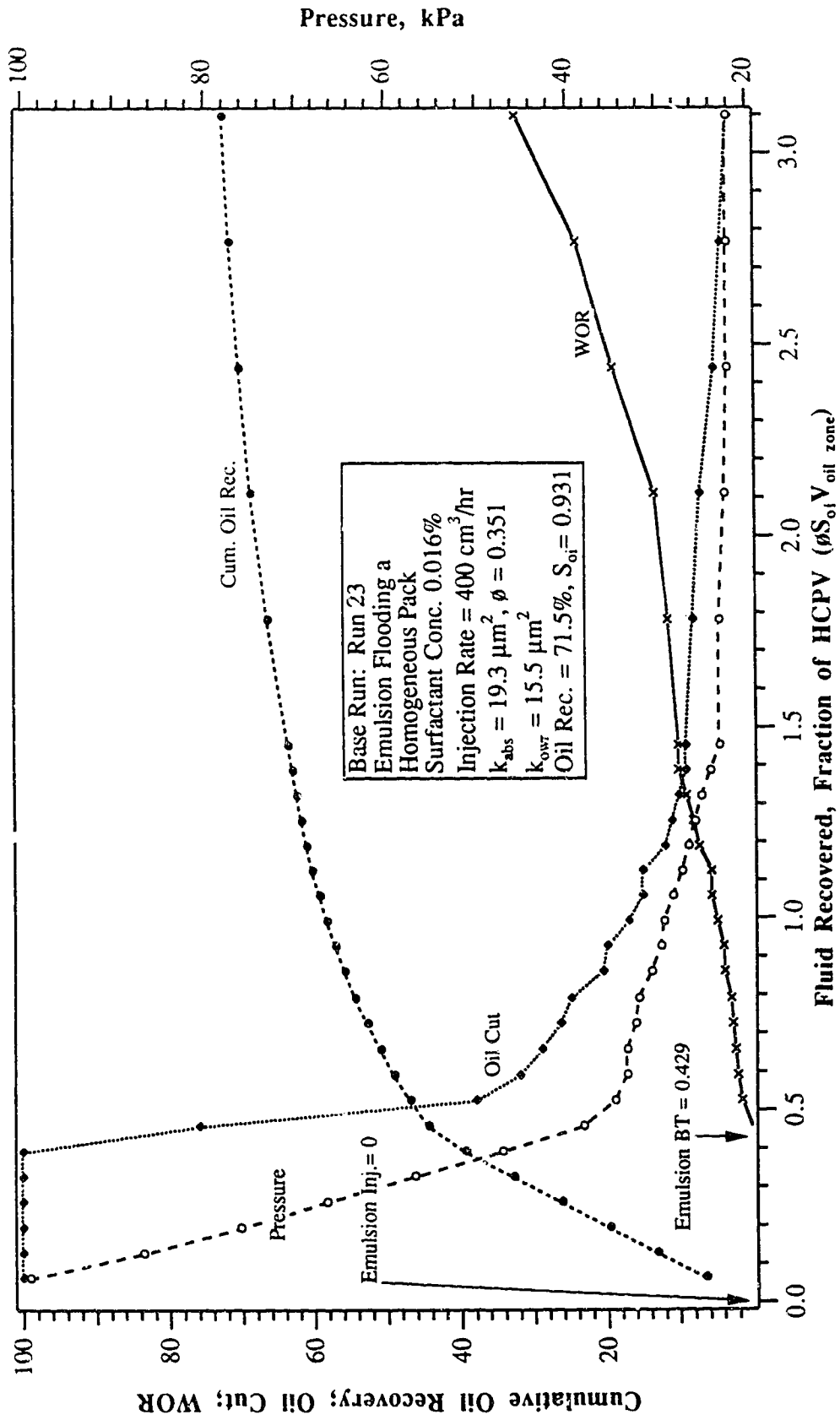


Fig. 7.24: Production History for Run 23. Emulsion Flooding a Homogeneous Pack (0.016% Surfactant Conc. Emulsion).

breakthrough, the WOR increased rapidly to over 20 when only 0.71 HCPV of fluid had been recovered. As a result, a low ultimate oil recovery of 43.4% IOIP was obtained.

Emulsions with a lower surfactant concentration in Runs 22 and 23 exhibited similar oil-cut curves with emulsion breakthrough at 0.419 and 0.429 HCPV of fluid production. However, despite the similarity of the emulsion breakthrough in the two runs, a lower surfactant concentration in Run 23 gave a much higher ultimate oil recovery of 71.5% IOIP as compared to 59.2% IOIP in Run 22. Thus, it can be concluded that surfactant concentration in the emulsion plays a major role in oil recovery.

Runs 24 and 25: Reproducibility of the Experiments

As described in the previous section, it can be seen that the experimental set-up and procedure is labour-intensive. Thus, experimental error is one of the major errors likely to occur in the experiments. However, it can be shown from Runs 24 and 25 that when a similar packing procedure was employed, error was about the same. That is, human error, if present, was consistent in the packing process. Therefore, experimental results can be meaningfully compared with each another.

Due to the long duration of the experiments, on the average 10 days for each run, only two runs were repeated to examine the reproducibility of the experiments. Runs 16 and 18 were repeated as Runs 24 and 25, respectively. Figures 7.25 and 7.26 show the production histories of these two runs. Comparing these runs with the previous Runs 16 and 18, Runs 24 and 25 exhibit almost identical production histories. Cumulative oil recovery for Runs 16 and 18 were 66% and 60% IOIP; for Runs 24 and 25, recoveries of 66.1% and 59.5% IOIP were obtained. Thus, it can be concluded that the experiments in this study were reproducible with an error of less than 1% recovery of IOIP.

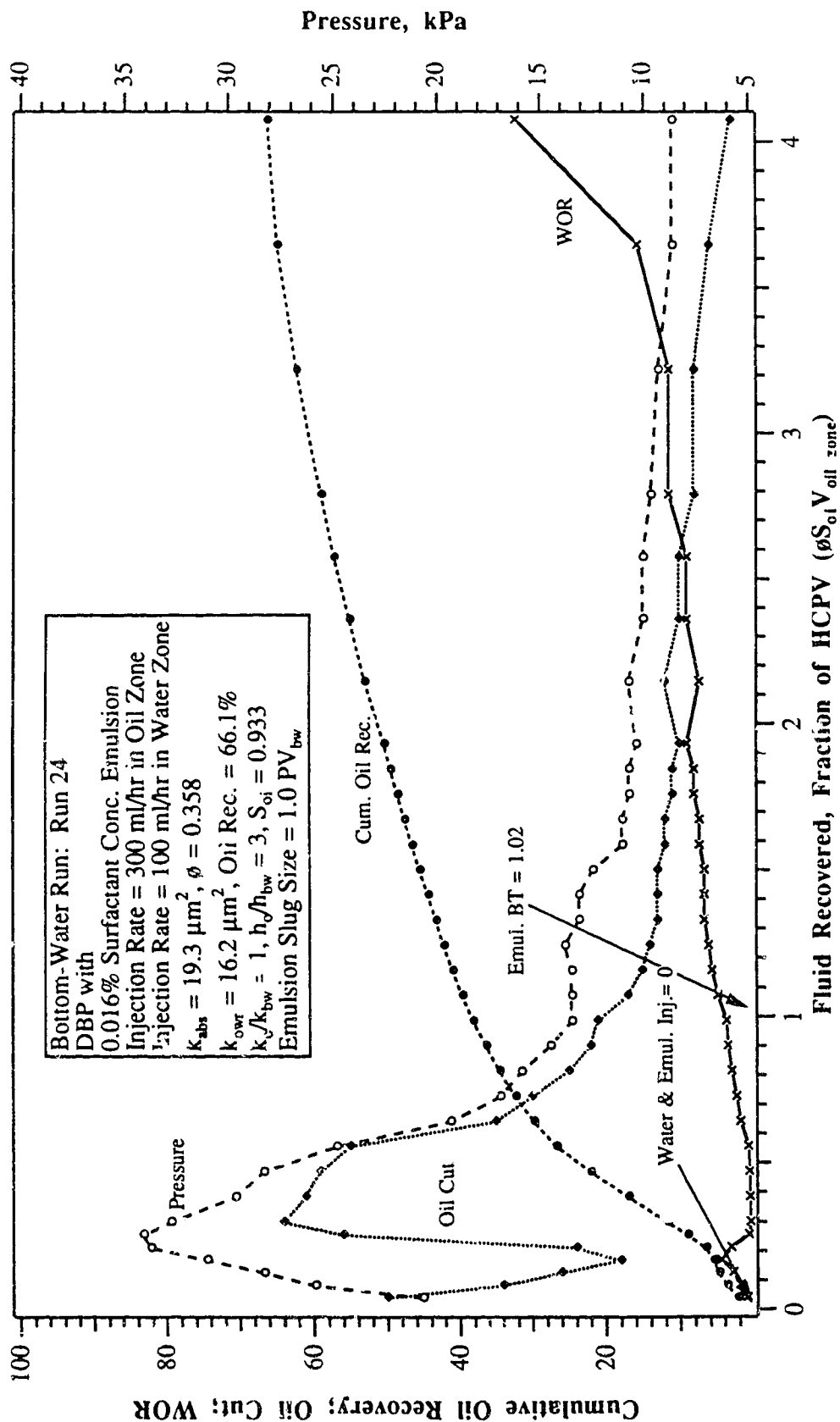


Fig. 7.25: Production History for Run 24. Emulsion Flooding a Bottom-Water Reservoir Using the DBP (0.016% Surfactant Conc. Emulsion).

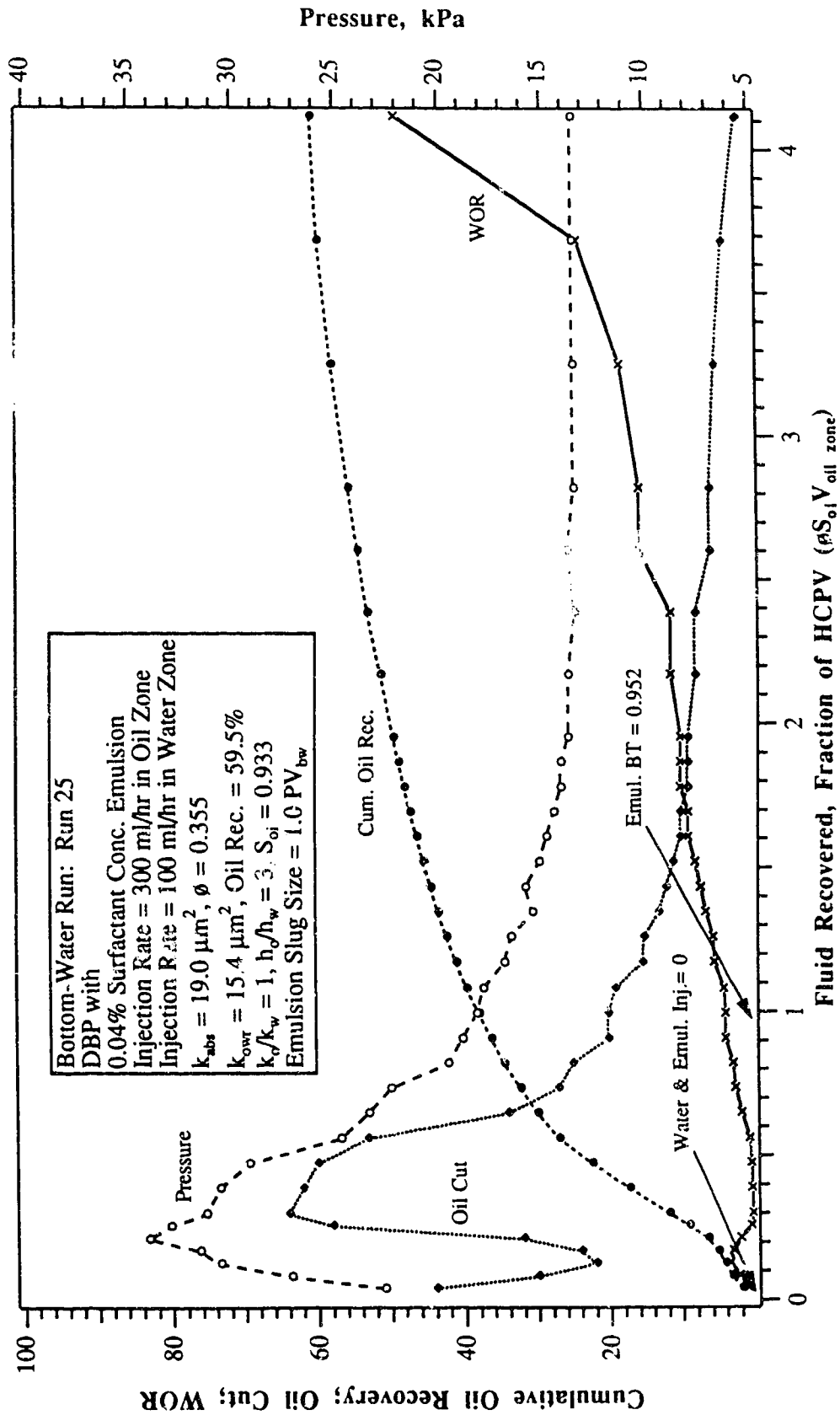


Fig. 7.26: Production History for Run 25. Emulsion Flooding a Bottom-Water Reservoir Using the DBP (0.04% Surfactant Conc. Emulsion).

8. DISCUSSION OF THE RESULTS

In this research, 25 experiments were conducted to study waterflooding under bottom-water conditions. The principal objectives were to study the crossflow effect and examine the use of emulsions as blocking agents under bottom-water conditions. This chapter is divided into two main sections. First, different aspects of crossflow are discussed, based upon the experimental results obtained in this study as well as the experimental results of previous studies^{3,5,6}. Second, different injection strategies for using an emulsion as a blocking agent are discussed.

8.1 Crossflow

Four experiments (Runs 7, 11, 12 and 20) were conducted to verify the crossflow equations. The equations were further confirmed using data from previous studies^{3,5,6}. In this section, different aspects of the crossflow equations are discussed.

8.1.1 The Effect of Injection Point on Crossflow

Runs 7, 12 and 20 were designed to study the effect of waterflood injection interval on oil recovery. The injection intervals were located in the oil zone, both oil and water zones, and the water zone, respectively in Runs 7, 12 and 20. The flow rate used in these runs was 400 ml/hr. In Run 12, the volumetric flow rates in the oil and bottom-water zones were proportional to the cross-sectional areas of the respective zones to simulate a vertical-front displacement. Figure 3.1, as well as the production history graphs in the previous section (Figs. 7.8, 7.13, and 7.21), show that the waterflood performance was very similar in that the cumulative oil recovery curves exhibited similar trends with a maximum deviation of 4%. Root and Skiba³⁰ concluded that oil recovery cannot be improved by blocking access to a high permeability zone in the injection well. Runs 7 and 12 showed that this is indeed the case: by restricting water injection to the oil zone, oil recovery improved only slightly; an increment of only 1.6% IOIP in ultimate oil recovery (from 48.5% IOIP in Run 12 to

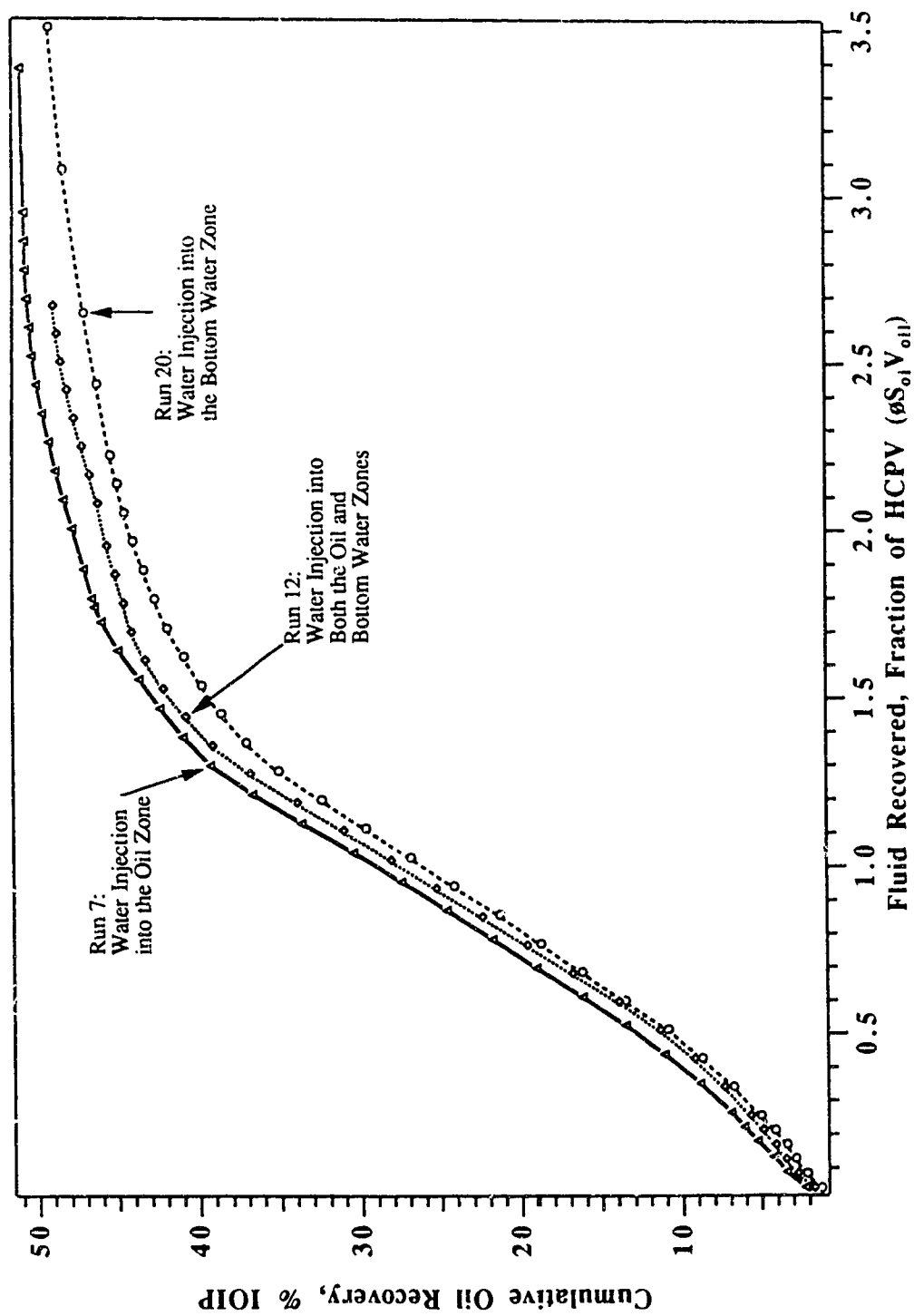


Fig. 8.1: The Effect of Injection Interval on Oil Recovery When Waterflooding a Bottom Water Reservoir.

50.1% IOIP in Run 7) was realized. In contrast, restricting water injection to the bottom-water zone in Run 20 did not affect the oil recovery adversely (an ultimate oil recovery of 46.6% IOIP). When water was injected into both layers proportionally in Run 12 (i.e., $q_o/h_o = q_w/h_w$, where subscripts refer to the respective layers), however, the oil recovery was between the two extremes.

Crossflow as a function of the flood-front position is plotted for Runs 7, 12, and 20 in Figs. 8.2a, 8.2b and 8.2c using Eqs. (4.12) and (4.13), respectively, in order to examine the similarity of the three runs. Notice that in all three figures, the amount of crossflow remained more or less unchanged after the flood front traversed less than 10% of the model length. In the case of injection into the oil zone, Run 7, 63.2% of the injected water channelled into the bottom-water zone, leaving 36.8% of the injected water to displace the oil (Fig. 8.2a). (Note: water channelling is approximated using Eq. (4.12) at $X_f = 1$.) Thus, theoretically, the oil cut should be constant at 36.8% before water breakthrough in the oil zone. The experimental value of the oil cut averaged 33.2% over 0.67 HCPV of fluid production (Fig. 7.8).

When water was injected into both the oil and water zones (75% into the oil zone and 25% into the bottom-water zone), in Run 12, 40.6% of the injected water channelled into the bottom-water zone (Fig. 8.2b). Therefore, the theoretical constant oil cut should be 34.4% (= 75% - 40.6%). The experimental value of the oil cut averaged 33.3% over 0.76 HCPV of fluid production (Fig. 7.13). When water was injected into the water zone only, in Run 20, 35.6% of the injected water channelled into the oil zone (Fig. 8.2c). Therefore, the theoretical constant oil cut should be 35.6%. The experimental value of the oil cut averaged 31.4% over 0.77 HCPV of fluid production (Fig. 7.21). On the whole, the agreement between the oil cut values calculated from the crossflow equations and those observed experimentally is good.

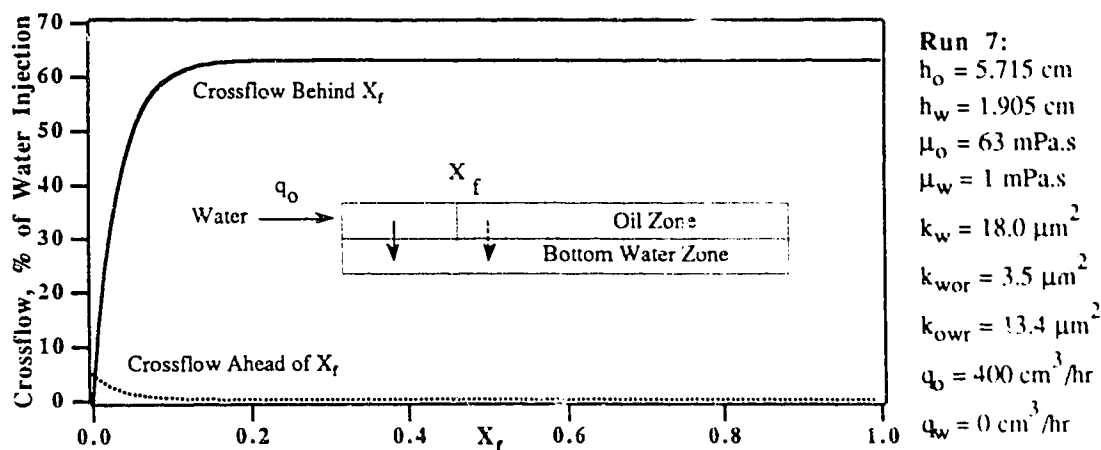


Fig. 8.2a: Crossflow as a Function of the Flood Front Position when Waterflooding the Oil Zone.

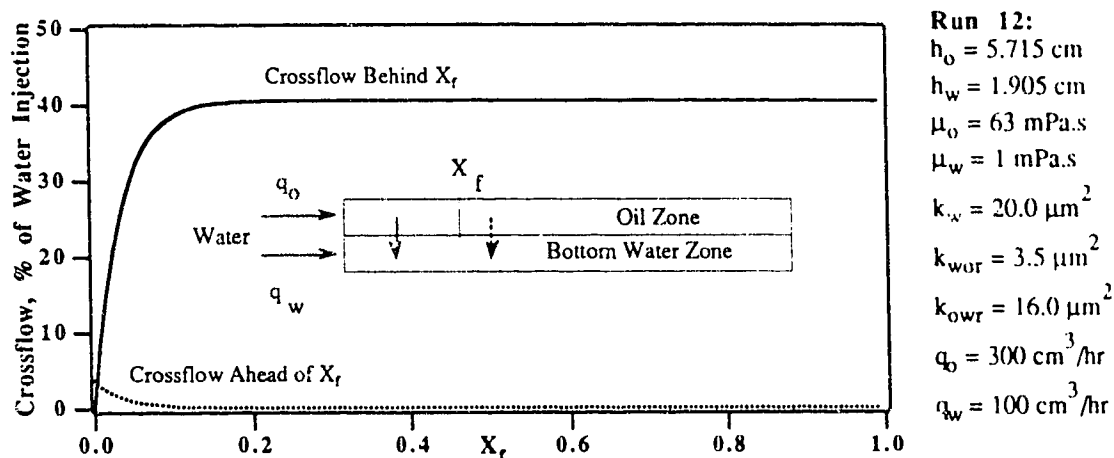


Fig. 8.2b: Crossflow as a Function of the Flood Front Position when Waterflooding Both the Oil and Water Zones.

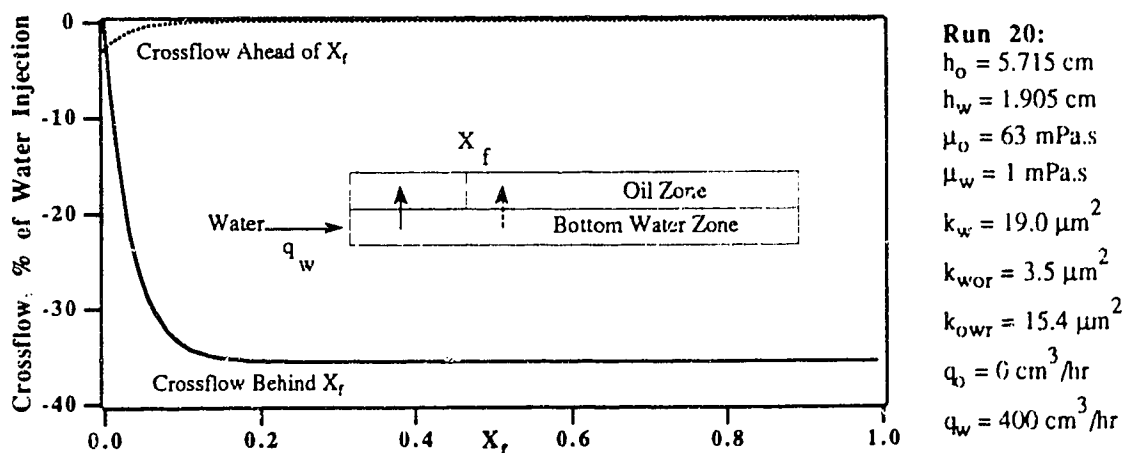


Fig. 8.2c: Crossflow as a Function of the Flood Front Position when Waterflooding the Water Zone.

In all three runs, the percentage of the injected water flowing in the oil zone, as given by the crossflow equation, is of the same order, viz. 36.8, 34.4 and 35.6% for Runs 7, 12 and 20, respectively. In fact, if the identical reservoir descriptions of the model (i.e., the permeabilities of the different zones) are used to calculate the percentage of the injected water flowing in the oil zone, identical values are obtained regardless of the interval of injection (i.e., using the crossflow Eq. (4.12) for any combination of flow rates in the oil and the bottom-water zones, the percentage of the injected water flowing in the oil zone is the same). Thus, it is concluded that the waterflood performance under bottom-water conditions is not a strong function of the water injection interval when crossflow exists. However, ignoring the effect of gravity, it is still preferable to inject water into the oil zone, as it is evident that a small oil bank forms in the bottom-water zone, leading to a decrease in the water mobility in this zone, eventually leading to a higher oil production rate. The small oil bank can be identified as the crossflow of oil into the bottom-water zone ahead of the flood front in Figs. 8.2a and 8.2b.

8.1.2 Verification of the Crossflow Equations

It can be seen from the previous section that the crossflow equations predicted the amount of water channelling under bottom-water conditions. In this section it is shown that the crossflow equations can be used to analyze Run 11, and selected results obtained in previous studies^{3,5}.

8.1.2.1 Zero Crossflow Case

The case of zero crossflow between the two layers is of special interest, because the displacement process is then similar to that in the case of a homogeneous porous medium.

The condition for zero crossflow between the layers was (Section 4.2):

$$\frac{q_w \mu_w}{A_w k_w} - \frac{q_o \mu_o}{A_o k_c} = 0, \quad \dots\dots\dots(8.1)$$

where subscripts w and o denote the properties of the bottom-water and oil zones behind the flood front, respectively, and q_w and q_o are the respective water injection rates.

In Run 11, oil (MCT-10) was injected into both the oil and bottom-water zones to satisfy the above condition. Since the same porous media were used for both zones and the injection rates in the oil and bottom-water zones were proportional to their cross-sectional areas (i.e., $q_w/A_w = q_o/A_o$), the above condition was satisfied. From the experimental results, Fig. 7.12, it can be seen that after 0.35 HCPV of fluid production, an oil cut of 76% was obtained (i.e., zero crossflow was attained, since $h_o/(h_o+h_w) = 75\%$). Despite the fact that the mobility ratios were favourable in both the oil and bottom-water zones, it took 0.35 HCPV of fluid production before the oil rate reached 76%. Thus, it seems that the low oil rate during the initial production stage of a bottom-water reservoir is unavoidable. However, once the system reached steady state, the oil cut was constant at an average of 76% for 0.37 HCPV of fluid production before the oil cut started to increase due to production of injected oil. Thus, the crossflow equation predicted the zero crossflow condition when the appropriate fluids were injected into the corresponding layers.

8.1.2.2 Previous Linear Waterflood Studies

Islam⁵ reported the only experimental investigation of waterflooding an oil zone with a communicating water zone. However, all of the waterfloods in that work were followed by various types of chemical floods. Thus, only the portion of the fluid production history prior to the chemical flood was used to verify the crossflow equation derived in this research. In Fig. 8.3, the oil cut (before a chemical flood) when waterflooding a bottom-water reservoir is plotted against fluid recovered, in pore volumes of the model. Notice that all of the oil cut curves exhibit a fairly constant value shortly after production started. This further supports the premise that crossflow is constant after the flood front is away from the injection well (approximately 0.1 of the model length, derived below in Section 8.1.3). Figure 8.3 shows that the crossflow equations predict water channelling into the

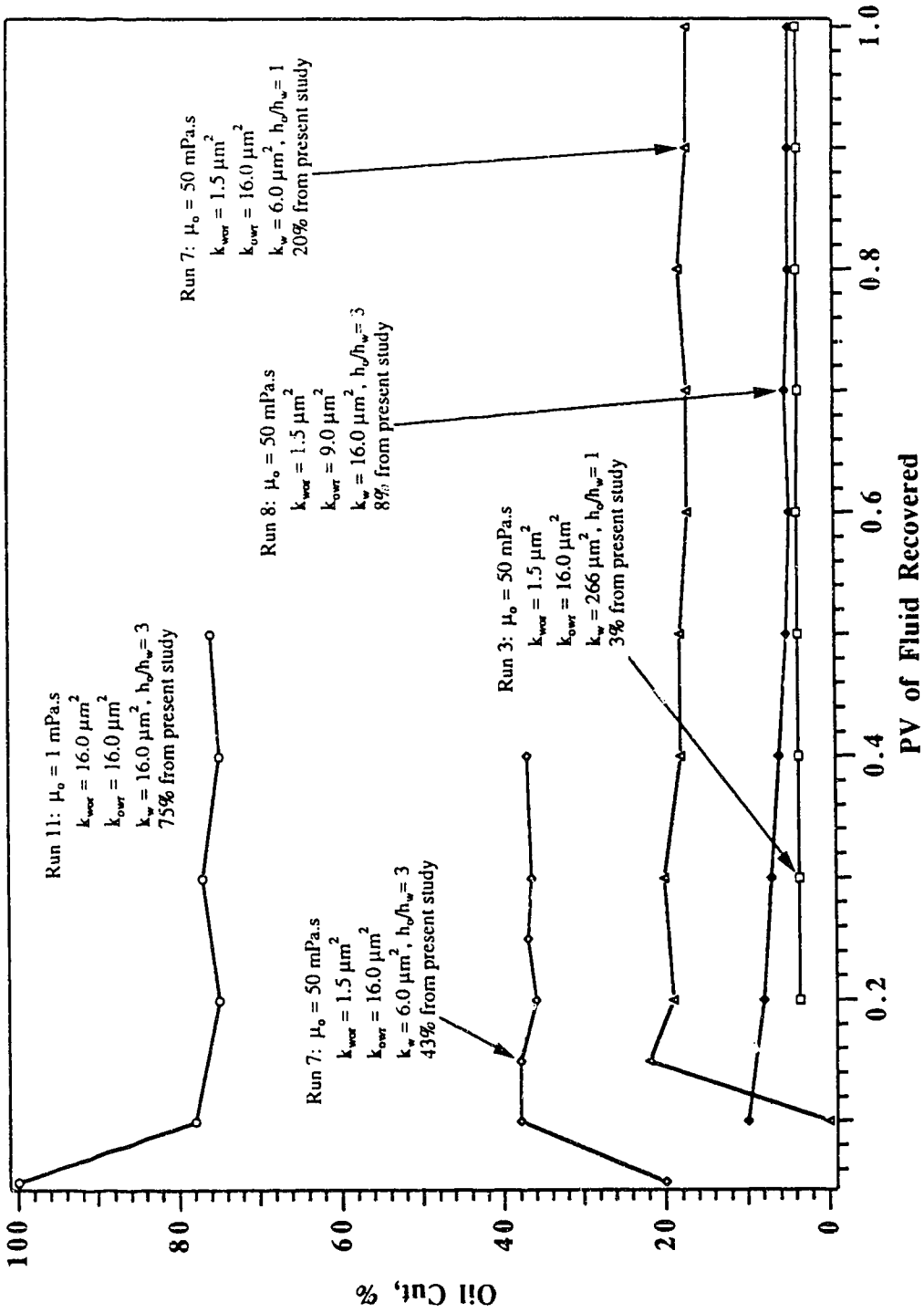


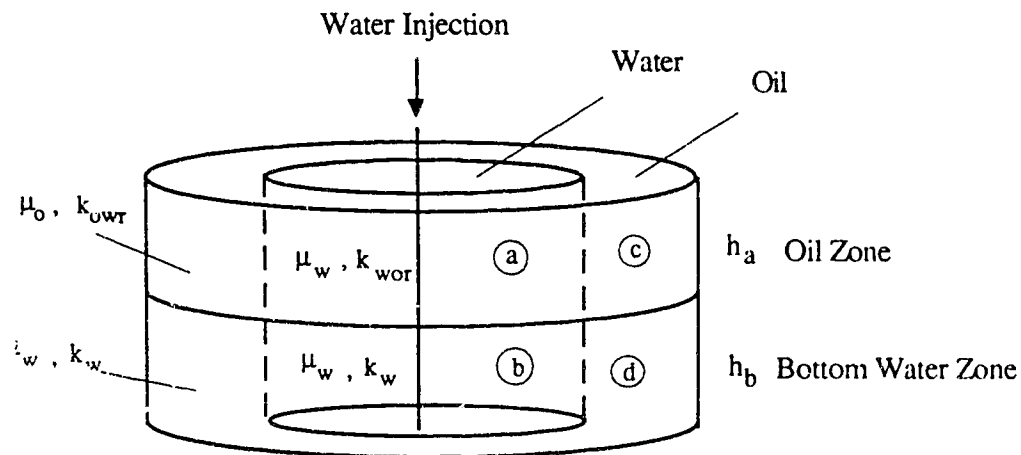
Fig. 8.3: Experimental Results of Oil Cut vs. Fluid Recovered from Islam⁵.

bottom-water zone with a maximum error of approximately 5%. Again, water channelling is predicted using Eq. (4.12) at $X_f = 1$.

8.1.2.3 Previous Radial Waterflood Studies

Although the crossflow equations were derived for a linear displacement case, it can be shown that crossflow between layers under bottom-water conditions is independent of geometry (i.e., linear and radial displacements exhibit similar pressure distributions when crossflow exists), and thus, can be used to examine a radial displacement case.

Consider the following radial displacement which is similar to the previous conditions:



The previous assumptions, as follows, apply in this case also:

- 1) flow is steady state;
- 2) crossflow is vertical;
- 3) crossflow does not alter the mobility in either layer;
- 4) fluids are incompressible;
- 5) displacement is piston-like;
- 6) only oil is flowing ahead of the flood front in the oil zone;
- 7) only water is flowing behind the flood front; and
- 8) capillary and gravity forces are negligible.